TAMPEREEN TEKNILLINEN YLIOPISTO
TAMPERE UNIVERSITY OF TECHNOLOGY

Jaakko Kleemola

Experimental Methods for the Evaluation of Lubrication Conditions in Gear Contacts

Julkaisu 894 • Publication 894

Tampere 2010

Tampereen teknillinen yliopisto. Julkaisu 894
Tampere University of Technology. Publication 894

Jaakko Kleemola

Experimental Methods for the Evaluation of Lubrication Conditions in Gear Contacts

Thesis for the degree of Doctor of Technology to be presented with due permission for public examination and criticism in Konetalo Building, Auditorium K1702, at Tampere University of Technology, on the 31st of May 2010, at 12 noon.

Tampereen teknillinen yliopisto - Tampere University of Technology
Tampere 2010

ISBN 978-952-15-2367-0 (printed)
ISBN 978-952-15-2815-6 (PDF)
ISSN 1459-2045

Abstract

The constant pressure to build lighter, more heavily loaded, more efficient and extremely reliable gearboxes defines the main requirements for gear design. In a typical elastohydrodynamic lubrication (EHL) contact, which occurs in gear contacts, the lubrication pressure rises to several GPa above ambient levels for times of 200 – 400 μs and the protecting film thickness is usually below the 1 μm. Operating under such conditions, a gearbox is required to last for more than 20 years, which sets strict requirements for the gears and for the lubrication itself. The standard calculation methods provide the safety factor against failure, but they give no detailed information on what is really happening in the gear contacts. To have a fuller understanding of lubricated contacts designed to minimize friction, heating and failure rates in modern gearboxes, it is important to analyze gear contact in more sophisticated ways.

The objective of this thesis is to increase the understanding of lubrication conditions in gear contacts. This involved the development of test devices and methods for determination of lubrication conditions and high pressure properties of lubricants in gear contacts as well as the evaluation of lubrication conditions in controlled elliptical contacts and in real gear contacts.

A high pressure twin-disc test device was developed where the grinding of discs has been done perpendicular to the rolling direction, which corresponds to real gear surfaces. This allowed the study of lubricant high-pressure properties and lubrication conditions by simulating the gear contact along the line of action. The test device was equipped to measure the mean contact resistance, the bulk temperature and the frictional force.

A method for determination of the limiting shear stress and actual viscosity of lubricants was developed using a numerical traction model based on elliptical EHL contact and traction curves measured over a wide range of temperatures and pressures with a twin-disc test device.

The transversely ground elliptical contact was studied under mixed lubrication conditions using a twin-disc test device. The calculated thermal Λ-values of real gears and the measured mean contact resistance correspond well. This kind of simulation gives more local information about the friction coefficients, lubrication conditions and temperatures along the line of action than can be obtained from real gear measurements. The simulation can be also used to provide reference data for testing of mixed lubrication models.

The contact resistance and bulk temperature measurement were applied to a modified FZG gear test device to detect on-line transient lubrication conditions in real transient gear contacts under mixed lubrication conditions. The trend in the curves of the measured mean contact resistance and the calculated steady-state based film thicknesses correspond well with different operating parameters such as load, pitch line velocity and oil inlet temperature. Some deviations were observed, which were explained as being the result of non-steady-state lubrication conditions.

Preface

This work was carried out in the Department of Mechanics and Design, Tampere University of Technology. I would like to express my appreciation to my supervisor Professor Arto Lehtovaara, who has provided support and guidance during the work and has also given me the opportunity to find my own way to the goal even if it has taken time.

I would like to thank all my colleagues in the Department of Mechanics and Design for their support. I am especially indebted to Lic.Tech. Olli Nuutila for guidance in the world of measuring techniques, Mr Matti Uotila for helping in numerous test rig installations and modifications and Mr Alan Thompson for the English language revision of the manuscript.

I wish to acknowledge the financial support of the Graduate School CE Tampere (Concurrent Engineering), Fortum foundation, Walter Ahlström foundation, Finnish foundation for technology promotion (TES) and the Yrjö and Senja Koivunen foundation.

I would also like to thank Mom and Dad, for all their support and for bringing me my up as they did. Finally I wish to express my heartfelt gratitude to my lovely wife Elina and my dear son Joni, for their patience and support throughout this work.

Tampere, January 2010

Jaakko Kleemola

List of appended papers and division of work

I. Kleemola, J. and Lehtovaara A. Development of a high pressure twin disc test device for the simulation of gear contact. Finnish Journal of Tribology, 2006, 25(2), 8-17.

II. Kleemola, J. and Lehtovaara A. Experimental evaluation of friction between contacting discs for the simulation of gear contact. TriboTest, 2007, 13(1), 13-20.

III. Kleemola, J. and Lehtovaara A. An approach for determination of lubricant properties at elliptical elastohydrodynamic contacts using a twin-disc test device and a numerical traction model. Proc. IMechE, Part J: J. Engineering Tribology, 2008, 222(7), 797-806.

IV. Kleemola, J. and Lehtovaara A. Experimental simulation of gear contact along the line of action. Tribol Int., 2009, 42(10), 1453-1459.

V. Kleemola, J. and Lehtovaara A. Evaluation of lubrication conditions in gear contacts using contact resistance and bulk temperature measurements. Proc. IMechE, Part J: J. Engineering Tribology, 2010, 224(4), 367-375.

In all these papers Kleemola performed the work and undertook the major part of the writing. Lehtovaara supervised the work and shared in the writing.

Contents

Abstract i
Preface ii
List of appended papers and division of work iii
Contents iv
Nomenclature v
1 Introduction 1
1.1 Tribology and lubrication 1
1.2 Lubrication of gearing 4
1.3 Scope and objectives 10
1.4 Outline and contribution of the thesis 10
2 High-pressure twin-disc test device 12
2.1 Base construction 12
2.2 Measured signals 12
2.3 Test discs and lubricants 13
2.4 Results 14
3 An approach for determination of lubricant high pressure properties 15
3.1 Description of the method 15
3.1.1 Viscosity 16
3.1.2 Limiting shear stress 17
3.2 Results 18
4 Lubrication conditions in simulated gear contact 21
4.1 Results 21
5 Lubrication conditions in real gear contact 26
5.1 Experimental 26
5.2 Results 26
6 Conclusions 30
References 32

Nomenclature

a	ellipse semi axis
$a_{1,2,3,4,5}$	constant
b	ellipse semi axis
C_Z	non-dimensional constant
D_Z	non-dimensional constant
G_0	non-dimensional constant
F_N	normal force
F_μ	traction/friction force
h	film thickness
n	rotation speed
p	Hertzian pressure
p_0	maximum Hertzian line pressure
$\bar{p}$	mean fluid pressure
S_0	non-dimensional constant
T	temperature
T_{ref}	reference temperature
T_{bulk}	disc bulk temperature
u	surface velocity
V_R	rolling velocity, $(u_1 + u_2)/2$
V_S	sliding velocity, $u_1 - u_2$
x	coordinate
y	coordinate
z	coordinate
φ_T	thermal reduction factor
Λ	lambda value, h/σ
μ	friction/traction coefficient
μ_{cal}	calculated traction coefficient
μ_{exp}	experimental traction coefficient
ν	kinematic viscosity
ρ	radius of curvature

σ	combined surface rms roughness
τ	shear stress
τ_0	shear stress at atmosphere pressure?
τ_L	limiting shear stress
$\bar{\tau}_L$	mean limiting shear stress
ω	angular velocity
ξ	density
η	actual viscosity
η_0	viscosity at atmospheric pressure

Subscripts:

1	surface 1
2	surface 2
f	fluid
max	maximum value

1 Introduction

This Chapter provides a background for the thesis. The “Tribology and lubrication” section gives an overview of tribology and lubrication generally. “Gear lubrication” summarizes the operating conditions and lubrication mechanisms where gears are working in addition to providing an introduction to modern gearbox requirements. The objectives, scope and contribution of the thesis are presented. Finally, the outline of the thesis gives an overall idea of the structure of the thesis.

1.1 Tribology and lubrication

Tribology comes from the Greek word “tribos”, which means rubbing and the first time the term was used in England in the 1960s [1]. As a science tribology is a quite broad area, but at its simplest it studies the interaction between surfaces in contact and moving relative to each other. It includes friction, wear and lubrication.

The history of tribology and lubrication can be traced back a long way. The evolution of tribology is very clearly summarized in Dowson’s “History of Tribology” [2]. A short overview is given here of the key moments in the history of tribology and lubrication. When mankind invented very simple machines like carriages, he realized the need for lubricants and lubrication to make the machines work better. For example, the oldest potter’s wheel so far discovered, dated at 3250 $\pm$ 250 B.C., shows a marks of bitumen used to reduce the friction and an Egyptian chariot, dated about 1400 B.C., shows the use of mutton or beef tallow as a lubricant. In the Middle Ages these vegetable oils or animal fats were still in general use as lubricants and the use of mineral oils was still a long way off. The Renaissance, circa A.D. 1450-1600, was dominated by one man as far as tribology is concerned: Leonardo da Vinci. Leonardo studied friction, wear, bearings materials, plain bearings, lubrication systems, gears, screw-jacks and, most importantly, rolling-element bearings. He also set out the two principles of frictional behaviour:

1. the friction created by the same weight will result in equal resistance at the beginning of its movement even though the contact area may be of different widths and lengths and
2. the frictional resistance produced will double if the weight is doubled.

These statements are known as “Amontons laws of friction”, because Leonardo did not publish his theories and Guillaume Amontons rediscovered these two basic laws of friction. Before the industrial revolution more theories and laws were presented such as Robert Hooke’s observations on rolling friction, Sir Isaac Newton’s Principia, which contained the foundation for the future understanding of fluid-film lubrication and Leonhard Euler’s research, which shows the difference between static and kinetic friction. The industrial revolution was a turning point for lubrication science because machines became more complex and machine element speeds increased. There were increasing demands to develop lubricants, lubrication and for the understanding of contact.

In 1883 Beauchamp Towers, a railway engineer reported that very high pressures were developed in the contact zone of lubricated locomotive journals and later Osborne Reynolds demonstrated Towers’ observations experimentally. These observations led to the very important discovery that a very thin microscopic film exists between the contacting surfaces and that viscosity plays a crucial role in lubricated bearings [3]. In the 1940s and 1950s it became clear that there really is a protecting film between the contact gear surfaces. This is possible because the viscosity of a lubricant increases by several decades, when it enters into pressurized gear contact and elastic deformation changes the shape of the surfaces in and near the contact [4]. The theory behind this phenomenon is now known as elastohyrodynamic lubrication (EHL). Dowson et al., [5] summarized the development of EHL theory in their book “Elasto-hydrodynamic lubrication”. The micro-level aspects in elastohydrodynamic lubrication (micro-EHL) are presented in reference [6].

In elastohydrodynamic contact two surfaces have relative motion and they are separated by a viscous lubricant film that is trapped in the converging gap. A load causes an elastic deformation of the contacting surfaces and the contact area increases. The load also subjects the lubricant to high pressure, which greatly increases its actual viscosity. As a result the lubricant cannot escape from the contact area, but it can carry the applied load. In a typical EHL contact, which arises in gear and bearing contacts, the lubricant pressure rises from ambient to several GPa in a time of 200 – 400 μs and the protecting film thickness is usually below the 1 μm. Lubricant high pressure properties such as viscosity and limiting shear stress are strongly dependent on both pressure and temperature in EHL contacts. In this kind of high pressure contact the lubricant may no longer behave like a Newtonian fluid, especially if sliding is present. Different kinds of rheological fluid models have been developed to describe the fluid behaviour [7].

The limiting shear stress τ_L was proposed by Paul and Cameron [8] and it describes the maximum shear stress, which a lubricant can sustain at a given pressure and temperature. It has an influence on the surface tangential stresses, which specify the friction coefficient of the contacting surfaces and also have an effect on surface lifetime. Actual lubricant viscosity η is defined as the resistance of the flow and it is also dependent on pressure and temperature. It has an influence on lubricant film thickness and the friction coefficient between the contacting surfaces. Determination of these parameters as a function of high pressure and temperature is a difficult task and values for these properties are not commonly available.

Friction or traction in an EHL contact can be defined as a force generated in the contact that resists relative motion of the contacting surfaces. Traction is mainly determined by what happens in the high pressure region: therefore, lubricant properties must be known at the high pressures (and temperatures) that prevail there. Johnson and Tevaarwerk analyzed traction in the 1970s using a twin disc test device and they were convinced of the importance of non-Newtonian fluid properties, as either the pressure or slide-to-roll ratio increases [9]. The overall behaviour of friction curves is characterized by three

different regions – the linear, non-linear and thermal regions, as shown in Fig. 1.

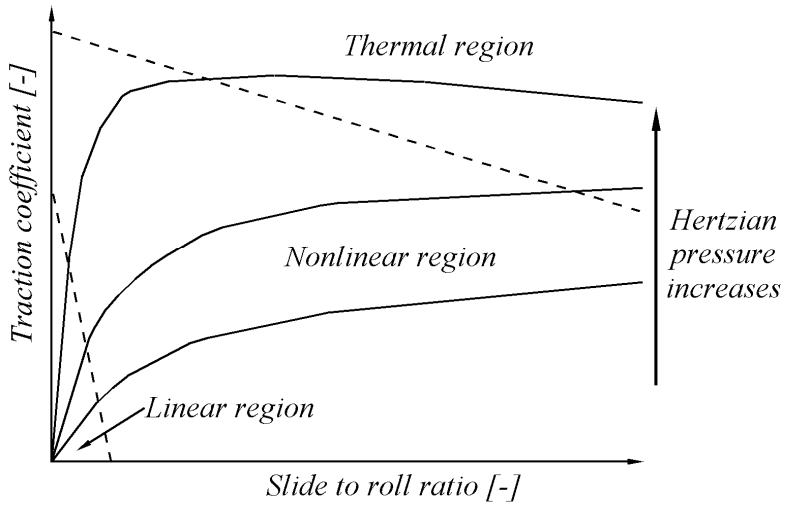

Fig. 1. Friction behaviour under the different regimes

The linear region appears with a very small slide-to-roll ratio while the lubricant retains Newtonian behaviour. When the slide-to-roll ratio increases, a shift occurs to a region, where the lubricant begins to behave in a non-Newtonian way. The friction coefficient is dominated by the lubricant limiting shear stress and friction may reach its maximum point. When the slide-to-roll ratio increases further, a thermal region is reached, where the increasing shearing of the lubricant raises the lubricant temperature and the friction may start to decrease slowly. In the mixed lubrication regime, asperity friction may contribute to the overall friction behaviour. Traction and friction are directly related to gear contact power loss and temperature rise.

1.2 Lubrication of gearing

Gears are one of man's oldest mechanical devices and have been used for over 5000 years [10]. The oldest known gearing from ancient times is the "South Pointing Chariot" circa 2600 BC, where the gears are made from wooden pins. According to Dudley [10], modern gearing began between 1600 AD and 1800 AD. During this period the theory of the gear tooth began to develop and even then the use of the involute tooth form was recommended.

However, at that time theory and practice did not converge because gear-making was a craft and an art. In the 19th century gear cutting machines started to improve, which made it possible to improve the quality of the gears. Modern cutting machines have developed much further and it is now possible to produce modified involute gear profiles at the micro level.

The simplest gear form is the external spur gear. To produce more silent operation, helical gears are often used. The disadvantage of these is that they produce an axial force and make the bearings more complicated than in a spur gear. Herringbone gears eliminate axial forces, but they are more complex to manufacture. Gearing may be internal or external. Internal gearing is used, for example, in planetary gears. In Fig.1 shows the difference between these gear types.

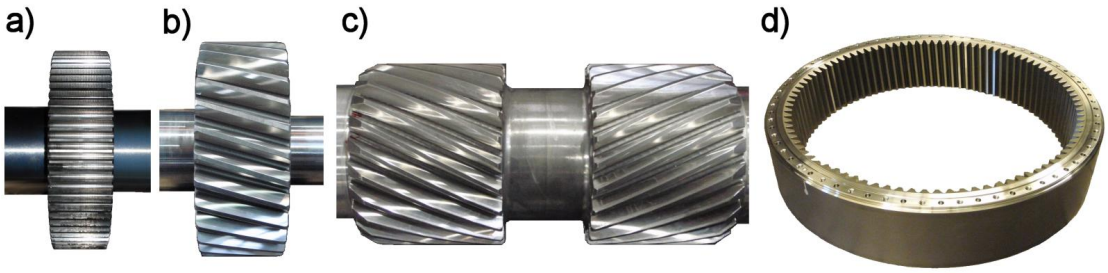

Fig. 2. a) Spur, b) helical, c) herringbone and d) internal gears.

In his book "Lubrication of gearing", Bartz [11] classified gears according to the position of the shaft axes, as shown in Fig. 3. He found this to be particularly suitable for the purposes of the lubrication. Spur gears have parallel axes, while normal bevel gears have intersecting axes. Both types of gear can be considered as rolling gears. If the axes cross, as with the offset bevel gears, worm gears, and crossed-axis helical gears, they are called rolling crossed-axis gears. Usually the lubrication of gearing has been performed using splash or pressure lubrication. In splash lubrication the gears are partly immersed in the lubricant and the rotating parts move lubricant to other lubrication points. In the pressure lubricated systems lubricant is pumped to lubrication points using pipes and the lubricant is often filtered during each lubrication cycle.

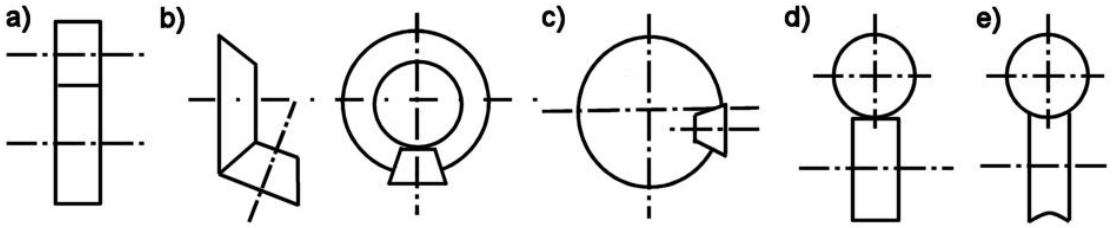

Fig. 3. Schematic views of basic gear types a) spur gear, b) bevel gear, c) offset bevel gear, d) worm gear and, e) crossed axis helical gears.

In the case of gears, contact conditions change greatly along the line of action, because load, surface velocities and radii are changing continuously. Fig. 4a shows the instantaneous spur gear teeth contact and Fig. 4b shows the gear contact along the line of action, where the dimensionless distribution of normal force (F_N/F_{Nmax}), Hertzian maximum line pressure (p_0/p_{0max}), surface velocities (u/u_{max}) and combined radius of curvature (ρ/ρ_{max}) are also shown. The tooth engagement starts at the left in Fig. 4b and the two sudden changes in load and pressure occur when two tooth engagement changes to single tooth engagement and the reverse. At the pitch point pure rolling is present, i.e. the sliding velocity ($V_S = u_1 - u_2$) is zero. The rolling velocity is given by $V_R = (u_1 + u_2)/2$. In static loading, the gear contact ratio at 1-2 and equal load distribution in the case of two teeth in contact (half of the single tooth load) were assumed.

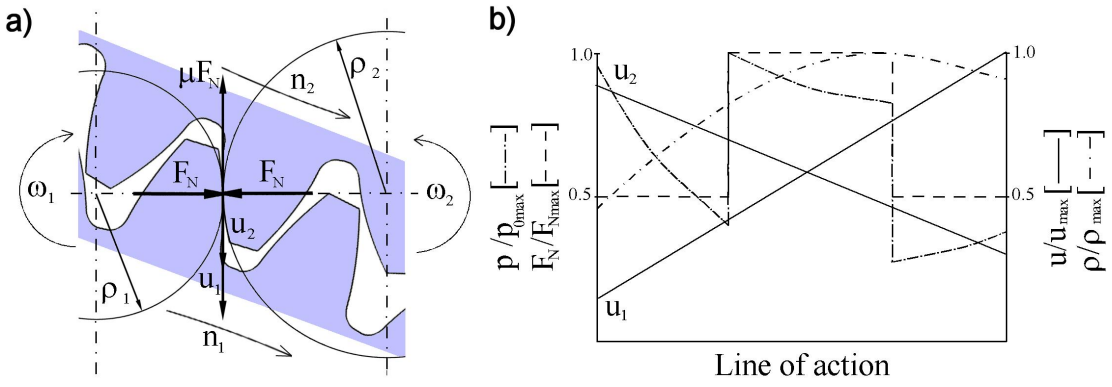

Fig. 4. Operating conditions along the line of action.

The instantaneous contact points along the line of action are very difficult to analyze in detail with real gears. Very often spur gear profiles are approximated by cylinders with the same radius of curvature (ρ_1,ρ_2) as the

gear teeth at the instant contact point, as shown in Fig. 4a. This provides the basis for the twin-disc test device, where steady-state operating conditions exist and most of the dynamics and manufacturing tolerances involved in real gears have been eliminated, resulting in accurately controlled contact conditions. This makes it possible to simulate various essential parameters and failures in gear contact such as scuffing, pitting, power loss, lubricant life and wear.

Gears often operate in boundary, mixed or (micro-) EHL regimes depending on operating conditions such as speed, actual viscosity and surface properties. The lubrication regimes and friction are typically described by using the EHL-Stribeck curve for highly loaded contacts [12]. This curve is shown in Fig. 5. The boundary lubrication regime can be related to low velocity (or low ηV_R – value). In this regime, the friction coefficient is typically high, because shear stress arises mainly from asperity contacts, which carry the load. The mixed lubrication regime is reached by increasing the velocity, which decreases the friction coefficient. With a further increase in velocity, the elastohydrodynamic lubrication regime is reached, where the hydrodynamic pressure generated in fluid film carries the load with no asperity contacts. In this regime the friction coefficient stays fairly constant.

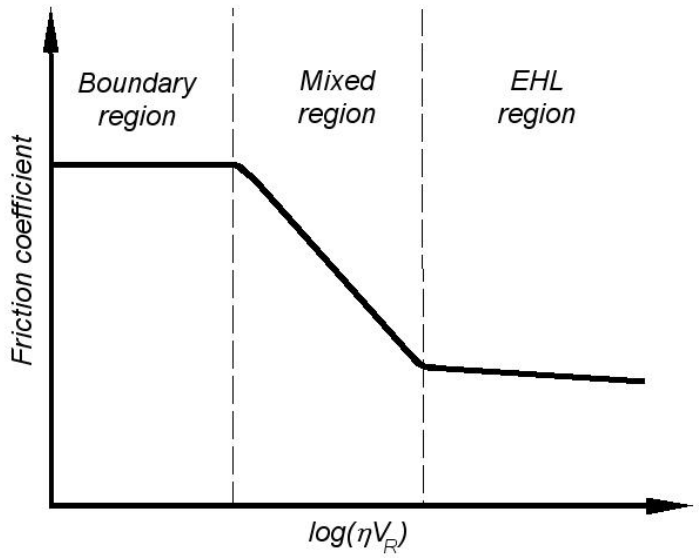

Fig. 5. Lubrication regimes described using the EHL-Stribeck curve for highly loaded contacts.

Traditionally a lubrication regime is defined by the ratio of the smooth surface oil film thickness to the composite surface roughness, $\Lambda = h/\sigma$, even though this parameter is known to have limitations in relation to thin film lubrication [13]. Determination of the lubrication regime at some level, however, is important. The thickness of the film is usually defined using the well-known Hamrock and Dowson film thickness formula, where the film thickness depends on velocities, lubricant, geometry, load and materials [7]. Especially in gear contacts at higher surface velocities, where sliding is present, the formula is multiplied by a thermal reduction factor φ_T [14]

When the gear contact condition changes greatly along the line of action, it leads to variations in the gear contact conditions. Typical gear failures including wear, scuffing, pitting, micro-pitting and tooth fracture take place at different positions along the tooth flank because the contact conditions are such as to cause certain types of failure at particular points. For example, pitting failure appears close to the pitch point where high pressure and negative sliding velocity are present. However, the scuffing failure appears close to the tooth tip, where the sliding velocity is maximum, which increases the temperature and decreases the protecting film thickness. All these failures, except tooth fracture, are influenced by the lubricant temperature [15]. High temperatures lead to low viscosity, which decreases the lubricant film thickness and usually increases the failure rate.

A wind turbine gearbox, as shown in Fig.6, is one example of modern gearbox technology. Today, the largest wind turbines have a nominal power of about 5 MW and a rotor diameter of more than 100 meter. The main design requirements for this kind of gearbox are low weight, high efficiency, extreme reliability and low vibration and noise levels. In a wind turbine, the speed of rotation of the high speed shaft can increase from 0 to 1800 rpm and power from 0 to two times nominal power in seconds. Under such operating conditions the gearbox should last for more than 20 years, which sets strict requirements for gears, bearings and the lubricant itself. This requires a high

level of understanding of what is happening in the lubricated contact and what can protect the surfaces from failure and decrease friction.

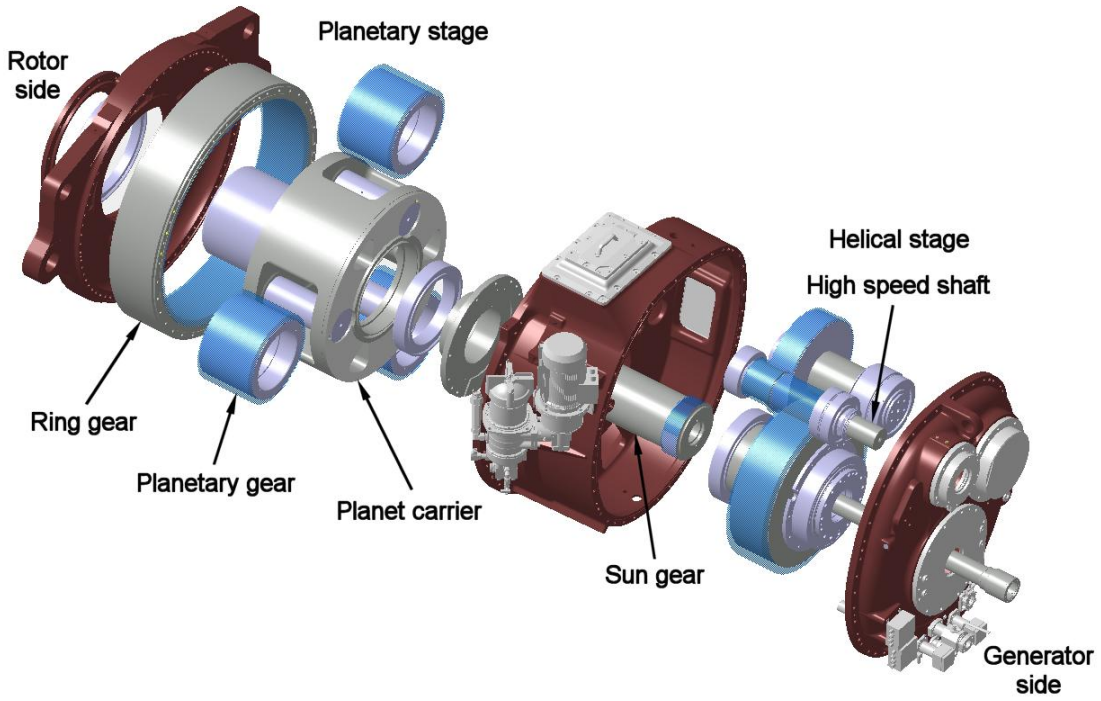

Fig. 6. Layout of a modern wind turbine gearbox (Published with permission of Moventas Wind Oy)

Today's standard gear calculations take account of tooth fracture, pitting durability and scuffing performance. Using modified geometry in gear tooth design, including tip relief and crowning, gear performance and dynamic behaviour can be greatly enhanced. In addition the lubrication may be improved by using chemical additives such as extreme pressure (EP) and antiwear (AW), which may improve the scuffing performance [15,16]. The standard calculation provides a safety factor against failure, but it gives no detailed information on what is really happening in the gear contact.

To gain a fuller understanding of the lubricated contact, to minimize friction, heat and reduce failure rates in modern gearboxes, it is important to analyze gear contact in more sophisticated ways. The main approaches may be:

- to develop a modern mixed lubrication model for rough surfaces and/or a gear-specific transient lubrication model [17-18]

- to develop or apply novel measurements techniques (sensors) in real gear contacts [19-22]
- to measure and/or analyze the lubrication conditions in simulated gear contacts with a series of steady-state contacts along the line of action with controlled elliptical contact [23-25]
- to determinate the high pressure properties of the lubricant [26-29]

1.3 Scope and objectives

The original objective of the thesis was to evaluate experimentally the lubrication condition in gear contacts, lubricant high pressure properties and their possible influence on pitting fatigue. During the work the objective of the thesis focused on increasing the understanding of lubrication conditions in gear contacts. This consists of a) the development of test devices and methods for determination of lubrication conditions and lubricant high pressure properties in gear contacts and b) evaluation of lubrication conditions in controlled elliptical contact and in real gear contact. This deeper knowledge will improve the basis and criteria for optimization of gear geometry, surface quality and for selection of lubricant properties to achieve gearboxes with low power losses, high load capacities and extended lifetimes.

1.4 Outline and contribution of the thesis

To achieve the goal of the thesis the gear contact was first simplified to a steady-state elliptical contact using a twin-disc test device. A high-pressure twin-disc test device was developed and Paper I deals with the development of this test device with elliptical contact. In Paper II, the measured signals and the test device are applied to study the friction behaviour and for verification of the test device. Special attention has been paid to creating conditions that correspond to the real industrial gear contact topography. In Paper III, lubricant high pressure properties were evaluated in a smooth elliptical contact under pure EHL conditions. A method to determine the limiting shear stress and the actual viscosity properties of lubricants was developed. In

Paper IV, the transversely ground elliptical contact was studied under mixed lubrication conditions. The gear contact was simulated along the line of action using a twin-disc test device focusing on friction, temperature and lubrication conditions. In Paper V, real gear contact lubrication conditions were observed and followed on-line using contact resistance and bulk temperature measurements, which were applied to a modified FZG gear test device.

The following original methods and devices have been developed during the course of this work:

a) Development of a high-pressure twin-disc test device with line-of-action simulation ability and transverse grinding of discs.
b) Development of a method for determination of lubricant high pressure properties based on a numerical traction model and a wide range of traction curves measured with the twin-disc device which had been developed
c) Application of contact resistance methods for detection of lubrication condition in simulated gear contacts and in real gear contacts
d) Measured lubrication conditions in the form of contact resistance, friction and temperature at a wide range of operating conditions in simulated and real gear contacts

2 High-pressure twin-disc test device

2.1 Base construction

The high-pressure twin-disc test device which has been developed is presented in Paper I and the follow-up Paper II, which includes presentation of measured signals and verification of the test device. The basic construction of the test device is shown in Fig. 7. Each disc is driven by a separate electric motor with adjustable rolling and sliding velocities. Loading and rotating speeds can be varied on-line with automated computer control, which allows flexible testing.

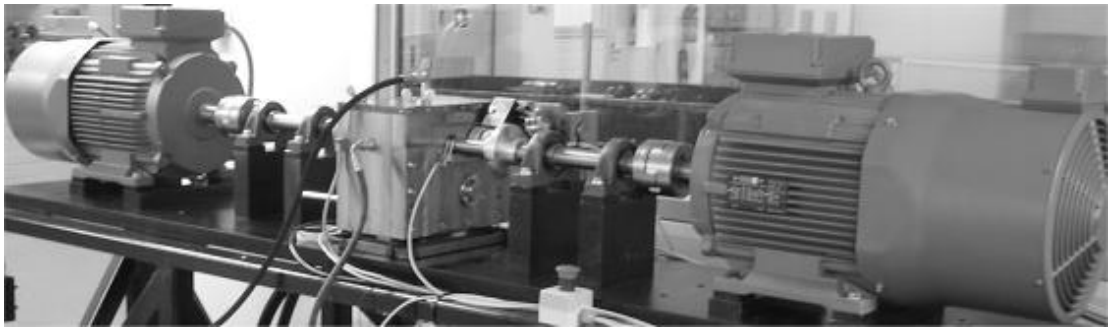

Fig. 7. The twin-disc test device that was developed

The electric motor can be driven at the maximum rotation speed of 6000 rpm, which provides a disc surface velocity of 22 m/s for the test disc radius used. The highest load is 11 kN, which gives a maximum Hertzian pressure close to 2.5 GPa in the disc contact. The oil inlet temperature and flow rate can be varied between 40 °C and 120 °C, and 0.5 l/min and 20 l/min, respectively. The lubrication of the test disc is performed with a circulating lubrication system.

2.2 Measured signals

Measured signals from the twin-disc test device include bulk disc temperature, mean contact resistance and friction moment in addition to load, shaft rotation speeds, oil inlet temperature and oil flow rate. The disc bulk temperature is

measured below the surface with a thermocouple as show in Fig. 8 and the signal is transmitted from the axle using a telemetry device. The mean contact resistance measurement was introduced into the test device to analyze the contact lubrication conditions. The friction moment measured from shaft 1 includes the bearing moments, but these can be excluded by calibration, which is described in Paper III. Signals are collected on a sampling card and are used both for on-line analysis and for subsequent processing.

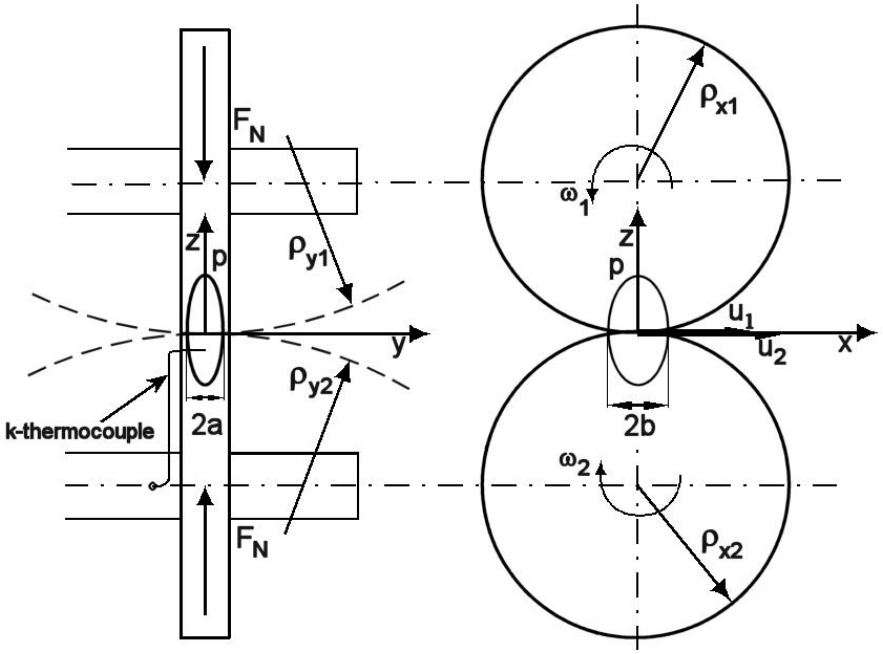

Fig. 8. Principles of a twin-disc test device.

2.3 Test discs and lubricants

The test disc material in all tests is case-hardening steel 20 NiCrMo2-2. The discs are case-hardened to a depth of 0.8 – 1 mm, with specific surface hardness of 60 – 62 HRC. The test discs have a diameter of 70 mm and a thickness of 10 mm. A special device for disc grinding was also developed and constructed, where grinding can be done perpendicular to the rolling direction to give a raised crown with a radius of 292 mm. This corresponds to the real gear flank surface topography, which is very seldom used in other twin-disc studies. The grinding is described in more detail in Paper I. In Paper

III polished surfaces was needed and after grinding the disc surfaces have been polished to a surface roughness Ra-value close to 0.05 µm.

All measurements have been made using either mineral base oil or synthetic PAO base oil or both. For this point on mineral base oil is denoted as MIN and synthetic polyalphaolefin base oil as PAO. Table 1 presents the basic viscosity properties, which manufacturers give for these lubricants. Paper III contains the viscosity and limiting shear strength properties of MIN and PAO oils as a function of temperature and pressure.

Table 1. Main viscometric properties of the lubricants tested.

Type	Min.	PAO
Kinematic viscosity, ν at 40 °C, mm^2/s	220	220
Kinematic viscosity, ν at 100 °C, mm^2/s	19	29.1
Density, ξ at 15 °C, kg/m^3	892	849
ISO viscosity grade, -	220	220

2.4 Results

Traditionally, the twin-disc test device slide-to-roll ratio is fixed and grinding of discs is done parallel to the rolling direction. In the twin-disc test device developed for this work loading, sliding and rolling as well as the lubricant inlet temperature can be varied independently and continuously. The grinding has been performed perpendicular to the rolling directions, which corresponds to the real gear surface. The mean contact resistance measurement indicates the contact lubrication conditions with support of bulk temperature and friction measurements. This provides an accurate and flexible test environment to study lubricant high-pressure properties and lubrication conditions by simulating the gear contact along the line of action as shown in Papers III and IV. The experience gained from the measuring arrangement in the twin-disc device has been transferred to the measuring arrangement in the FZG gear test device, which is used in Paper V.

3 An approach for determination of lubricant high pressure properties

The friction behaviour in gear contact is a complicated result of the interaction of many different parameters leading to different outcomes, depending on the operating conditions. One way to study gear contact behaviour is to measure the lubrication conditions and traction in simulated gear contact with a series of steady-state contacts along the line of action. In Paper III, lubricant high pressure properties were evaluated in smooth elliptical contact under pure EHL conditions. A method for determination of limiting shear stress and actual viscosity properties of lubricants was developed using a numerical traction model based on elliptical EHL contact and traction curves measured at a wide range of temperatures and pressures with a twin-disc test device. The tests were performed in pure fluid film conditions at high Hertzian pressures with fine polished surfaces. Each of the two lubricants was tested at 135 test points, where traction coefficients and bulk temperatures were measured. The lubricant parameters in the traction model were adjusted so that the calculated results match the experimental measurements for all the test points.

3.1 Description of the method

The upgraded numerical traction model is based on the model [30,31] developed earlier for calculation of sliding friction and power loss in spur gear contacts. In this model the line contact geometry was upgraded to correspond to the elliptical contact which is found in the twin-disc test device used in this study. Another major change was made for characterization of lubricant limiting shear stress properties at high pressures.

In this model Herzian pressure distribution and constant film thickness are assumed. It is well known that these profiles do not differ greatly from the real profiles and they usually provide a reasonable approximation for traction studies, at least under heavily loaded conditions. The constant film thickness

is calculated from the isothermal central film thickness formula [7] by taking into account a thermal reduction factor φ_T [14]. The non-Newtonian model proposed by Gecim and Winer [32] for fluid shear stress-strain rate relationship is assumed. The first term, i.e., the elastic strain component has been neglected in numerical studies. The strain rate across the film is assumed to be constant. The sliding traction force can be integrated from the lubricant shear stress over the contact zone, where the corresponding traction coefficient is determined. The dominant mode of heat generation is assumed to be frictional heating resulting from the lubricant sliding. It is assumed that half the heat is conducted to the surface on each side, the surface temperature can be calculated by flash temperature equations for fast moving surfaces [14,33]. The estimation of the contact traction requires estimation of an effective temperature of the lubricant within the film, which, in turn, can be used to estimate the lubricant shear stress and viscosity. The equation for lubricant thermal conductivity dependence on pressure is given in [34]. These calculations lead to an iterative solution, where the contact temperature field must be harmonized with the friction force, i.e., frictional heating, at every mesh point. The model is presented in more detail Paper III.

3.1.1 Viscosity

Lubricant viscosity is strongly dependent on pressure and temperature in the EHL contacts. This can be taken into account by using Roelands equation [35], which can be written as follows:

$$\eta(p,T_f)=\eta_0(T_f)\exp\left\{\left(\ln\left(\eta_0\left(T_f\right)\right)+9.67\right)\cdot\left[-1+\left(1+5.1\cdot10^{-9}\,p\right)^{Z\left(T_f\right)}\right]\right\} \quad (1)$$

where the $\eta_0(T_f)$ and $Z(T_f)$ can be defined as [34]:

$$\log(\log\eta_0+4.2)=-S_0\log(1+T_f/135)+\log G_0 \quad (2)$$

$$Z(T_f)=D_Z+C_Z\log(1+T_f/135) \quad (3)$$

The lubricant parameters S_0 and G_0, which describe viscosity dependence on temperature, were set according to the information from the manufacturers. Other parameters, C_Z and D_Z, were defined by iteration so that the calculated results correlated with experimental results. In non-linear traction regimes and at low pressures actual lubricant viscosity is the major determinant of the shape of the traction coefficient curve.

3.1.2 Limiting shear stress

When the traction coefficient is studied as a function of sliding velocity, three different (linear, non-linear and thermal) regimes can typically be found. The limiting shear stress has the major role in defining the traction coefficient in a non-linear traction regime. At the maximum point of the traction curve, the traction coefficient can be estimated as follows:

$$\mu = \frac{F_\mu}{F_N} = \frac{\bar{\tau}_L}{\bar{p}} \tag{4}$$

In equation (4), $\bar{\tau}_L$ is the mean value of the limiting shear stress and $\bar{p}$ is the mean Hertzian pressure. Equation (4) can be written as follows:

$$\bar{\tau}_L = \mu \cdot \bar{p} \tag{5}$$

The traction coefficient μ is calculated from the measured traction force F_μ and the normal load F_N. The measured traction data with an inlet temperature of 50 °C was used for creation of the master curve for limiting shear stress. Initially, the maximum traction coefficients were chosen from the measured traction curves at five Hertzian pressure levels. Using equation 5, the mean limiting shear stress can be calculated and the results are plotted (circles) against the mean Herzian pressure in Fig. 9. The traction points are then fitted into the quadratic master curve equation $\tau(p)$ and the equation constants a_1, a_2 and τ_0 are determined.

The limiting shear stress at an effective fluid temperature of T_f is obtained by multiplying the master curve by the temperature function $g(T_f)$, as shown in Fig. 9. In this function the constants a_3, a_4 and a_5 are unknown and these constants are defined by iterating the lubricant parameters of the traction model so that the calculated results correlated with experimental results in all test cases.

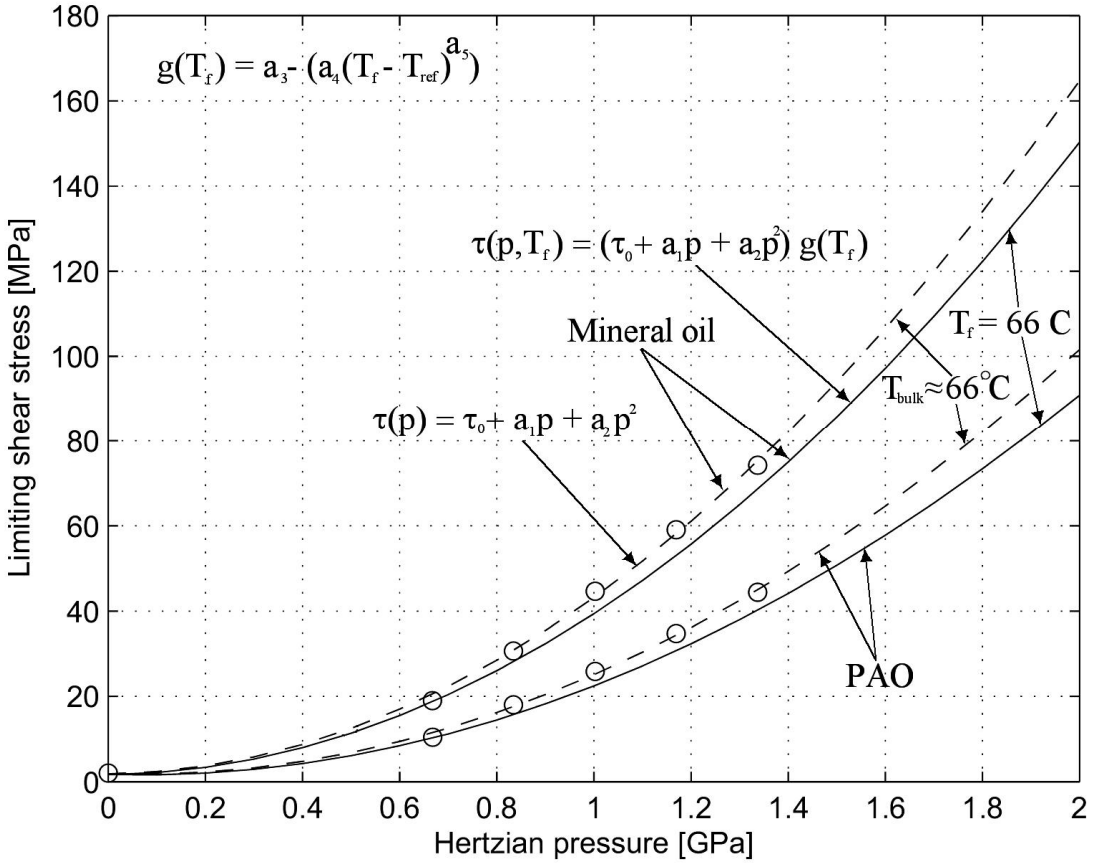

Fig. 9. Limiting shear stress curve-fitting for tested lubricants

3.2 Results

In general, the calculated results correlate well with the experimental results. Some experimental and calculated results are shown in Fig. 10. The shape of the traction curves is familiar to those from other works, where traction curves have been measured using twin-disc test devices [36-38].

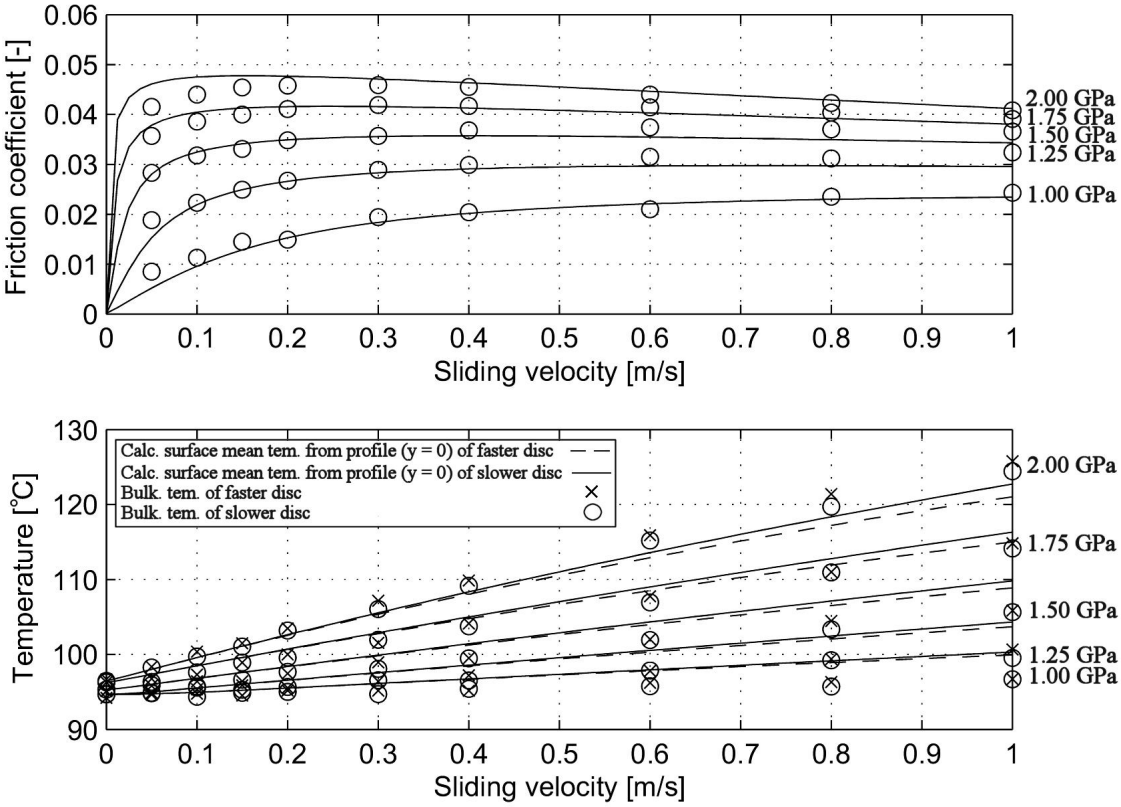

Fig. 10. Mineral oil traction coefficient and corresponding temperatures as a function of sliding velocity at maximum Hertzian pressure of 1.00, 1.25, 1.50, 1.75 and 2.00 GPa and an oil inlet temperature of 90 °C.

Fig. 11 shows the relative difference between traction model calculations and experimental traction results for all test points. The full test conditions for each case are shown in Paper III. The mean percentage difference for all PAO oil test points is 9 % and for mineral oil test points it is 4 %. The largest differences are mainly related to the lowest sliding velocities and lowest pressures, where the percentage difference is high due to the small traction values. Under these operating conditions, the actual viscosity dominates the traction coefficient values. However, there were no parameters such as C_Z and D_Z that would have made the difference substantially less than that between the experimental and traction model results. This may indicate that the model described is not flexible enough in this regime.

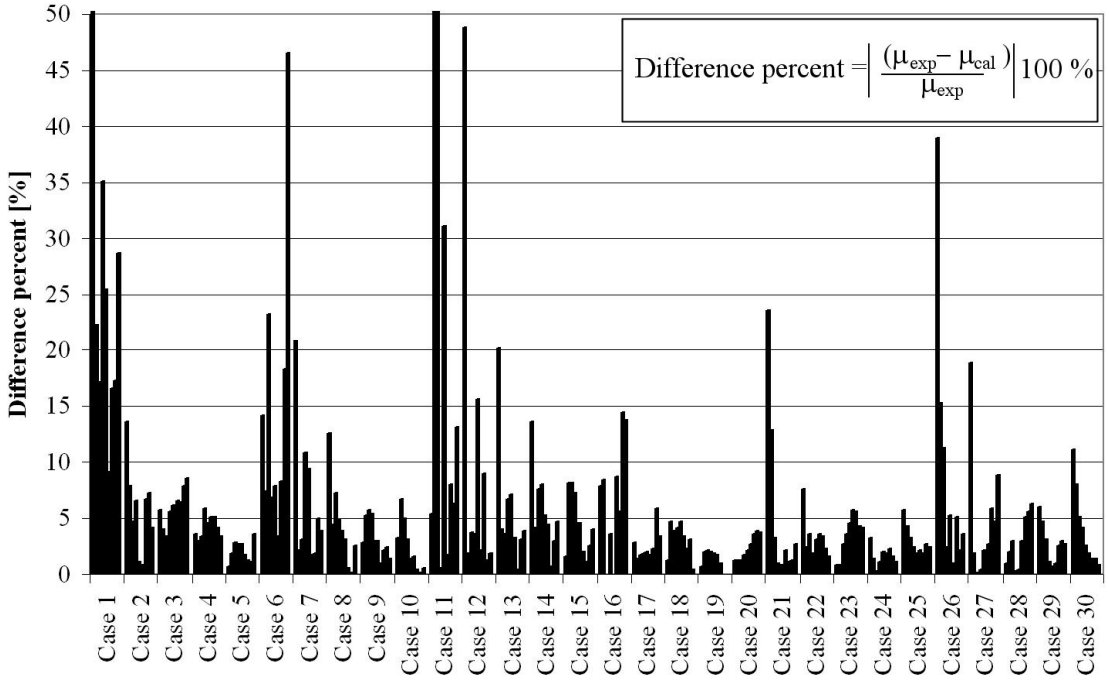

Fig. 11. Difference between the measured and the calculated traction coefficient results for all cases. Sliding velocities for each case, from left to right, are 0.05, 0.1, 0.15, 0.2, 0.3, 0.4, 0.6, 0.8 and 1.0 m/s. Cases 1-15 are results for PAO oil and cases 16-30 are results for mineral oil

Henceforth, the method developed can be utilized to estimate lubricant traction properties in pure EHL contact and to determine the input values for the numerical friction model.

4 Lubrication conditions in simulated gear contact

The transversally ground elliptical contact was studied under mixed lubrication conditions in Paper IV. Single spur gear geometry was simulated at 38 steady-state measuring points along the line of action using a twin-disc test device focusing on the friction coefficient and on temperature and lubrication conditions. Twin-disc simulations were adjusted to match real gear experiments by using similar maximum Hertzian pressure and surface velocities.

4.1 Results

Firstly, it was necessary to ascertain how well the trends in lubrication conditions in real gears match those in the twin-disc device along the line of action. This evaluation was done by calculating the isothermal and thermal Λ-values of real gears along the line of action and comparing these with the measured mean contact resistance, as shown in Fig. 12.

The shape of the curves of the thermal Λ-values and the measured mean contact resistance corresponds well, indicating that twin-disc measurements properly simulate the change of lubrication conditions in real gears. In disc contact the thermal Λ-values (0.5 … 2) are higher than in real gear contact due to lower surface roughness. At the lowest Λ-values measured mean contact resistance values no longer have a clear dependence on Λ-values and in the full EHL regime it will only indicate a possible disturbance of the film. Each test case condition is shown in detail in Paper IV.

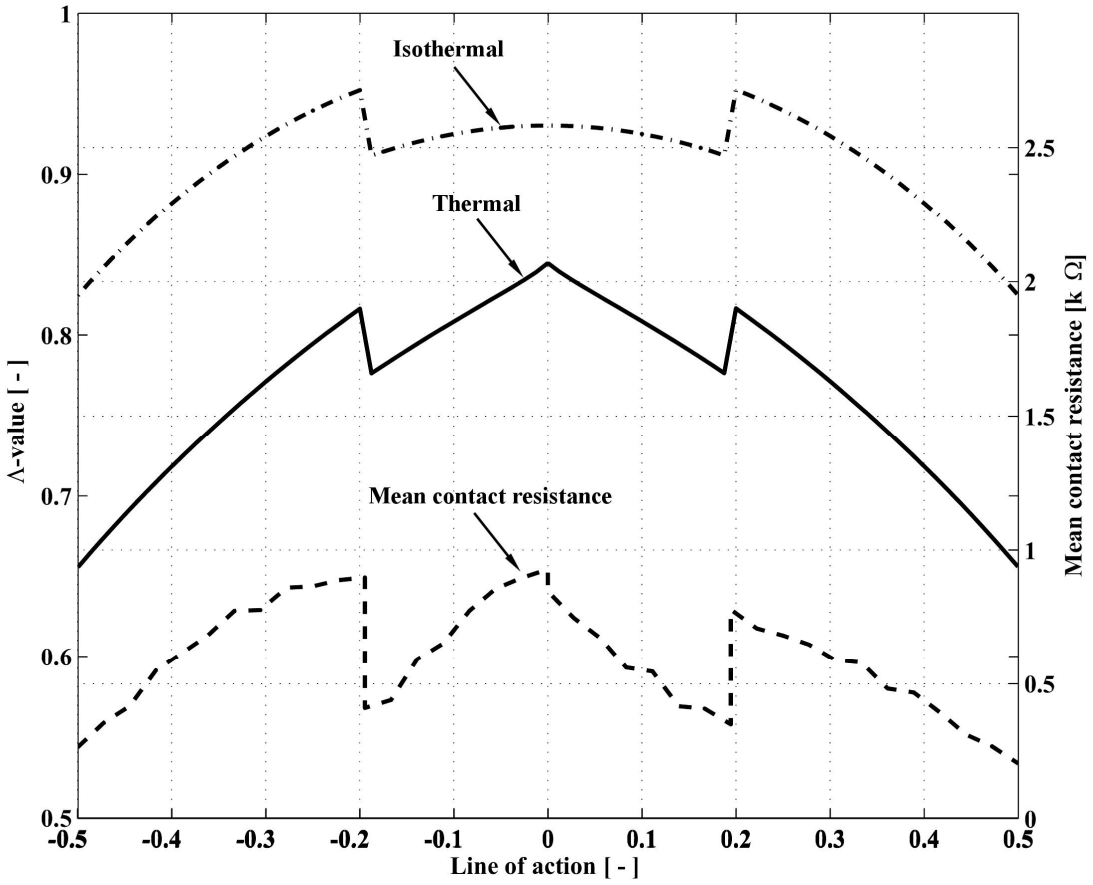

Fig. 12. The calculated isothermal (dash dot line) and thermal (solid line) Λ-values in gear line contact together with the measured mean contact resistance (dashed line).

The second essential issue is to study the behaviour of the mean friction coefficient along the line of action, which can also be measured in real gears. In the twin-disc case, the mean friction coefficient is a mean value of the friction based on 38 separate test points along the line of action. Fig. 13 presents the mean friction coefficients for mineral and PAO lubricants from real gears [39] and from corresponding twin-disc simulations, as a function of gear pitch line velocity.

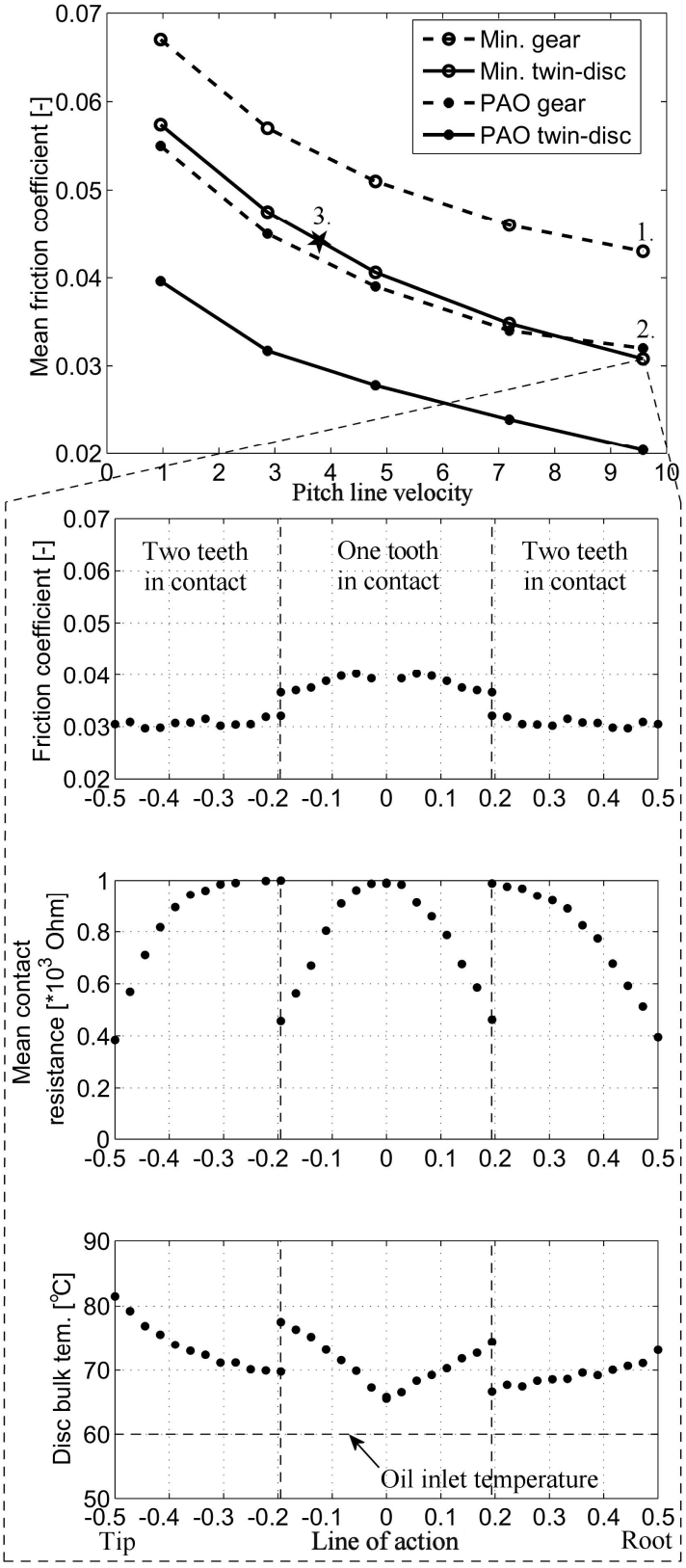

Fig. 13. The mean friction coefficient as a function of pitch line velocity from real gear tests and corresponding twin-disc tests together with the detailed view of simulated friction results.

Fig. 13 shows that the shape of the mean friction coefficient curves are similar for both lubricants, indicating that the twin-disc measurements properly simulate the friction behaviour trends in real gears. However, there are clear differences in absolute friction values. It was concluded that the main reason for the difference in absolute friction coefficient values is obviously caused by surface roughness differences in discs and gears. A previous study [40] also supports this conclusion.

The results in Fig. 14 summarize all friction simulations made at different rolling and sliding velocities with twin-discs.

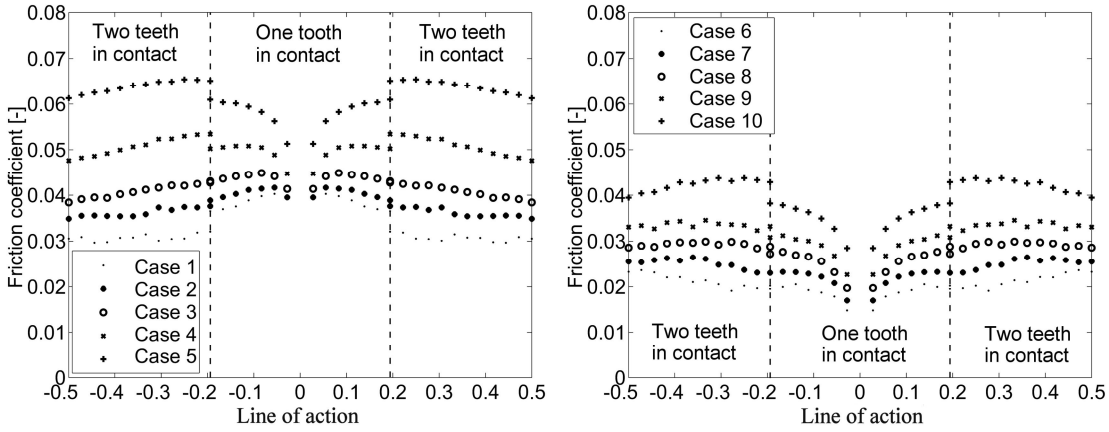

Fig. 14. The simulated friction coefficients along the line of action for mineral oil (left) and for PAO oil (right).

Fig. 14 shows that in all cases mineral base oil gives higher friction coefficients than PAO base oil. The measured results show that mineral base oil reaches the thermal friction region with a lower sliding velocity than with PAO. The step-type increase in the friction coefficient was observed at low rolling velocities when single tooth engagement changes to two tooth engagement, i.e., load decreases, but a reverse step occurs at high rolling velocities.

It can be concluded that the twin-disc simulations give more local information about the friction coefficients, lubrication conditions and temperature along the line of action than the real gear measurements. This has potential when the mechanisms and risks of gear failures such as pitting and scuffing are being evaluated. However, it should be noted that temperature build up, especially at the tip and at the root of the tooth flank, may include differences between simulated disc and real gear results. This detailed (local) information can be also utilized as reference data for testing of the mixed lubrication models. This kind of simulation would also be a very suitable classification for surface roughness, coatings, lubricants and additives.

5 Lubrication conditions in real gear contact

The real gear contact was studied at transient lubrication conditions, which was detected on-line using contact resistance and bulk temperature measurements that were applied to a modified FZG gear test device. Measurements were made in mixed lubrication conditions with polished gear surfaces; otherwise the operation conditions were similar to those in a typical industrial gear. The detailed description of the method and results are presented in Paper V.

5.1 Experimental

Gear tests were carried out using a modified FZG test device. The bulk temperature of the gear tooth was measured from one tooth at four different positions. This was done using k-thermocouples and a telemetry device. A contact resistance measuring device was incorporated into the test device to analyze relative changes in the oil film thickness. The total loss of torque from two gear pairs was obtained by using the torque meter. The test arrangement is presented in more detail in Paper V.

The material for the test gears is case-hardening steel 20 NiCrMo2-2. The gears are case-hardened to a depth of 0.8 – 1 mm, with specific surface hardness of 60 – 62 HRC. Test gears were case hardened, ground and polished, which gives the gear surfaces a mirror-like finish. The test lubricant was mineral base oil.

5.2 Results

The contact resistance and bulk temperature were measured as functions of pitch line velocity, load and oil inlet temperature in a mixed lubrication regime. The mean contact resistance and pitch line velocity are shown as a function of time in Fig. 15.

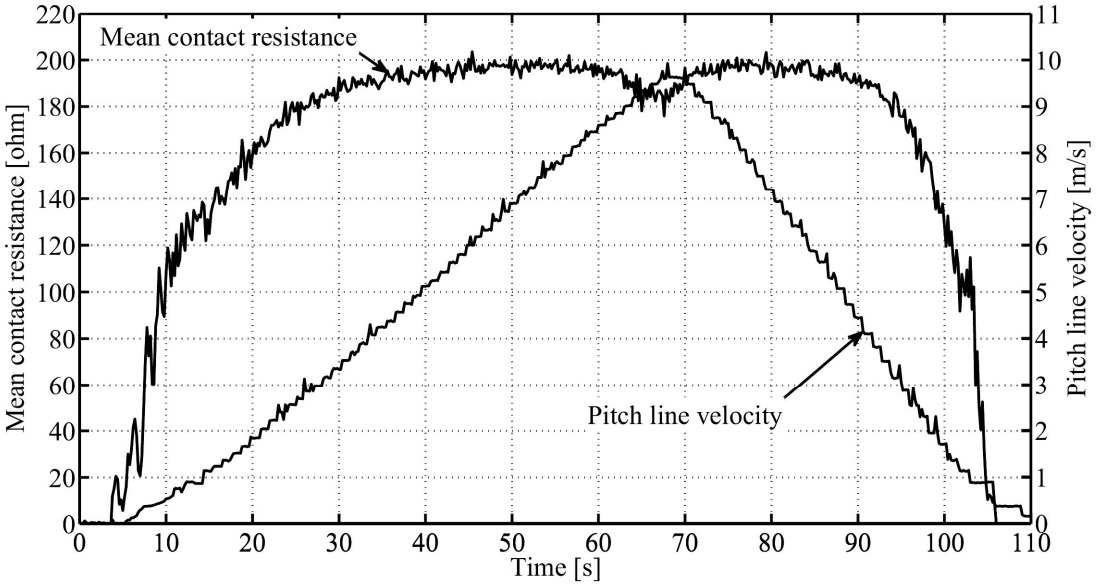

Fig. 15. The measured mean resistance and pitch line velocity as a function of time at an oil inlet temperature of 40 ºC and a torque of 135 Nm.

Fig. 15 shows that the measured mean contact resistance curve is fairly smooth with the mean value period used and that the signal is very sensitive to the change of pitch line velocity. The single mean contact resistance value is a mean value for a period of 0.2 s with a sampling period of 1 ms. This means that the mean value includes the data points in different positions along the line of action and thus takes into account transient effects. The measured contact resistance does not have a linear correlation with oil film thickness, at least when it approaches the maximum or minimum values. The test device used has two gear pairs and each gear pair with one and two tooth pairs in contact, which makes it impossible to evaluate a single tooth contact. In the 1950s Lane and Hughes [41] also studied the oil film formation in one gear pair using electrical resistance measurements. They found out that it was possible to identify resistance change along the line of action. However, their study does not include, for example, the gear geometry data (and surface velocities), which prevented a fuller evaluation of their results.

In Fig. 16 the behaviour of mean contact resistance is shown at three different oil inlet temperatures 40, 60 and 80˚C, together with the calculated thermal film thickness trends at the pitch point. In this study, the measured bulk temperature related film thickness was also included because it takes account

of the temperature behaviour when the real gear operating conditions, such as pitch line velocity, are varied. Bulk temperature measurements give the actual temperature for gear contact and support the estimates of actual film thickness and lubrication conditions. The bulk temperature is closely linked to scuffing failure.

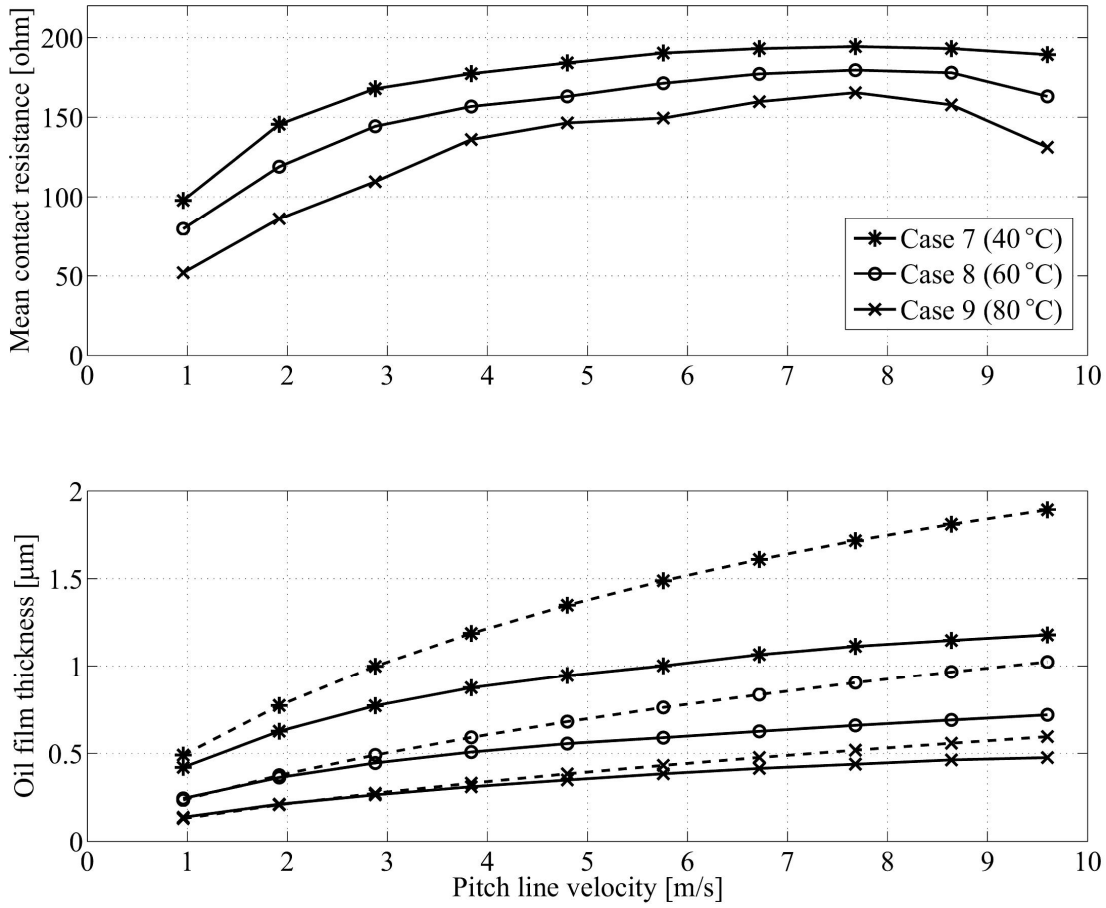

Fig. 16. The measured mean contact resistance, the calculated bulk temperature related (solid line) and thermal (dashed line) central film thicknesses at pitch point.

Fig. 16 shows that the trend of the curves of the measured mean contact resistance and the calculated film thicknesses match well, indicating that the mean contact resistance measurement reflects the changes in oil film thickness under real gear operating conditions. The mean contact resistance begins to drop at higher pitch line velocities, especially with an oil inlet temperature of 80 ºC. This might be due to the dynamics of the gear contact, the fact that the oil film has to build up with every new engagement and/or

that the increase in oil film temperature with increasing velocity has the potential to reduce the oil film thickness despite the increase in entrainment velocity. These reasons are related to non-steady-state lubrication conditions and cannot be derived with the film thickness calculations used.

In the future, the mean contact resistance measurement should be evaluated with ground gear surfaces. Further study is also needed to adapt the measurement system to different lubrication and operating conditions. These actions should show whether this method can contribute to or offer an alternative method for diagnosing faults in gearboxes. Bulk temperature measurement may have potential, when the gearbox conditions are analyzed on-line.

6 Conclusions

The objective of the thesis is to increase the understanding of lubrication conditions in gear contacts. This consists of the development of test devices and methods for determination of lubrication conditions and lubricant high pressure properties in gear contacts with, in addition, the evaluation of lubrication conditions in controlled elliptical contact and in real gear contact.

In the high-pressure twin-disc test device developed here the loading, sliding and rolling as well as the lubricant inlet temperature can be varied separately and continuously and the grinding has been carried out perpendicular to the rolling directions, which corresponds to the real gear surface. The mean contact resistance measurement indicates the contact lubrication conditions with support from bulk temperature and friction measurements. This provides an accurate and flexible test environment to study lubricant high-pressure properties and lubrication condition by simulating real gear conditions along the line of action.

A method for determination of limiting shear stress and actual viscosity properties of lubricants was developed using a numerical traction model based on elliptical EHL contact and traction curves measured at a wide range of temperatures and pressures with a twin-disc test device. The viscosity and limiting shear stress values used in the traction model were adjusted by iteration so that the calculated results correlated with experimental values under the same conditions. In general, the calculated values correlate well to the experimental results. These specified properties can be utilized to estimate lubricant traction properties in pure EHL contact and to determine the input values for the numerical friction model from now on.

The transversely ground elliptical contact was studied under mixed lubrication conditions using a twin-disc test device, focusing on the friction coefficient and temperature and lubrication conditions. The simulations were adjusted to match real gear experiments by using similar maximum Hertzian pressure and

surface velocities, along the line of action. The calculated thermal Λ-values of real gears and the measured mean contact resistance correspond well. The results indicated also that the twin-disc measurements accurately simulate the friction behaviour trends in real gears. This kind of simulation gives more local information about the friction coefficients, lubrication conditions and temperature along at the line of action than the real gear measurements. It has potential in the evaluation of gear failures and in the classification of surface roughness, coatings, lubricants and additives. It can be also utilized as reference data for testing of the mixed lubrication models.

The contact resistance and bulk temperature measurements were applied to a modified FZG gear test device to detect on-line lubrication conditions in real transient gear contact under mixed lubrication conditions. The mean contact resistance presented includes data points in different positions along the line of action and thus also allows for transient effects. The trend in the curves of the measured mean contact resistance and the calculated steady-state based film thicknesses correspond well with different operating parameters such as load, pitch line velocity and oil inlet temperature. Some deviations were observed, which were explained by taking into account non-steady-state lubrication conditions. Bulk temperature measurements give the actual temperature for gear contact and support the estimates of actual film thickness and lubrication conditions.

References

1. **Jost, P.** *Lubrication (Tribology) education and research*. UK Department of education and science, HMSO, 1966.
2. **Dowson, D.** *History of tribology*. 1979, p. 677 (Longman Group Limited, London)
3. **Dragon, R.J.** *Fundamentals of gear design*. 1988, p. 560 (Butterworths, cop., Boston).
4. **Olver, A.V.** Gear lubrication – a review. *Proc. IMechE, Part J: J. Engineering Tribology*, 2005, **216**(5), 255-267.
5. **Dowson, D., Higginson, G.R., Archard, J.F.** and **Crook, A.W.** *Elasto-hydrodynamic lubrication, the fundamentals of roller and gear lubrication*. 1966, p. 235 (Pergamon press, Oxford).
6. **Dowson, D.** Elastohydrodynamic and micro-elastohydrodynamic lubrication. *Wear*, 1995, **190**(2), 125-138
7. **Hamrock, B.** *Fundamentals of fluid film lubrication*, 1994, p. 690 (McGraw-Hill, Inc., New York)
8. **Paul, G.R.** and **Cameron, A.** The ultimate shear stress of fluids at high pressures measured by a modified impact microviscometer. *Proc. R. Soc., Ser. A*, 1979, **365**(1720), 31-41.
9. **Johanson, K.L.** and **Tevaarwerk, J.L.** Shear Behaviour of Elastohydrodynamic Oil Films. *Proc. R. Soc., Ser. A*, 1977, **356**(1685), 215-236.
10. **Dudley, D.W.** The *Evolution of the gear art*. 1969, p. 93 (American Gear manufacturers Association, Washington, D.C.)
11. **Barzt, W.J.** *Lubrication of gearing*. 1993, p. 510 (Mechanical Engineering Publications Limited, London).
12. **Spikes, H.A.** Mixed lubrication – an overview. 1997, *Lub. Sci.* **9**(3), 221-253.
13. **Cann, P., Ioannides, E., Jacobson, B.** and **Lubrecht, A.A.** The lambda ratio – a critical re-examination. *Wear*, 1994, **175**(1-2), 177-188.
14. **Wu, S.** and **Cheng, H.S.** A friction model of partial-EHL contacts and its application to power loss in spur gear. *Trib. Trans.*, 1991, **34**(3), 398-407.

15. **Höhn, B.-R.** and **Michaelis, K.** Influence of oil temperature on gear failures. *Trib. Int.,* 2004, **37**(2), 103-109.
16. **Snidle, R.W.** and **Evans H.P.** Some aspects of gear tribology. *Proc. IMechE, Part C: J. Mechanical Engineering Science*, 2009, **223**(1), 103-141.
17. **Evans, H.P., Snidle, R.W.** and **Sharif, K.J.** Deterministic mixed lubrication modeling using roughness measurements in gear applications. *Trib. Int.,* 2009, **42**(10), 1406-1417.
18. **Larsson, R.** Transient non-Newtonian elastohydrodynamic lubrication analysis of an involute spur gear. *Wear*, 1997, **207**(1–2), 67–73.
19. **Höhn, B.-R., Michaelis, K.** and **Kopatsch, F.** Determination of film thickness, pressure and temperature in elastohydrodynamic lubrication in the past 20 years in Germany. *Proc. IMechE, Part J: J. Engineering Tribology*, 2001, **215**(3), 235-242.
20. **Jia, Y.** and **Araya, G.** Dynamic performance of a thin film temperature sensor in a lubricated contact. *Proc. IMechE, Part J: J. Engineering Tribology*, 2008, **220**(6), 487-497.
21. **Deng, G., Kato, M., Maruyama, N., Morikawa, K.** and **Hitomi, N.** Initial temperature evaluation for flash temperature index of gear tooth. *Trans. ASME J. Tribol.*, 1995, **117**(3), 476-481.
22. **Kleemola, J.** and **Lehtovaara, A.** Evaluation of lubrication conditions in gear contacts using contact resistance and bulk temperature measurements. Proc. IMechE, Part J: J. Engineering Tribology, 2010, 224(4), 367-375.
23. **Patching, M.J., Evans, H.P.** and **Snidle, R.W.** Micro-EHL analysis of ground and superfinished steel discs used to simulate gear tooth contacts. *Trib. Trans.* 1996, **39**(3), 595-602.
24. **Alanou, M.P., Evans, H.P.** and **Snidle, R.W.** Effect of different surface treatments and coatings on the scuffing. *Trib. Int.,* 2004, **37**(2), 93-102
25. **Kleemola, J.** and **Lehtovaara, A.** Experimental simulation of gear contact along the line of action. *Trib. Int.,* 2008, **42**(10), 1453-1459.
26. **Johnson, K.L.** and **Cameron, R.** Shear behaviour of ehd oil film at high rolling contact pressure. *Proc. IMechE, Part I*, 1967, 182, 307-319.

27. **Johanson, K.L.** and **Tevaarwerk, J.L.** Shear Behaviour of Elastohydrodynamic Oil Films. *Proc. R. Soc., Ser. A,* 1977, **356**, 215-236.
28. **Fang N., Chang L., Johnston G.J., Webster M.N.** and **Jackson A.** An experimental/theoretical approach to modeling the viscous behavior of liquid lubricants under EHL conditions. *Tribology Research: From model experiment to industrial problem, Dalmaz G. et al., (editors),* Elsevier Science B.V., 2001, 769-778.
29. **Kleemola, J.** and **Lehtovaara, A.** An approach for determination of lubricant properties at elliptical elastohydrodynamic contacts using a twin-disc test device and a numerical traction model. *Proc. IMechE, Part J: J. Engineering Tribology*, 2008, **222**(7), 797-806.
30. **Lehtovaara, A.** Calculation of Sliding Power Loss in Spur Gear Contacts. *Tribotest*, 2002, **9**(1), 23-34.
31. **Hedlund, J.** and **Lehtovaara, A.** Influence of Lubricant on Sliding Friction in Spur Gear Contacts. Proc. of 10th Nordic Symposium on Tribology, 2002.
32. **Gecim, B.** and **Winer, W.O.** Lubricant limiting shear stress effect on ehd film thickness. *J. Lubr. Tech.*, 1980, **102**(2), 213-221.
33. **Jaeger, J.C.** Moving sources of heat and the temperature at sliding contacts. *Proc. R. Soc.*, 1942, 203-224.
34. **Larsson, R., Larsson, P.O., Eriksson, E., Sjöberg, M.** and **Höglund, E.** Lubricant properties for input to hydrodynamic and elastohydrodynamic lubrication analyses. *Proc. IMechE, Part J: J. Engineering Tribology*, 2000, **214**(1), 17-27.
35. **Roelands, C.J.A.** *Correlation aspects of the viscosity-temperature-pressure relationship of lubricating oils*. 1966 (Druk. V.R.B., Groningen, The Netherlands).
36. **Johanson, K.L.** and **Tevaarwerk, J.L.** Shear Behaviour of Elastohydrodynamic Oil Films. *Proc. R. Soc., Ser. A*, 1977, **356**, 215-236.
37. **Wu, S.** and **Cheng, H.S.** Empirical determination of effective lubricant rheological parameters. *Trib. Trans.*, 1994, **37**(1), 138-146.

38. **Jacobson B.O.** High-pressure chamber measurements. *Proc. IMechE, Part J: J. Engineering Tribology*, 2006, **220**(3), 199-206.

39. **Järviö, O**. and **Lehtovaara, A.** Experimental study of influence of lubricants on friction in spur gear contacts. *Finn. J. Tribol.,* 2002, **21**(1), 20-27.

40. **Johnson, K.L.** and **Spence, D.I.** Determination of gear tooth friction by disc machine. *Tribol. Int.*, 1991, **24**(5), 269-275.

41. **Lane T.B.** and **Hughes, J.R.** A study of the oil film formation in gears by electrical resistance measurements. *Brit. J. Appl. Phys.* 1952, **3**, 315-318.

Paper I

Kleemola, J. and Lehtovaara A.

Development of a high pressure twin disc test device for the simulation of gear contact

Finnish Journal of Tribology, 2006, **25**(2), 8-17.

DEVELOPMENT OF A HIGH PRESSURE TWIN DISC TEST DEVICE FOR THE SIMULATION OF GEAR CONTACT

JAAKKO KLEEMOLA and ARTO LEHTOVAARA
Tampere University of Technology, Machine Design
Box 589, FIN-33101 Tampere, Finland
Email: jaakko.kleemola@tut.fi, arto.lehtovaara@tut.fi

ABSTRACT

Gear contact behavior has been a subject of study for many decades, but it is still a challenging engineering problem. Instant gear contact can be simulated with contacting discs, which provides steady operating conditions and eliminates most of the dynamics and manufacturing tolerances involved in real gears, resulting in an accurately controlled contact condition. A high-pressure twin disc test device was developed, where loading, rolling and sliding velocity together with lubricant inlet temperature can be varied continuously. A special device for disc grinding was also developed, where grinding can be done transversally to the disc rolling direction with proper crowning corresponding to the real gear flank properties. The study includes the preliminary friction results and some aspects of gear related lubrication.

Keywords: gear, twin disc, lubrication mechanism, elastohydrodynamic lubrication, friction

INTRODUCTION

Gear contact behavior has been a subject of study for many decades, but it is still a challenging engineering problem. In power transmissions there are continuous requirements to apply higher Hertzian pressures and speeds but, at same time, gears should be more effective and compact. Therefore, a lot of research is going on for the modeling and experimental analysis of gear contact, including geometry, surface finishing, materials and coatings.

Many different types of gear test devices have been developed to study gear contact. In the gear contact load, surface velocities and radiuses are changing continuously along the line of action and instantaneous contact points are difficult to analyze in detail with real gears. Instant gear contact can be simulated with contacting discs, which are shown in Fig. 1. Contacting disc arrangements, which form the basis of the twin disc test device, provide steady state operating conditions and eliminate most of the dynamics and manufacturing tolerances involved in real gears, resulting in an accurately controlled contact condition.

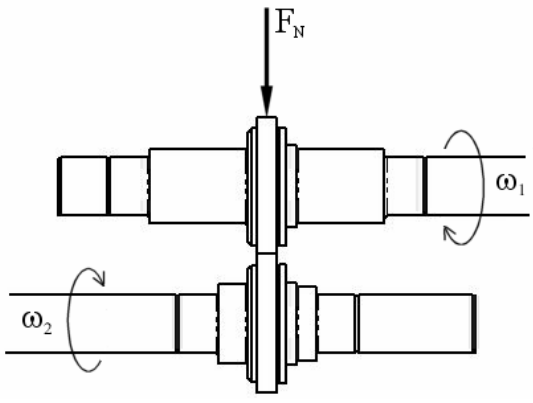

Figure 1. Basic idea of twin disc device.

This work is focused on the development of a high-pressure twin disc test device. The work also includes the preliminary results and some aspects of gear related lubrication.

GEAR LUBRICATION MECHANISM

Gear profile

Spur gear profiles are commonly approximated to be cylinders with equivalent radius of curvature as gear teeth at instant contact point, as shown in Figure 2.

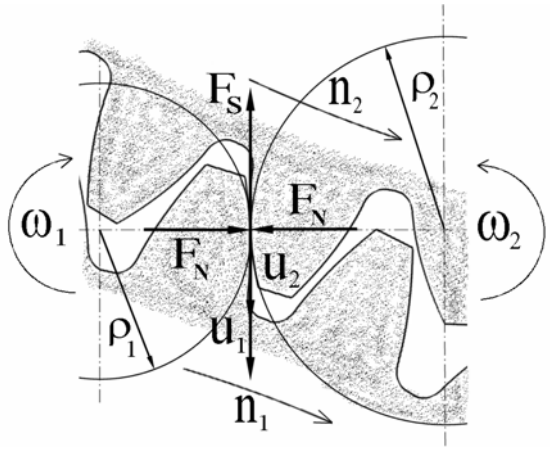

Figure 2. Instant gear teeth contact and its approximation with equivalent cylinders.

The velocities of the teeth contacting surfaces (u_1, u_2) act in same direction, but they are equal only at the pitch point. This is why sliding velocity ($V_S = u_1 - u_2$) is zero at the pitch point, but its absolute value increases towards the start and end points of the line of action. Rolling velocity ($V_R = ½(u_1 + u_2)$), reduced radius of curvature ($1/\rho = 1/\rho_1 + 1/\rho_2$) and load F_N change also during meshing. This leads to a slide-to-roll ratio ($SR = V_S / V_R$) of zero at the pitch point, whereas its absolute value increases towards the start and end points of the line of action.

In principle, any instant point on the line of action of any spur gear pair can be simulated under steady state conditions by properly chosen disc angular velocities (ω_1, ω_2) and diameters (ρ_1 , ρ_2). In practice, however, disc diameters are fixed in the test devices, which limits the operation conditions. This actually means that in the given gear pair only one operation contact point can be simulated exactly by using the fixed diameter twin disc device.

Lubrication regimes

Heavily loaded gears typically operate in boundary, mixed or elastohydrodynamic regimes depending on operating conditions (speed, viscosity, etc.), material and surface properties. In particular, mixed and boundary lubrications together with micro-elastohydrodynamics are challenging, ongoing, research topics. A comprehensive mixed lubrication overview is presented in ref. [1].

The lubrication regimes and friction are typically described by using the Stribeck curve for highly loaded contacts [1], as shown in Figure 3. The boundary lubrication regime can be related to low velocity (or low ηV_R – value). In this regime, friction coefficient is typically rather high, because shear stress mainly comes from asperity contacts, which carries the load. The mixed lubrication regime is reached by increasing the velocity, which decreases the friction coefficient. With further increase of velocity, the elastohydrodynamic lubrication regime is reached, where the hydrodynamic pressure generated in fluid film carries the load with no asperity contacts. In this regime, friction coefficient stays rather constant.

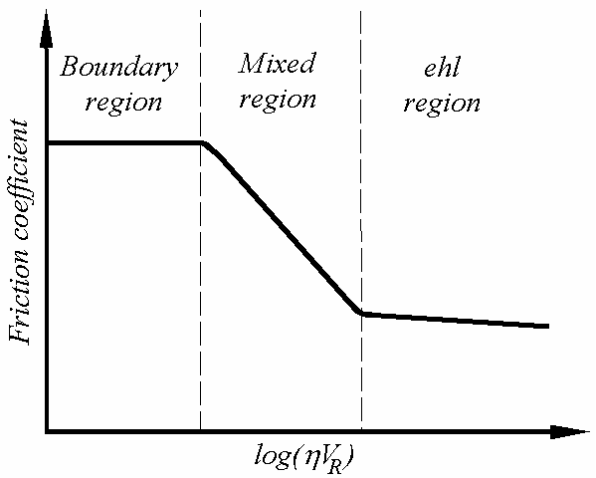

Figure 3. Lubrication regimes and friction.

As a first estimation, the lubrication regime may be characterized with film parameter $\Lambda = h_c/\sigma$, even if this parameter is known to have limitations in connection with thin film lubrication [2]. Determination of the lubrication regime at some level, however, is important, because the tendencies of certain contact parameters can be contradictory in different lubrication regimes. Film parameter Λ is defined as:

$$\Lambda = \frac{h_c}{\left(R_{q,1}^2 + R_{q,2}^2\right)^{1/2}} \qquad (1)$$

where h_c is central film thickness (eq. 2) and $R_{q,1,2}$ are surface roughness rms values.

Film thickness

The well-known Hamrock and Dowson film thickness formula depends on velocities, lubricant, geometry, load and materials. The isothermal central film thickness in elliptical contact can be determined with equation 2 [3], which is corrected by thermal reduction factor φ_T [4].

$$h_c = \varphi_T \cdot 2.69U^{0.67}G^{0.53}W^{-0.067}R \cdot (1 - 0.61e^{-0.73k}) \qquad (2)$$

Film thickness is created in contact inlet. Flow of lubricant in inlet and the forming of film thickness is presented in ref. [5].

Lubricant properties

Lubricant viscosity is strongly dependent on pressure and temperature in ehl conjunction. In high pressure contact the lubricant may no longer behave like a Newtonian fluid, especially if sliding is present. Different kind of rheological fluid models have been developed to describe the fluid behaviour [3]. The non-Newtonian model proposed by Gecim&Winer [6] for fluid shear stress – strain rate relationship is written as follows:

$$\dot{\gamma} = \frac{1}{G_\infty}\frac{d\tau}{dt} + \frac{\tau_L}{\eta}\tanh^{-1}\left(\frac{\tau}{\tau_L}\right) \qquad (3)$$

The first term, i.e. elastic strain component in Eq. (3), may be neglected in gear related cases and the strain rate across the film can be assumed to be constant, i.e. $\dot{\gamma} = |u_1 - u_2|/h_c$. τ_L represents the limiting shear stress that a lubricant can sustain. It depends on pressure and temperature. Figure 4 shows lubrication shear strain in an ehl contact.

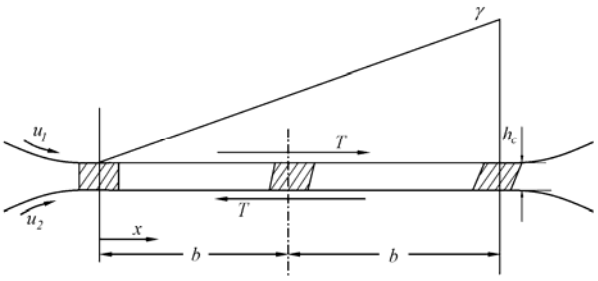

Figure 4. Shear strain γ in an elastohydrodynamic film.

The selection of lubricants in industry is traditionally based on lubricant viscosity, but its high-pressure rheological properties also have a major effect on gear contact.

Friction and traction

Friction or traction in an ehl contact can be defined as a force generated in the contact that resists relative motion of the contacting surfaces. Traction is mainly determined by what happens in the high pressure region: therefore, lubricant properties must be known at the high pressure (and temperature) that prevails there [7]. Traction is directly related to gear contact power loss and temperature rise. Johnson and Tevaarwerk analyzed traction in the 1970s using a twin disc test device and they were convinced of fluid non-Newtonian properties, when pressure or slide-to-roll ratio increases [8]. Figure 5 shows a principle of traction behaviour in an ehl contact.

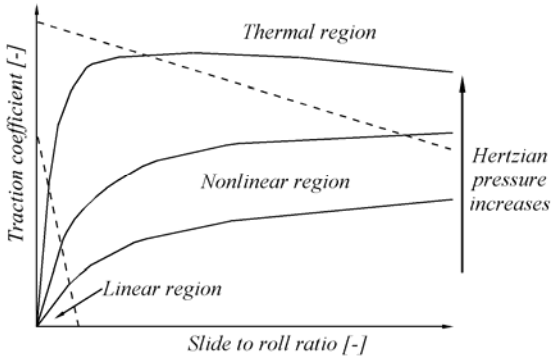

Figure 5. Principle of traction behaviour in an ehl contact.

The overall behavior of friction curves is characterized by three different regions - linear, non-linear and thermal region. The linear region appears on a very small slide-to-roll ratio while the lubricant retains Newtonian behavior. When the slide-to-roll ratio increases, a shift occurs to a region, where the lubricant begins to behave in a non-Newtonian way. The friction coefficient is dominated by lubricant limiting shear stress and friction may reach its maximum point. When the slide-to-roll ratio increases further, a thermal region is reached, where the increasing shearing of the lubricant raises lubricant temperature and the friction may start to fall slowly. In the mixed lubrication regime, asperity friction may contribute to the overall friction behavior.

Friction in gear contact

Friction is directly related to gear contact power loss and temperature rise, which are critical parameters in gear behavior. Gears are often operated in mixed or boundary lubrication regimes.

In the mixed lubrication regime, the total sliding friction force F_s basically consists of two components, the shear stress of lubricant and the shear stress of asperity contact, as follows [4], [9]:

$$F_s = \int_{-b}^{b} \left[\tau(x) + f_a p_a \left(1 - \frac{x^2}{b^2} \right)^{1/2} \right] B dx \quad (4)$$

At the instant gear contact point, the approximation of the friction force is an iterative process and needs calculation of the central film thickness, pressure distribution and the distribution of the average surface temperature and mid-film temperature in a given geometry. Material properties, lubricant properties and operating conditions are also needed. Numerical studies of friction and the power loss in gear contact are presented in references [9] and [10].

Experimental studies with modified FZG test rig show (Figure 6) that base PAO oil has about 20 – 30 % lower mean friction coefficient than base mineral oil [11]. Lubricant viscosities are in both cases ISO VG 220.

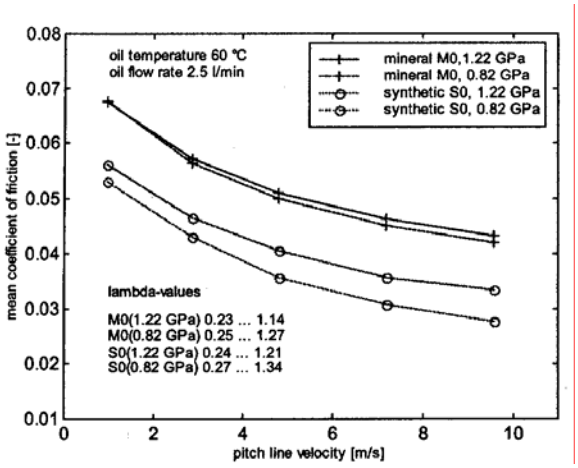

Figure 6. Mean coefficient of friction in gear mesh with base lubricants M0 and S0 [11].

The results also show the decreasing trend of friction coefficient as the pitch line velocity increases. Similar kinds of results have been obtained with numerical studies [10].

EXPERIMENTAL

The developed high-pressure twin disc test device is shown in Fig. 7. The test device consists of two parallel shaft lines with a central distance of 70 mm and a loading frame, where the tests discs are located. Loading and rotating speeds can be varied on-line with automated computer control, which allows flexible testing.

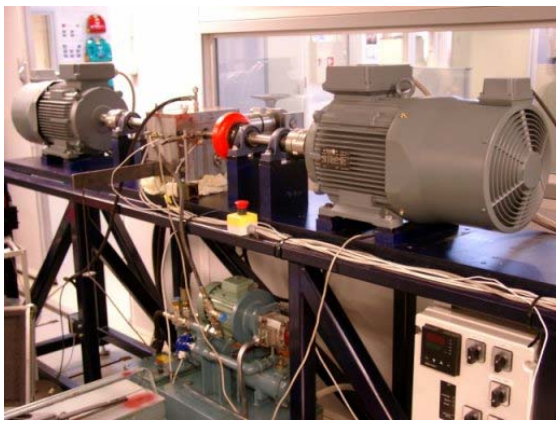

Figure 7. The developed high-pressure twin disc test device.

A closed structural force loop will act on the loading frame and the load cylinder will not exert forces in the other parts of the test device, as shown in Figure 8.

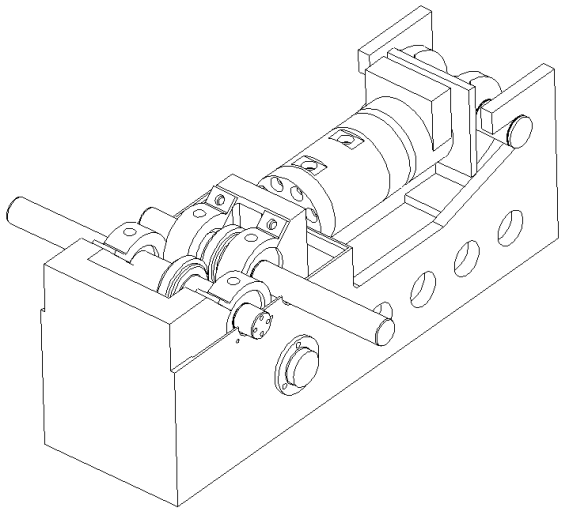

Figure 8. Loading frame.

This makes it possible to determine the friction coefficient below the loading frame, as described later.

Speed control

Each disc is driven by a separate electric motor with adjustable rotating speed resulting in a continuous change of slide-to-roll ratio in disc contact. Feedback signals from tachometers situated in shaft lines perform the rotational speed control of the motors. This enables an accurate control of slide-to-roll ratio. Rotating speeds can be varied on-line, which allows the testing procedure with various speeds.

Loading system

The discs are loaded with a hydraulic cylinder, which is controlled by a high response regelvalve together with a control unit, as shown in Figure 9.

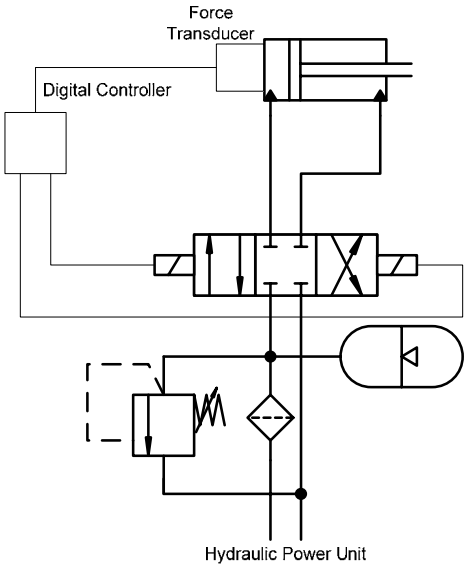

Figure 9. Hydraulic loading unit.

A force sensor behind the load cylinder allows force feedback control. The load is computer controlled and can follow a certain program so that, for example cumulative fatigue tests with various loads can be performed automatically.

Lubrication system

The test discs are lubricated in a circulating lubrication system, the layout of which is shown in Figure 10.

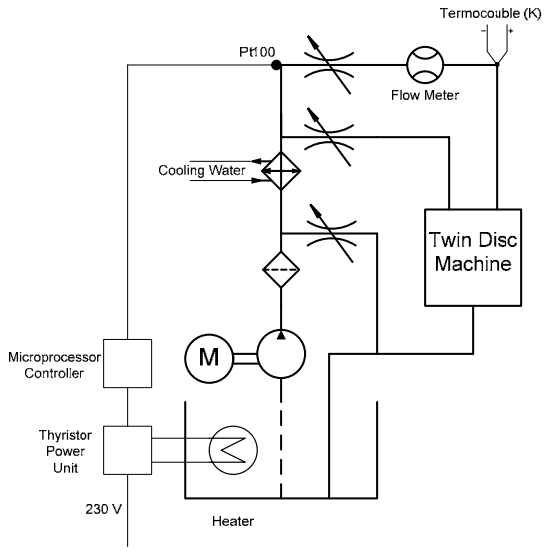

Figure 10. Schematic layout of lubricating unit and temperature control.

The lubricant in the tank can be heated with the heater, which is controlled with a thyristor power unit and a microprocessor controller. The system has a feedback temperature control. The lubricant can be cooled with a heat exchanger, which has been connected to a closed water system. The circulating lubricant is filtered and two different lines are directed to the test device. The first line lubricates the bearings and the second line the discs. Lubricant flow rate to the discs is measured. The temperature of the lubricant is measured just before the discs contact with the thermocouple.

Operation conditions and signals

The measured signals are collected to a sampling card to be analyzed later in detail. The measured data is also used for on-line analyses, for example to count the slide-to-roll ratio. The range of operating parameters is shown in Table 1.

Table 1. Operation conditions and ranges.

Measured signals	Range
Rotating speed	150 - 6000 rpm
(Rolling velocity)	(max. 22 m/s)
Load	30 - 11 000 N
(max. Hertz pressure)	(max. 2.5 GPa)
Lubricant inlet temperature	50 - 120 °C
Lubricant flow rate	0.5 - 20 l/min

Principle of friction measurement

The loading frame was designed with a closed structural force loop so that hydraulic loading cylinder will not exert any force on the surrounding constructions, as shown in Fig. 8 and 11. This also makes it possible to measure friction moment below the loading frame with the plate type moment sensor based on strain-gauges.

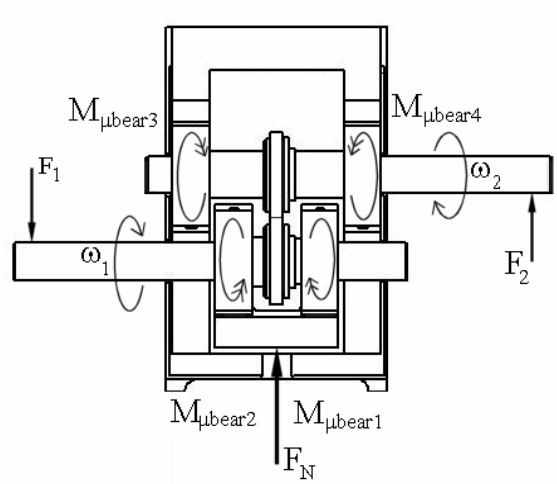

Figure 11. Forces and moments that effect the moment sensor below the loading frame. Force F_N has no direct effect on the moment sensor.

The measured moments below the loading frame represented the friction force exerted by disc contact. The slight measured moment changes caused by bearings (that mainly compensate each other), shaft bending and clutches can be ruled out by calibration.

Similar bearings in each shaft are rotating in different directions and they compensate each other's friction moments if their speeds are the same. With different bearing speeds, the friction moment compensation is no longer complete and minor friction moment may be introduced to the moment sensor. However, according to the bearing calculations, this additional moment typically causes an error less than 2 percent in the overall friction coefficient. In this kind of twin disc devices, friction coefficient is usually defined from the shaft torque. In these cases, bearing friction moments cause a 10 – 20 percent error in overall friction coefficients, unless they are ruled out with calibration. The load caused by shaft bending and forces F_1 and F_2 must be taken into account when the zero of the friction moment is determined.

Disc specification and manufacture

The test disc diameters are 70 mm and their width is 10 mm. A special device for disc grinding was also developed and constructed, where grinding can be done transversally to the disc rolling direction with proper crowning, with a radius of 292 mm. This corresponds to the real gear flank surface topography, as shown in Figure 12. The principle of the device is based on references [12, 13].

Figure 12. The test disc surface has been finished perpendicular to the rotating direction.

The grinding was performed with a grinding tool, which is shown in Figure 13.

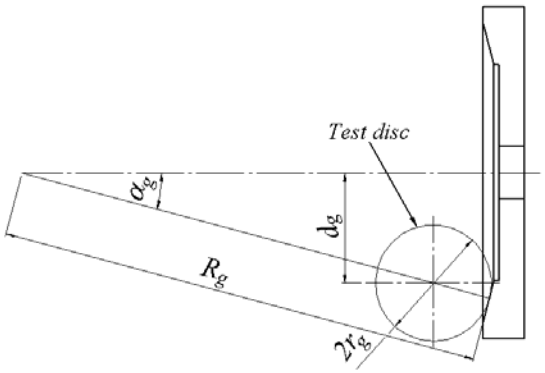

Figure 13. The profile of the grinding tool.

The radius of the crown R_g is defined from the equation (5),

$$d_g = (R_g - r_g) \cdot \sin(\alpha_g) \qquad (5)$$

where r_g is the radius of the test disc, α_g is the grinding angle and d_g is the distance between the centers of the grinding tool and the test disc. The grinding of discs was performed with the test discs fastened to the shafts before grinding. In this way the eccentricity of the test discs was minimized. Surface topography and roughness can also be varied to some extent by using different grain sizes and alloying elements on the grinding tool. After grinding the surface roughness of the test discs was measured with Talysurf 10.

Test procedure

In preliminary tests, the test device was warmed up for 1 hour before start by circulating lubricant in the test device at the test temperature and by rotating the test shafts without any load to achieve constant temperature conditions. The test started by keeping the velocity of the disc 1 constant and by decreasing disc 2 velocity from disc 1 velocity until the slide-to-roll ratio of -0.4 was reached. Disc 2 velocity was then increased until the slide-to-roll ratio was 0.4. The second measuring cycle was performed by keeping the velocity of the disc 2 constant. The velocity was varied at certain steps and the running time of each step was one minute.

The test was performed using base mineral oil ISO VG 220, whose viscosity index is 95. The lubricant flow rate was 6 l/min and inlet temperature 60 °C. The test disc material was case-hardening steel 20 NiCrMo2-2 and the discs were case-hardened into the depth of 0.8 – 1 mm, with specific surface hardness of 60 – 62 HRC. Maximum Hertzian pressure was 1.00 GPa and disc constant velocity was 3.00 m/s. The friction moment sensor was calibrated before and after the test.

RESULT

The measured preliminary result is shown in Figure 14.

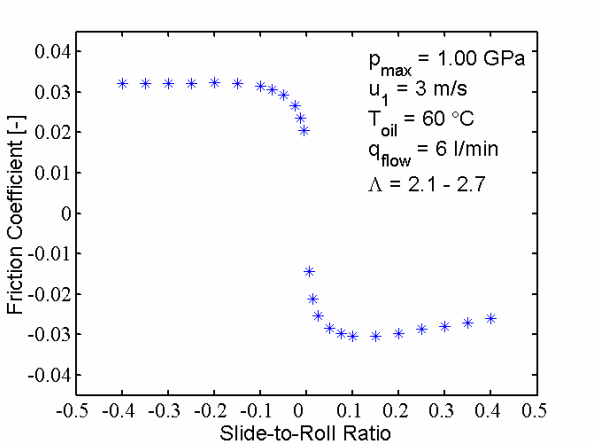

Figure 14. Preliminary result from the friction test.

Fig. 14 shows that the measured friction coefficient behavior correlates with earlier published results, and three different regions can be detected; linear, nonlinear and thermal region.

CONCLUSIONS

1. A high-pressure twin disc test device was developed, where loading, rolling and sliding velocity together with lubricant inlet temperature can be varied continuously.
2. Some aspects of gear related lubrication were presented.
3. A special device for disc grinding was also developed, where grinding can be done transversally to the disc rolling direction with proper crowning corresponding to the real gear flank properties.
4. The measured preliminary result shows that the measured friction coefficient behavior correlates with earlier published results and three different regions can be detected; linear, nonlinear and thermal region.

ACKNOWLEDGEMENT

The authors wish to thank Neste Oil for providing the test oils and Jorma Niskala for discussions on lubricants, Olli Nuutila for experimental support and Matti Uotila for his help with the twin disc device.

REFERENCES

1. Spikes, H.A. 1997. Mixed Lubrication – an Overview. Lubrication Science. 9. n3. 221-253.

2. Cann, P., Ioannides, E., Jacobson, B. and Lubrecht, A.A. 1994. The Lambda Ratio – a Critical Re-examination. Wear. 175. 177-188.

3. Hamrock, B. 1994. Fundamentals of Fluid Film Lubrication, McGraw-Hill, Inc. ISBN 0-07-025956-9. 690 p.

4. Wu, S. and Cheng, H.S. 1991. A Friction Model of Partial-EHL Contacts And Its Application to Power Loss in Spur Gears. Trib. Trans. 34. 398-407.

5. Wang, S., Cusano, C. and Conry T.F. 1991. Thermal Analysis of Elastohydrodynamic Lubrication of Line Contacts Using the Ree-Eyring Fluid Model. Trib. Trans. 113. 138-146.

6. Gecim, B. and Winer, W.O. 1980. Lubricant Limiting Shear Stress Effect on EHD Film Thickness. J. Lubr. Tech. 102. 213-221.

7. Höglund, E. 1999. Influence of Lubricant Properties on Elastohydrodynamic Lubrication. Wear 232. 176-184.

8. Johanson, K.L., and Tevaarwerk, J.L. 1977. Shear Behaviour of Elastohydrodynamic Oil Films. Proc. R. Soc. London, Ser. A 356. 215-236.

9. Lehtovaara, A. 2002. Calculation of Sliding Power Loss in Spur Gear Contacts. Tribotest. 9. n1. 23-34.

10. Hedlund, J., Lehtovaara, A. 2003. Influence of Lubricant on Sliding Friction in Spur Gear Contacts. Finnish Journal of Tribology. 22. n3. 11-25.

11. Järviö, O. and Lehtovaara, A. 2002. Experimental Study of Influence of Lubricants on Friction in Spur Gear Contacts. Finnish Journal of Tribology 21. n2-3. 22-29.

12. Patching, M.J. 1994. The Effect of Surface Roughness on the Micro-elastohydrodynamic Lubrication and Scuffing Performance of Aerospace Gear Tooth Contacts. Dissertation. University of Wales. 259 p.

13. Simon, M. 1984. Messung von elasto-hydrodynamischen parametern und ihre auswirkung auf die grübchentragfähigkeit vergüteter scheiben und zahnräder. Dissertation. Technischen Universität München. 203 p.

NOMENCLATURE

b	=	Half-width of Hertzian contact region, $b = (8wR/(\pi E'))^{0.5}$
B	=	Face width of the teeth
d_g	=	Distance
$E_{1,2}$	=	Elasticity modulus
E'	=	Reduced modulus of elasticity, $1/E' = ½[(1-\nu_1^2)/E_1 + (1-\nu_2^2)/E_2]$
f_a	=	Coefficient of asperity friction
$F_{1,2}$	=	Force
F_N	=	Normal force
F_S	=	Friction force caused by sliding
G	=	Material parameter, $G = \alpha E'$
G_∞	=	Limiting shear modulus
h_c	=	Central film thickness
k	=	Ellipticity parameter
$M_{\mu bear1,2,3,4}$	=	Bearing friction moments
$n_{1,2}$	=	Rotation speed
p_a	=	Asperity contact pressure
p_{max}	=	Max. Hertzian pressure
q_{flow}	=	Lubricant flow rate
r_g	=	Radius of test disc
R	=	Reduced radius of curvature, $1/R = 1/R_1 + 1/R_2$
$R_{1,2}$	=	Radius of curvature
R_g	=	Radius of crown
$R_{q,1,2}$	=	Surface roughness rms value
SR	=	Slide-to-roll ratio, $SR = V_S/V_R$
t	=	Time
T	=	Traction force
T_{oil}	=	Lubricant inlet temperature
$u_{1,2}$	=	Surface velocity
U	=	Dimensionless speed parameter, $U = \eta_o V_R/(E'R)$
V_R	=	Rolling velocity, $V_R = (u_1 + u_2)/2$
V_S	=	Sliding velocity, $V_S = u_1 - u_2$
w	=	Load per unit width
W	=	Dimensionless load parameter, $W = F_N / (E'R^2)$
x	=	Coordinate
α	=	Pressure-viscosity index (Barus)
α_g	=	Grinding angle
γ	=	Limiting shear stress-pressure coef.
$\dot{\gamma}$	=	Shear strain rate
η	=	Viscosity
η_0	=	Viscosity at atmospheric pressure
φ_T	=	Thermal reduction factor
Λ	=	Film parameter, $\Lambda = h_c / \sigma$
$\rho_{1,2}$	=	Radius of curvature $(R_{1,2})$
σ	=	Combined surface rms roughness,
τ	=	Shear stress
τ_a	=	$f_a \cdot p_a$
τ_L	=	Limiting shear stress
$\nu_{1,2}$	=	Poisson ratio
$\omega_{1,2}$	=	Angular velocity

Paper II

Kleemola, J. and Lehtovaara A.

Experimental evaluation of friction between contacting discs for the simulation of gear contact

TriboTest, 2007, **13**(1), 13-20.

TRIBOTEST
Tribotest 2007; **13**: 13–20
Published online 8th December 2006 in Wiley InterScience
(www.interscience.wiley.com) DOI: 10.1002/tt.29

tribo Test

Experimental evaluation of friction between contacting discs for the simulation of gear contact

J. Kleemola*,† and A. Lehtovaara
Tampere University of Technology (TUT), Tampere, Finland

Instant gear contact can be simulated with contacting discs, which provides steady operating conditions and eliminates most of the dynamics and manufacturing tolerances involved in real gears, resulting in an accurately controlled contact condition. A high-pressure twin-disc test device was developed, where loading and rolling velocity can be varied continuously. It is equipped with disc bulk temperature, mean contact resistance and friction moment measurements. The test discs were grinded transversal to the disc rolling direction with proper crowning corresponding to the real gear flank properties. The test device was applied by studying the friction behaviour against the slide-to-roll ratio at different contact pressures, rolling velocities and surface roughness. The measurements were performed using mineral base oil in the range of operation conditions often used in industrial gears. In general, the measured friction coefficient behaviour correlates with earlier published results and is logical with measured bulk temperature and mean contact resistance. The limiting shear stress of the lubricant has an essential role in friction behaviour. Copyright © 2006 John Wiley & Sons, Ltd.

KEY WORDS: twin-disc; friction; gear; contact resistance

1 INTRODUCTION

Gear contact behaviour has been a subject of study for many decades, but it is still a challenging engineering problem. In power transmissions, there are continuous requirements to apply higher Hertzian pressures and speeds but, at the same time, gears should be more effective and compact. Therefore, a lot of research is going on for the modelling and analysis of gear contact, including geometry, surface finishing, materials and coatings.

* Correspondence to: Jaakko Kleemola, Tampere University of Technology (TUT), P.O. Box 589 33101 Tampere, Finland.
† E-mail: jaakko.kleemola@tut.fi

Many different types of gear test devices have been developed to study gear contact. In the gear contact load, surface velocities and radiuses are changing continuously along the line of action, and instantaneous contact points are difficult to analyse in detail with real gears. Instant gear contact can be simulated with contacting discs, as shown in Figure 1. Contacting disc arrangements, which form the basis of the twin-disc test device, provide steady-state operating conditions and eliminate most of the dynamics and manufacturing tolerances involved in real gears, resulting in an accurately controlled contact condition.

Twin-disc test devices have been used to simulate various essential parameters and failures in gear contact such as scuffing, pitting, power loss, lubricants life and wear.[1–3] It is concluded[3] that twin-disc testing for gear lubricants provides good absolute correlation for frictional behaviour, good relative correlation for pitting results, but poor correlation for scuffing results. However, most of twin-disc tests are performed with discs where grinding has been done longitudinal to the disc rolling direction, which do not simulate the gear contact properly.

In this work, the developed twin-disc test device with measured signals is presented and is applied for studying friction behaviour. Special attention is paid to creating conditions that correspond to the real industrial gear contact topography.

2 EXPERIMENTAL

2.1 Twin-disc test device

The basic construction of the test device is shown in Figure 2. Each disc is driven by a separate electric motor with adjustable rotating speed resulting in a continuous change of slide-to-roll ratio (*SR*-ratio). Loading and rotating speeds can be varied on-line with automated computer control, which allows flexible testing.

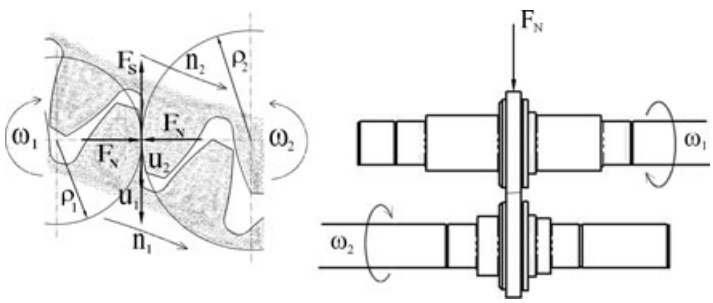

Figure 1. Simulation of gear contact with contacting discs

Figure 2. The developed twin-disc test device

DOI: 10.1002/tt

The electric motor can be driven at the maximum rotating speed of 6000 1/min, which provides a disc surface speed of 22 m/s for the given test disc radius. The highest load is 11 kN, which gives a maximum Hertzian pressure close to 2.5 GPa in the disc contact. Oil inlet temperature and flow rate can be varied between 50 and 120°C, and 0.5 and 20 l/min, respectively. The lubrication of the test disc is performed with a circulating lubrication system. A more detailed presentation of the twin-disc test device is shown in a previous study.[4]

2.2 Measured signals

The test device is equipped with disc 2 bulk temperature, contact resistance and friction moment measurements in addition to load and shafts rotating speeds. The loading frame is designed with a closed force loop so that the hydraulic loading cylinder will not exert any force on the surrounding constructions, as shown in Figure 3. This makes it also possible to measure the friction moment (M_μ) below the loading frame. The measured moments below the loading frame represented the direct friction force exerted by disc contact. The slight measured moment changes caused by bearings (mainly compensate each others), shafts bending and clutches can be ruled out by calibration.[4]

Disc bulk temperature is measured at 4.5 mm below the surface with a thermocouple and the signal is transmitted from the axel using a telemetry device. The contact resistance measurement was implemented into the test device to analyse the contact situation. The contact resistance and capacity measurement techniques have been shown in detail in previous works.[5,6] Signals are collected to a sampling card and are used for on-line analyses.

2.3 Test discs

The test discs material is case-hardening steel 20 NiCrMo2-2 and the discs were case-hardened into the depth of 0.8–1 mm, with specific surface hardness of 60–62 HRC. The test discs diameter is 70 mm and the width is 10 mm. A special device for disc grinding was also developed and constructed, where grinding can be done transversal to the disc rolling direction with proper crowning, with a radius of 292 mm. This corresponds to the real gear flank surface topography, as shown in Figure 4. The surface topography and roughness can also be varied to some extent by using different grain side and alloying elements on the grinding tool. The principle of the device is based on studies by Patching[1] and Simon[6] and is presented in more detail in a previous paper.[4]

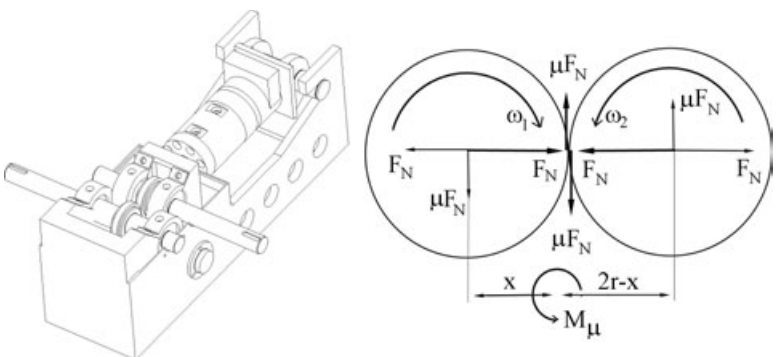

Figure 3. The loading frame and force caused friction moment (M_μ)

DOI: 10.1002/tt

Figure 4. The test disc surface has been finished perpendicular to the rotating direction

Table 1. Test matrix

Case	p_{max} (GPa)	u_1 (m/s)	T_{oil_inlet} (°C)	σ_{be} (μm)	σ_{af} (μm)	*SR*-ratio (–)	*q* (l/min)
1	1.00	3.0	50	0.43	–	–0.4 to 0.4	6
2	1.00	3.0	60	–	–	–0.4 to 0.4	6
3	1.00	2.0	60	–	–	–0.4 to 0.4	6
4	1.00	4.0	60	–	–	–0.4 to 0.4	6
5	1.00	3.0	70	–	–	–0.4 to 0.4	6
6	1.25	3.0	60	–	–	–0.4 to 0.4	6
7	1.50	3.0	60	–	0.41	–0.4 to 0.4	6
8	1.00	3.0	60	0.71	0.69	–0.4 to 0.4	6

The surface roughness of the test discs was measured with Talysurf 10 (Taylor Hobson Ltd., Leicester, England) with a metre cut-off value of 0.25 mm. R_a-value is the average of 12 independent measurements from four different places. In cases 1–7 (Table 1), the R_a-values were close to 0.2 μm and in case 8 close to 0.4 μm.

2.4 Test procedure and test matrix

The tests were performed on two test disc pairs. Cases 1–7 were measured with the same test disc pair. The test device was warmed up for 1 hour before starting by circulating lubricant in the test device at the test temperature and by rotating the test shafts without any load to achieve constant temperature conditions. The test started by keeping the velocity of disc 1 constant and by decreasing disc 2 velocity from disc 1 velocity until the *SR*-ratio of –0.4 was reached. Then the disc bulk temperature was allowed to stabilise in pure rolling conditions, after which disc 2 velocity was increased until the *SR*-ratio was 0.4. The second measuring cycle was done by keeping the velocity of disc 2 constant. The velocity was varied at certain steps and the running time of each step was 1

DOI: 10.1002/tt

minute. The test case conditions are presented in Table 1. All the tests were performed using base mineral oil ISO VG 220, whose viscosity index is 95. The friction moment sensor was calibrated before and after the test.

SR-ratio is specified by dividing sliding velocity by mean rolling velocity, i.e. $SR = (u_1 - u_2)/((u_1 + u_2)/2)$. The mean combined surface rms roughness was defined before (σ_{be}) and after (σ_{af}) the test as $\sqrt{(1.3 \cdot R_{a1})^2 + (1.3 \cdot R_{a2})^2}$. Lubrication regime was estimated by using lambda value Λ, which was obtained by dividing the isothermal central film thickness (h_c) by mean combined rms surface roughness (σ).

3 RESULTS AND DISCUSSION

The measured results are shown in Figures 5-7. From each case, one measuring cycle is presented. The maximum differences between the two measuring cycles were typically less than 6% when absolute *SR*-ratio was higher than 0.025.

The overall behaviour of friction curves is characterised by three different regions, linear, non-linear and thermal region. The linear region appears on a very small *SR*-ratio while the lubricant retains a Newtonian behaviour. When the *SR*-ratio increases, a shift occurs to a region; where the lubricant begins to behave in a non-Newtonian way. The friction coefficient is dominated by lubricant limiting shear stress and friction may reach its maximum point. When the *SR*-ratio increases further, a thermal region is reached, where the increasing shearing of the lubricant raises lubricant temperature and the friction may start to fall slowly. This description matches lubricated high pressure, non-conformal rolling/sliding contacts, where lubricant controls the frictional properties of a contact, as presented by Johnson and Cameron.[7] In mixed lubrication regimes, boundary friction may bring its own contribution to the overall friction behaviour.

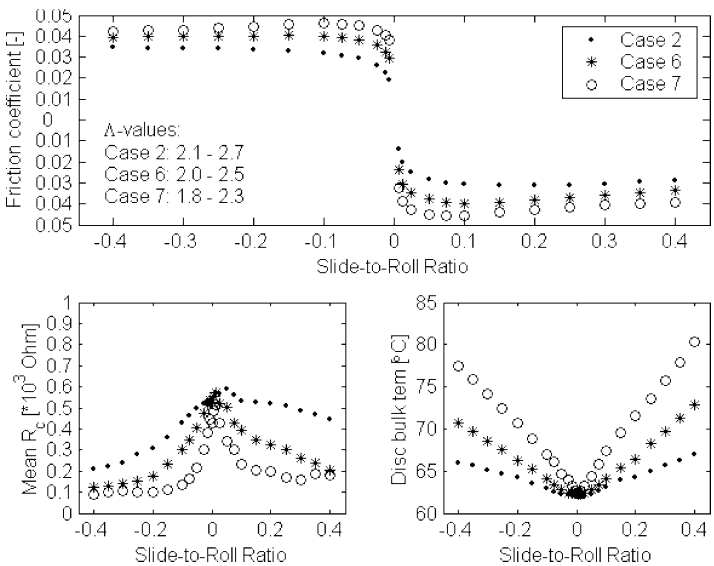

Figure 5. Maximum Hertzian pressure influence on friction coefficient, mean contact resistance and bulk temperature; u_2 = 3.0 m/s, T_{oil_inlet} = 60°C

DOI: 10.1002/tt

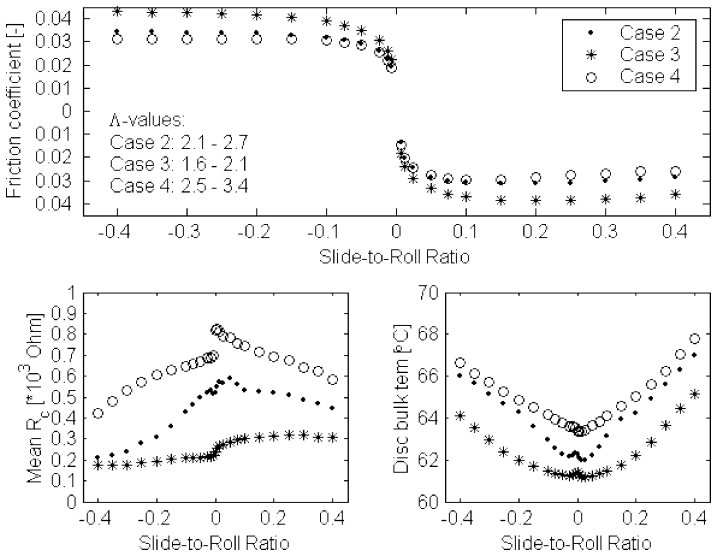

Figure 6. Rolling velocity influence on friction coefficient, mean contact resistance and bulk temperature; p_{max} = 1.00 GPa, T_{oil_inlet} = 60°C

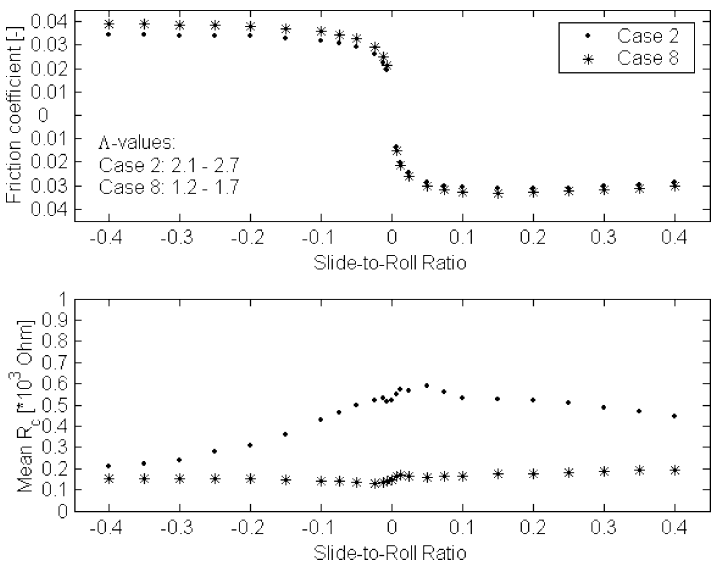

Figure 7. Combined surface roughness influence on friction coefficient and mean contact resistance; p_{max} = 1.00 GPa, u_2 = 3.0 m/s, T_{oil_inlet} = 60°C

3.1 Load

Figure 5 shows that friction coefficient increases with increasing contact pressure, especially at a non-linear region. At higher pressures, the limiting shear stress of lubricant plays an increasingly dominant role in friction behaviour. The disc bulk temperature increases with increasing *SR*-ratio and pressure due to increasing frictional power. The mean contact resistance measurement indicates

DOI: 10.1002/tt

decreasing film thickness with increasing pressure, which is mainly due to the higher temperature and lower effective viscosity.

The measured mean contact resistance indicates relative changes in film thickness. Decreasing mean contact resistance means that asperity contacts increase. There is not much experience yet about the severity of the asperity contact, when the measured value stabilises close to zero. However, it seems to behave logically in the range where it changes.

3.2 Rolling velocity

Figure 6 shows that an increase in rolling velocity decreases friction coefficient, especially at the thermal region. This correlates with an earlier description of the thermal region. The corresponding behaviour can also be seen, for instance, in the study of Simon.[6] The bulk temperature measurement shows that rolling point temperatures were not exactly at the same level as in the different cases, but this is not expected to have a major effect on the results. The power loss in different cases is close to each other resulting in that the rise of bulk temperature is quite similar in all cases.

3.3 Surface topography

The two measured cases only differed in surface roughness and they were measured in the same operation conditions. The overall friction difference should come from differences in micro-elastohydrodynamic lubrication (micro-EHL) friction, i.e. the bulk properties of the lubricant at the local conditions of asperity interaction in this lubrication regime.[8]

In Figure 7, the measured mean contact resistance logically shows that a rougher surface has more asperity contacts than a smoother one. Only a slight difference between the friction coefficients can be observed at high negative *SR*-ratios, where the Λ-values are the lowest ($\Lambda > 1.2$). This result corresponds to the earlier observations, that a greater difference in friction can be expected when $\Lambda < 1.0$,[2,8,9] i.e. in a more severe mixed (micro-EHL) lubrication regime.

4 CONCLUSIONS

A high-pressure twin-disc test device was developed, where loading and rolling velocity can be varied continuously. It is equipped with disc bulk temperature, mean contact resistance and friction moment measurements. The test discs were grinded transversal to the disc rolling direction with proper crowning corresponding to the real gear flank properties. The test device was applied by studying the friction behaviour against the *SR*-ratio at different contact pressures, rolling velocities and surface roughness. The measurements were performed using mineral base oil in the isothermal Λ-value range of 1.2–3.4 and maximum Hertzian pressure of 1.0–1.5 GPa, representing values often used in industrial gears. In general, the measured friction coefficient behaviour correlates with earlier published results and is logical with measured bulk temperature and mean contact resistance. More experience is needed to interpret the severity of the asperity contact, when the measured value stabilises close to zero. However, it seems to behave logically in the range where it changes.

It can be concluded that friction coefficient increases with increasing contact pressure, especially at a non-linear region. At higher pressures, the limiting shear stress of lubricant plays an increasingly dominant role in friction behaviour. An increase in rolling velocity decreases friction coefficient, especially at the thermal region. An increase in surface roughness increases friction coefficient only slightly in the applied lubrication regime.

DOI: 10.1002/tt

Nomenclature

F_N	normal force
F_S	friction force caused by sliding
h_c	central film thickness
M_μ	friction moment
n	rotation speed
p_{max}	max. Hertzian pressure
q	oil flow rate
r	disc radius
R_a	surface R_a-value
R_c	contact resistance
SR-ratio	slide-to-roll ratio $(u_1 - u_2)/((u_1 + u_2)/2)$
T_{oil_inlet}	oil inlet temperature
u	velocity
x	distance from moment sensor central point
Λ	h_c/σ
μ	friction coefficient
ρ	radius of curvature
σ	combined surface rms roughness $\sqrt{(1.3 \cdot R_{a1})^2 + (1.3 \cdot R_{a2})^2}$
ω	angular velocity

Subscripts

1	refers to disc 1
2	refers to disc 2

Acknowledgement

The authors gratefully acknowledge Neste Oil Oyj for providing the test lubricants.

REFERENCES

1. Patching MJ. The effect of surface roughness on the micro-elastohydrodynamic lubrication and scuffing performance of aerospace gear tooth contacts. Dissertation, University of Wales, College of Cardiff, 1994.
2. Wu S, Cheng HS. A friction model of partial-EHL contacts and its application to power loss in spur gears. *Trib. Trans.* 1991. **34**(3):398–407.
3. Hoehn B-R, Michaelis K, Doleschel A. Limitations of bench testing for gear lubricants. *ASTM Spec. Tech. Publ.* 2001. **1404**:15–32.
4. Kleemola J, Lehtovaara A. Introduction on high pressure twin disc test device. *Finnish J. Tribology* 2006. **25**(2):8–17.
5. Lord J. Thin lubricating film in elastohydrodynamic contacts experimental techniques and applications. Dissertation, Luleå University of Technology, 2004.
6. Simon M. Messung von elasto-hydrodynamischen parametern und ihre auswirkung auf die grübchentragfähigkeit vergüteter scheiben und zahnräder. Dissertation, Technischen Universität München, 1984.
7. Johnson KL, Cameron R. Shear behavior of elastohydrodynamic oil films at high rolling contact pressures. *Proc. Inst. Mech. Eng.* 1967. **182**(1):223–9.
8. Evans CR, Johnson KL. The influence of surface roughness on elastohydrodynamic traction. *Proc. Inst. Mech. Eng.* 1987. **201**(2):145–50.
9. Bair S, Winer WO. Friction/traction measurements with continuously variable slide-roll ratio and slide slip at various lambda ratios. *Proc. of the Leeds-Lyon Symposium on Tribology*, Leeds, 1981, pp. 296–301.

Paper III

Kleemola, J. and Lehtovaara A.

An approach for determination of lubricant properties at elliptical elastohydrodynamic contacts using a twin-disc test device and a numerical traction model

Proceedings of the Institution of Mechanical Engineers, Part J: Journal of Engineering Tribology, 2008, **222**(7), 797-806.

An approach for determination of lubricant properties at elliptical elastohydrodynamic contacts using a twin-disc test device and a numerical traction model

J Kleemola* and **A Lehtovaara**
Department of Mechanics and Design, Tampere University of Technology, Tampere, Finland

The manuscript was received on 28 April 2008 and was accepted after revision for publication on 27 June 2008.

DOI: 10.1243/13506501JET447

Abstract: High-pressure lubricant properties are important when friction coefficients and power losses are evaluated in elastohydrodynamic (EHL) contacts. An approach was developed to determine the limiting shear stress and actual viscosity properties of lubricants using a numerical traction model based on elliptical EHL contact and traction curves, measured at a wide range of temperatures and pressures with a twin-disc test device. The tests were carried out in pure fluid film at high Hertzian pressures with finely polished surfaces. Each lubricant was tested at 135 test points, where traction coefficients and bulk temperatures were measured. The lubricant parameters in the traction model were adjusted so that the calculated results matched the experimental measurements at all test points. In general, there is a good correlation between the calculated results and the experimental measurements. The influence of pressure on limiting shear stress and actual viscosity is less significant for polyalphaolefin (PAO) oil than for mineral oil.

Keywords: limiting shear stress, actual viscosity, twin-disc device, elastohydrodynamic, elastohydrodynamic traction model

1 INTRODUCTION

High-pressure lubricant properties are important when friction coefficients and power losses are evaluated in elastohydrodynamic (EHL) contacts. This type of contact is typical in machine elements such as gears and bearings. To determine the actual viscosity and the limiting shear stress at high pressures is a difficult task, and values of these properties are not commonly available. Many studies have been undertaken to develop a method for determining these properties [**1**–**9**].

The devices most commonly used to determine the limiting shear stress at high pressures are a ball-impacting apparatus, a pressure chamber, a ball-on-disc, or a twin-disc device. Jacobson [**10**] devised a ball-impacting apparatus, where the maximum pressure during impact was 5.5 GPa, and it was later improved and used by several researchers [**11**–**13**]. In 1967, Jacobson also developed the first high-pressure chamber [**14**], which has been updated several times since then [**3**, **5**, **15**, **16**]. In the most recent set-up, the lubricant's limiting shear stress was evaluated at pressures up to 3.3 GPa [**5**].

Bair [**8**] divided high-pressure viscometers into four categories. Rotational concentric cylinder (Coutte) viscometer [**17**] and capillary viscometer measurements are usually limited to low pressures. Diamond-anvil cells have been used as rolling ball viscometers [**18**] with pressures up to 10 GPa, but typically, only at ambient temperature. A falling body viscometer has been long in use, and the pressure range of the modern instrument [**8**, **19**] is up to 1.6 GPa.

Johnson *et al.* [**20**, **21**] developed an experimental method using a twin-disc device, where the rheological parameters were determined as an average value over the EHL contact. The disadvantage of rheological parameters so defined is that the lubricant is not subjected to the same conditions at all points of contact because of the Hertzian pressure distribution. Fang *et al.* [**2**] continued the development of the method using a rheological model based on the local rheological traction variables rather than the global-averaged quantities and evaluated contacts with pressures up

**Corresponding author: Department of Mechanics and Design, Tempere University of Technology, PO Box 589, Tampere 33101, Finland. email: jaakko.kleemola@tut.fi; arto.lehtovaara@tut.fi*

to 1.5 GPa. This model assumes a Hertzian shear stress distribution, and it is concluded that this assumption is reasonably valid at loading conditions of Hertzian maximum pressures >0.8 GPa. Generally, the advantage of a twin-disc device is that lubricant traction measurements can be carried out over a wide range of operating parameters and with transient loading conditions closely simulating the EHL contacts in machine elements.

The objective of the work was to evaluate, and develop further, a method to determine the limiting shear stress and actual viscosity properties of lubricants using a traction model based on an elliptical EHL contact and traction curves, measured at a wide range of temperatures and pressures using twin-disc test devices. Measurements were made with mineral and polyalphaolefin (PAO) base oils, which are generally used in industrial gears. The measured lubricant parameters can be used as input values in gear-contact power-loss calculations in future work.

2 EXPERIMENTAL

2.1 Twin-disc test device

Traction tests were performed using a previously developed high-pressure twin-disc test device, which is presented in more detail in references [**22**] and [**23**]. The principle used for the test device and the coordinate system is shown in Fig. 1. In the test device, each disc is driven by separate electric motors with adjustable rotation speeds, resulting in a continuous variable sliding velocity. Loading and rotation speeds can be varied on-line with automated computer control.

Measured signals from the twin-disc test device include bulk disc temperature, mean contact resistance, and traction moment in addition to load and shaft rotation speeds. The bulk disc temperature is measured 3 mm below the surface with a thermocouple, and the signal is transmitted from the axle using a telemetry device. The mean contact resistance measurement was introduced into the test device to analyse the contact lubrication conditions. The traction moment measured from shaft 1 includes the bearing moments, but these can be excluded by calibration, as described later. Signals are collected on a sampling card and are used for both on-line analysis and later processing.

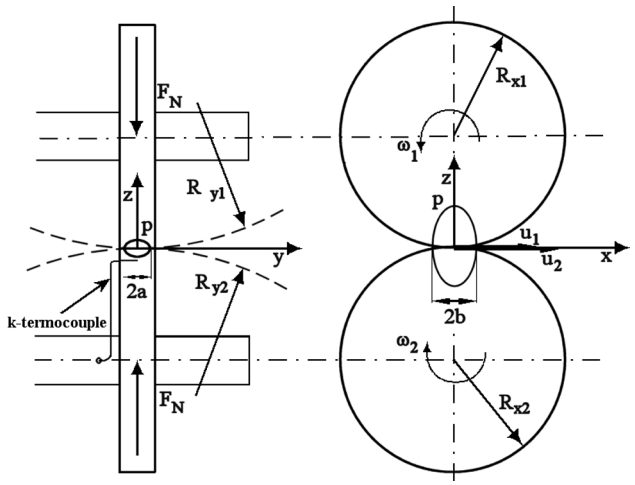

Fig. 1 Principles of a twin-disc test device

2.2 Test discs and lubricants

The material for the test discs is a case-hardening steel 20 NiCrMo2-2. The discs are case-hardened to the depth of 0.8–1 mm, with specific surface hardness of 60–62 HRC. The test discs have a diameter of 70 mm and a thickness of 10 mm. They were ground in a direction perpendicular to the rolling direction to give a raised peak with a radius of 292 mm. After grinding the disc, surfaces have been polished to a surface roughness Ra-value ∼0.05 μm. The surface roughness of the test discs was measured with a Wyko NT1100 optical profiler.

The test lubricants are mineral and PAO base oils. The main viscometric properties of lubricants are shown in Table 1. The tests were carried out at steady oil inlet temperatures of 50, 70, and 90 °C and at a lubricant flow rate of 5 l/min.

2.3 Test procedure and test matrix

The test conditions were selected to provide pure fluid film at high Hertzian pressures. This was possible only because of the fine by polished surfaces. The lubrication regime was monitored on-line with the measurement of mean contact resistance, which can indicate the possibility of metal-to-metal contact. The calculated thermal Λ-value varied between 4.6 and 12 in the measured test conditions.

The test device was warmed up for 1 h, before taking measurements, by circulating lubricant in the test device at the test temperature and by rotating the shafts without any load to achieve constant temperature. The pure rolling velocity point with load

Table 1 Main viscometric properties of the lubricants tested

Type	Mineral	PAO
ν at 40 °C (mm^2/s)	220	220
ν at 100 °C (mm^2/s)	19	29.1
ρ at 15 °C (kg/m)^3	892	849
VG class (–)	220	220

was tested in steady-state conditions after 20 min. Then the first stage was begun, in which sliding velocity was introduced in nine steps from 0 to 1 m/s, simultaneously by increasing the velocity of disc 1 and decreasing that of disc 2 by a similar amount, while maintaining a constant rolling velocity of 7.50 m/s. The duration of each step was 7 min, and after the final step, the system was taken back to the pure rolling velocity situation and kept in a steady state for 20 min. In the second stage, the sliding velocity was again increased from 0 to 1 m/s, but in this case the disc 1 velocity was decreased and disc 2 velocity was increased. In this way, bearing losses can be eliminated from the traction results. The supporting bearing friction moments were assumed to be equal, because all bearings are similar and the speed differences between the slower and the faster shafts are small. The direction of disc traction moments changes between stages 1 and 2, because the direction of sliding velocity changes, but the bearing friction moments are in the same direction at all instances. The net traction moment, without bearing losses at each sliding velocity, is the difference between the traction moment in stages 1 and 2 divided by two. The system allows measurement of the bulk temperatures of both the slower and faster discs.

The test matrix covers a wide range of parameters, which are shown in Table 2. Hertzian maximum pressure varied from 1 to 2 GPa, in steps of 0.25 GPa. A fairly high rolling velocity was chosen to achieve pure fluid film lubrications. The sliding velocity range was selected to include the maximum traction value. The lubricant inlet temperature varied (50, 70, and 90 °C) to understand the effects of temperature on the traction curve.

3 TRACTION MODEL

The upgraded numerical traction model is based on the model [**24**, **25**] developed earlier for the calculation of sliding friction and power loss in spur-gear contacts. In this model, the line contact, geometry was upgraded to correspond to the elliptical contact which is found in the twin-disc test device. Another major change was made for the characterization of lubricant limiting shear stress properties at high pressures.

Herzian pressure distribution and constant film thickness are assumed. It is well known that these profiles do not differ greatly from the real profiles and usually provide a reasonable approximation for traction studies, at least under heavily loaded conditions. The Hertzian normal contact pressure distribution for

Table 2 Test matrix

Case	Hertzian pressure (GPa)	Rolling velocity (m/s)	Sliding velcity (m/s)	Oil inlet temperature I oil (°C)	Oil type
1	1.00	7.50	0–1	50	PAO
2	1.25	7.50	0–1	50	PAO
3	1.50	7.50	0–1	50	PAO
4	1.75	7.50	0–1	50	PAO
5	2.00	7.50	0–1	50	PAO
6	1.00	7.50	0–1	70	PAO
7	1.25	7.50	0–1	70	PAO
8	1.50	7.50	0–1	70	PAO
9	1.75	7.50	0–1	70	PAO
10	2.00	7.50	0–1	70	PAO
11	1.00	7.50	0–1	90	PAO
12	1.25	7.50	0–1	90	PAO
13	1.50	7.50	0–1	90	PAO
14	1.75	7.50	0–1	90	PAO
15	2.00	7.50	0–1	90	PAO
16	1.00	7.50	0–1	50	Mineral
17	1.25	7.50	0–1	50	Mineral
18	1.50	7.50	0–1	50	Mineral
19	1.75	7.50	0–1	50	Mineral
20	2.00	7.50	0–1	50	Mineral
21	1.00	7.50	0–1	70	Mineral
22	1.25	7.50	0–1	70	Mineral
23	1.50	7.50	0–1	70	Mineral
24	1.75	7.50	0–1	70	Mineral
25	2.00	7.50	0–1	70	Mineral
26	1.00	7.50	0–1	90	Mineral
27	1.25	7.50	0–1	90	Mineral
28	1.50	7.50	0–1	90	Mineral
29	1.75	7.50	0–1	90	Mineral
30	2.00	7.50	0–1	90	Mineral

PAO, polyalphaolefin.

two elastic bodies with convex surfaces is stated as

$$p(x,y) = p_o \left(1 - \frac{x^2}{b^2} - \frac{y^2}{a^2}\right)^{1/2} \quad (1)$$

The constant film thickness is calculated from the isothermal central film thickness formula [**26**] by taking into account a thermal reduction factor φ_T [**27**]. The actual film thickness h for an elliptical contact can be written as

$$h = \varphi_T \cdot 2.69U^{0.67}G^{0.53}W^{-0.067}(1 - 0.61 \cdot e^{-0.73k_e}) \quad (2)$$

The non-Newtonian model proposed by Gecim and Winer [**28**] for fluid shear stress–strain rate relationship is assumed to be

$$\dot{\gamma} = \frac{1}{G_\infty}\frac{d\tau}{dt} + \frac{\tau_L}{\eta}\tanh^{-1}\left(\frac{\tau}{\tau_L}\right) \quad (3)$$

The first term, i.e. the elastic strain component in equation (3), has been neglected in numerical studies. The strain rate across the film is assumed to be constant, i.e. $\dot{\gamma} = |u_1 - u_2|/h$.

The sliding traction force, F_μ, can be integrated from the lubricant shear stress over the contact zone as follows

$$F_\mu = \int_{-a}^{a}\int_{-b}^{b} \tau(x,y)\,dx\,dy \quad (4)$$

The corresponding traction coefficient is determined as

$$\mu = \frac{F_\mu}{F_N} \quad (5)$$

The dominant mode of heat generation is assumed to be frictional heating, resulting from the lubricant sliding as follows

$$q(x,y) = \tau(x,y) \cdot V_s \quad (6)$$

where the coordinates x and y are parallel and perpendicular to the sliding direction. Assuming that half the heat is conducted on each side of the surface, the surface temperature can be calculated by flash temperature equations for fast-moving surfaces [**27**, **29**]

$$T_1(x,y) = T_0 + \frac{1}{\sqrt{\pi\rho_1 c_1 k_1 u_1}}\int_{-\infty}^{x}\left\{\frac{q(x',y)}{2}\right\}\frac{dx'}{\sqrt{x-x'}} \quad (7)$$

$$T_2(x,y) = T_0 + \frac{1}{\sqrt{\pi\rho_2 c_2 k_2 u_2}}\int_{-\infty}^{x}\left\{\frac{q(x',y)}{2}\right\}\frac{dx'}{\sqrt{x-x'}} \quad (8)$$

The estimation of the contact traction requires an estimation of an effective temperature of the lubricant within the film, which in turn can be used to estimate the lubricant shear stress and viscosity. This is described as follows

$$T_f(x,y) = \frac{1}{2}[T_1(x,y) + T_2(x,y)] + \frac{\tau(x,y)V_S h}{8k_f(x,y)} \quad (9)$$

The equation for lubricant thermal conductivity, k_f, dependence on pressure is given in reference [**30**]. The equations described earlier led to an iterative solution, where the contact temperature field must be harmonized with the frictional force, i.e. frictional heating, at every mesh point.

The current traction model, shearing is assumed to be constant across the film, which leads to parabolic temperature distribution across the fluid film. This assumption appears reasonable for small and moderate sliding velocities, which was the case in these experiments. Clarke *et al.* [**31**] studied the high sliding velocity case and concluded that shearing occurs near the faster surface, with effects on temperature distribution and heat transfer of the contact surfaces.

4 MODELLING OF LIMITING SHEAR STRESS AND ACTUAL VISCOSITY

An approach to determine the limiting shear stress and actual viscosity properties of a lubricant is developed using a traction model and traction curves, measured at a wide range of temperatures and pressures with the twin-disc test device. The limiting shear stress and actual viscosity have important effects on traction at different points of the traction curve under various traction regimes.

4.1 Viscosity

Lubricant viscosity is strongly dependent on pressure and temperature in the EHL contacts. This can be taken into account by using Roelands equation [**32**], which can be written as

$$\eta(p,T_f) = \eta_0(T_f)\exp\{[\ln(\eta_0(T_f)) + 9.67] \cdot [-1 + (1 + 5.1\cdot 10^{-9}p)^{Z(T_f)}]\} \quad (10)$$

where $\eta_0(T_f)$ and $Z(T_f)$ can be defined as [**20**]

$$\log(\log\eta_0 + 4.2) = -S_0\log\left(\frac{1+T_f}{135}\right) + \log G_0 \quad (11)$$

$$Z(T_f) = D_Z + C_Z\log\left(\frac{1+T_f}{135}\right) \quad (12)$$

The lubricant parameters S_0 and G_0, which describe viscosity dependence on temperature, were set according to the information provided by the manufacturers. Other parameters C_Z and D_Z were defined by

iteration so that the calculated results correlated with experimental results. In non-linear traction regimes and at low pressures, actual lubricant viscosity is the major determinant of shape of the traction coefficient curve.

4.2 Limiting shear stress

When the traction coefficient is studied as a function of sliding velocity, three different (linear, non-linear, and thermal) regimes can be found. The limiting shear stress plays the major role in defining the traction coefficient in a non-linear traction regime. At the peak point of the traction curve, the traction coefficient can be estimated as

$$\mu = \frac{F_\mu}{F_\mathrm{N}} = \frac{\bar{\tau}_\mathrm{L}}{\bar{p}} \tag{13}$$

In equation (13), $\bar{\tau}_\mathrm{L}$ is the mean value of the limiting shear stress and $\bar{p}$ is the mean Hertzian pressure. Equation (13) can be written as

$$\bar{\tau}_\mathrm{L} = \mu \cdot \bar{p} \tag{14}$$

The traction coefficient μ is calculated from the measured traction force F_μ and the normal load F_N. The measured traction data with an inlet temperature of 50 °C were used for the creation of the master curve for limiting shear stress. First, the maximum traction coefficients were chosen from the measured traction curves at five different Hertzian pressure levels. Using equation (14), the mean limiting shear stress can be calculated and the results are plotted (circles) against the mean Herzian pressure in Fig. 2. The traction points are then fitted into the quadratic master curve equation $\tau(p)$ and the equation constants a_1, a_2, and τ_0 are determined.

The limiting shear stress, at an effective fluid temperature of T_f, is obtained with multiplying the master curve with the temperature function $g(T_\mathrm{f})$, as shown in Fig. 2. In this function, the constants a_3, a_4, and a_5 are unknown and are defined by iterating the lubricant parameters of the traction model so that the calculated results correlated with experimental results in all the test cases.

Traction curve measurements were carried out at three different lubricant inlet temperatures. The measured traction data with an inlet temperature of 50 °C were used for the creation of the master curve for limiting shear stress. At this temperature and at the maximum traction coefficient points, the difference between the measured bulk temperatures T_bulk was the smallest, with tested Herzian pressure being <5 °C for mineral oil and <3 °C for PAO oil. This minimizes bulk temperature effects on limiting shear stress results.

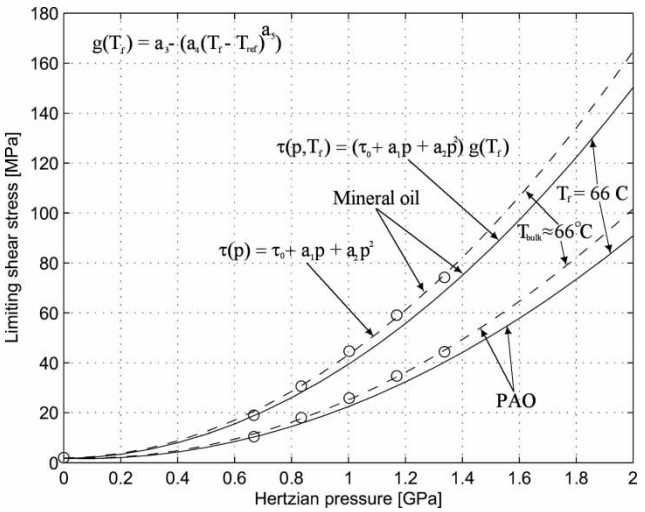

Fig. 2 Limiting shear stress curve-fitting for tested lubricants

The calculated limiting shear stress and actual shear stress distribution at operating conditions, corresponding to the maximum traction points (circles in Fig. 2) with mineral oil, are shown in Fig. 3. It was seen that the distribution of calculated and measured values was similar and the mean values was close to each other. This indicates that estimation of limiting shear stress using equations (13) and (14) is justified.

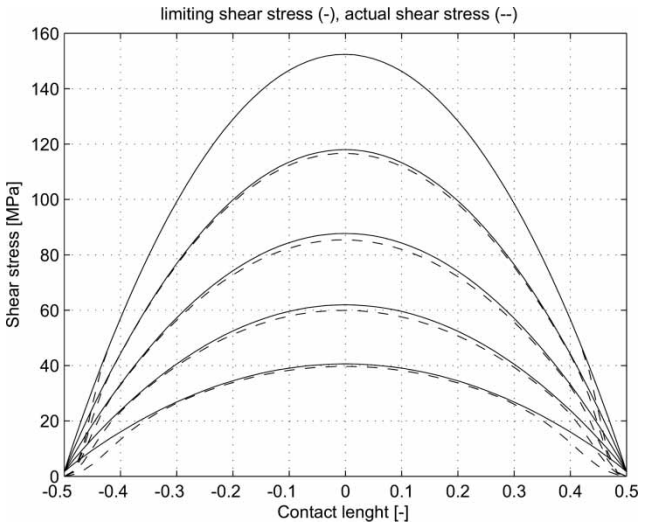

Fig. 3 The profiles ($y = 0$) of limiting shear stress (solid lines) and traction model shear stress distribution (dashed lines) at maximum Herzian pressures from top to bottom 2.00, 1.75, 1.50, 1.25, and 1.00 GPa, corresponding to sliding velocities 0.05, 0.1, 0.2, 0.3, and 0.3 m/s at an oil inlet temperature of 50 °C

5 RESULTS AND DISCUSSION

The properties of two different lubricants were determined by a wide range of operating conditions using the previously developed method. Each lubricant was tested under 15 sets of conditions, and each of which has nine separate test points. This results in 135 test points, where traction coefficient and bulk temperature were obtained as a function of the sliding velocity, the Hertzian pressure, and the oil inlet temperature. The parameters of actual viscosity and limiting shear stress in the traction model were adjusted by iteration, so that the calculated values match the experimental results for all the test points. Generally, calculated results correlate well with experimental results.

Some experimental and calculated results are shown in Figs 4 and 5. The shape of the traction curves are similar to other works, where traction curves have been measured using twin-disc test devices [**5**, **6**, **21**]. The calculated mean surface temperatures along the elliptical contact profile $y = 0$ and the measured bulk temperatures behave in a similar way, i.e. they increase almost linearly with increasing sliding velocity. The properties of the two lubricants tested, as expected with PAO, produce lower traction values, as shown elsewhere in the literature [**33**, **34**].

Figure 6 shows the relative difference between traction model calculations and experimental traction results for all test points. For each case, the percentage difference on the left is a sliding velocity of 0.05 m/s, while the last bar in each set is 1 m/s. The mean percentage difference for all PAO oil and mineral oil test points is 9 and 4 per cent, respectively. The largest differences are mainly related to the lowest sliding velocities and pressures, where the percentage difference is high due to small traction values. Under these operating conditions, the actual viscosity dominates the traction coefficient values. However, there were no such parameters, C_Z and D_Z, that would have made the difference substantially less than that between the experimental and traction model results. This may indicate that the model described earlier is not flexible in this regime, but in heavily loaded gear contacts this will not be a major problem.

In traction model calculations, the measured bulk temperature in rolling situations was used as the lubricant inlet temperature T_0. In rolling situations, no frictional heat generation effect is caused by sliding velocity, which contributes to the flash temperature, as shown in equations (7) and (8). The preliminary infrared temperature measurement from the disc 2 surface, just before contact, supported the view that, in a rolling situation, both surface and bulk temperatures were close to each other.

The experimental results showed that the bulk temperature of the faster disc is higher than the slower disc, but the differences were always $< 3\,^{\circ}\mathrm{C}$, because the values of sliding velocities were very less. The traction model gives the same level of difference for surface temperatures, but in the opposite direction. This was mainly because of the assumed heat division between the surfaces (half to each surface), and fluid temperature distribution across the film. However, the difference between the model and experiments was

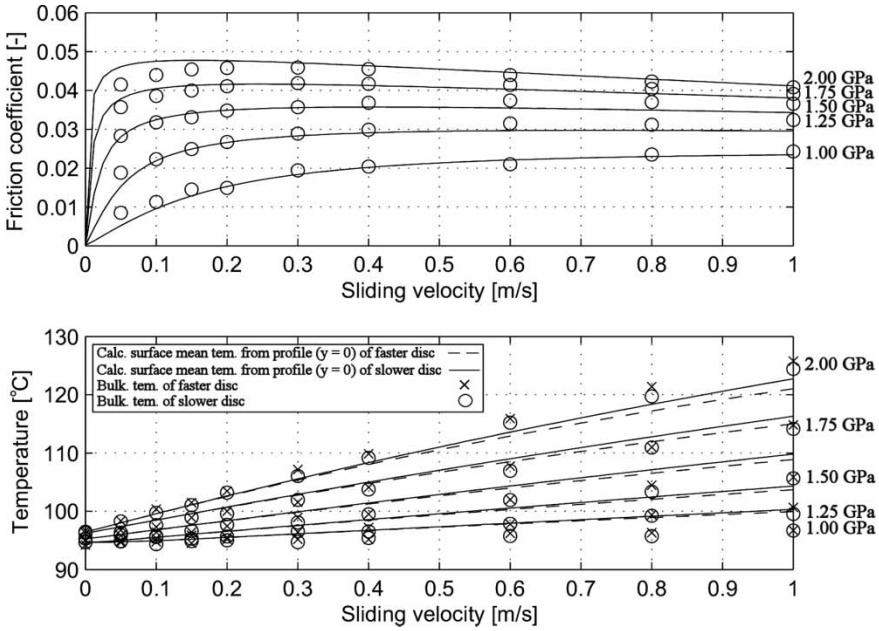

Fig. 4 Mineral oil traction coefficient and corresponding temperatures as a function of sliding velocity at maximum Hertzian pressures 1.00, 1.25, 1.50, 1.75, and 2.00 GPa, and an oil inlet temperature of 90 °C

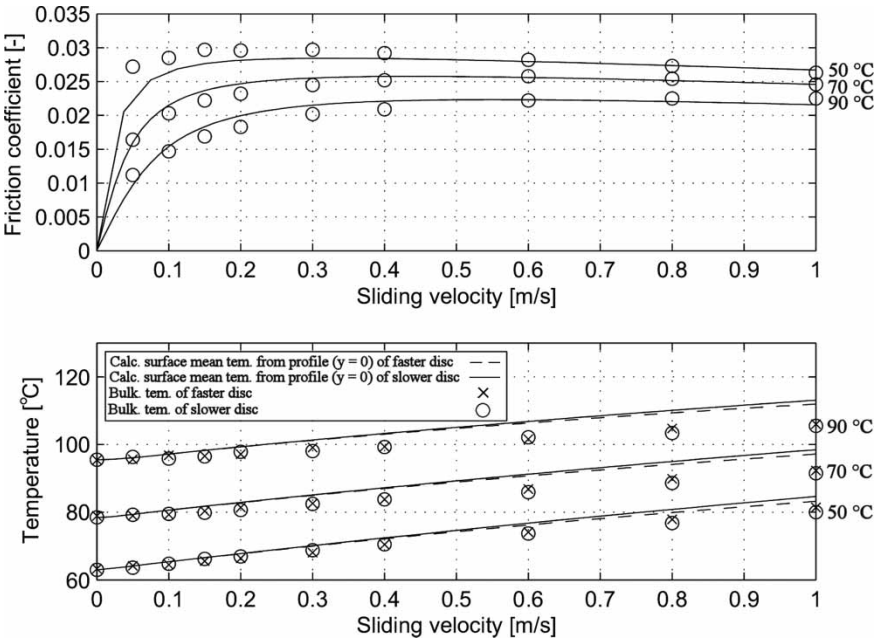

Fig. 5 PAO oil traction coefficient and corresponding temperatures as a function of sliding velocity at 50, 70, and 90 °C, at a maximum Hertzian pressure of 1.75 GPa

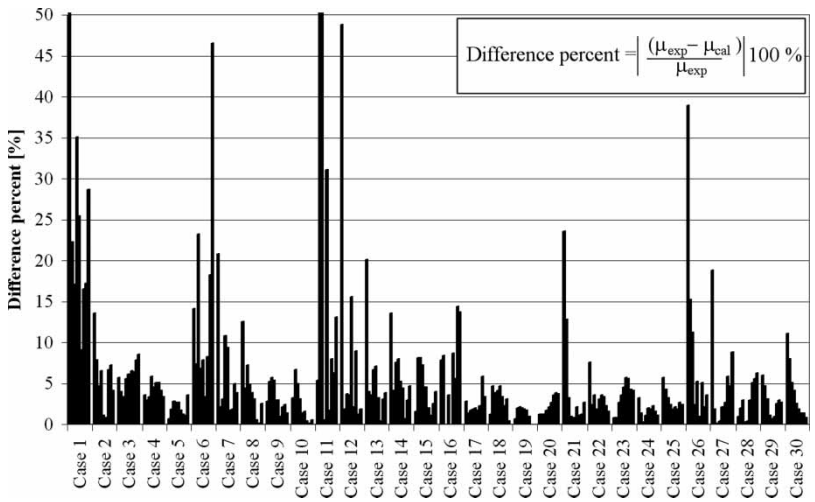

Fig. 6 The difference between the measured and calculated traction coefficient results for all the cases. Sliding velocities for each case, from left to right, are 0.05, 0.1, 0.15, 0.2, 0.3, 0.4, 0.6, 0.8, and 1.0 m/s. Cases 1–15 are results of PAO oil and cases 16–30 are results of mineral oil

less and it does not have a substantial effect on the traction results. Clarke *et al.* [**31**] also concluded, in their work with higher sliding velocities, that the faster surface is warmer than the slower disc. These results indicate that a more sophisticated model should be used if sliding velocities are very high.

Figures 7 and 8 show lubricant limiting shear stress and actual viscosity properties as a function of Hertzian pressure at several effective fluid temperatures. Lubricant properties were determined by the traction model, with the parameters fitting the experimental results. Fluid effective temperature is an estimate, is calculated in the model according to equation (9), and includes assumptions on the fluid inlet temperature and the temperature distribution across the film. However, the evaluation of the cases 1–5 with extended sliding velocity up to 3 m/s showed that the model and experimental traction coefficients accord well while using obtained lubricant properties from sliding velocity range 0–1 m/s.

The shapes of the limiting shear stress curves are fairly similar to corresponding results obtained in other measuring methods using a high-pressure chamber [**5**]. The results show that a decrease in temperature increases the limiting shear stress. The temperature behaviour is similar for both lubricants,

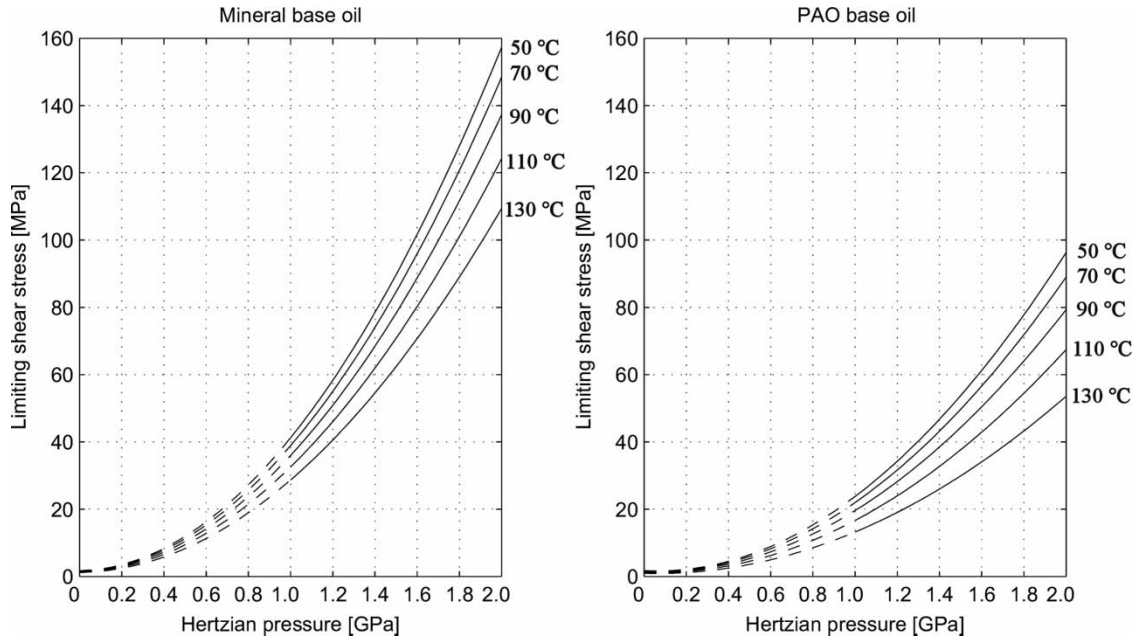

Fig. 7 The limiting shear stress of mineral and PAO oils as a function of pressure at different fluid temperatures

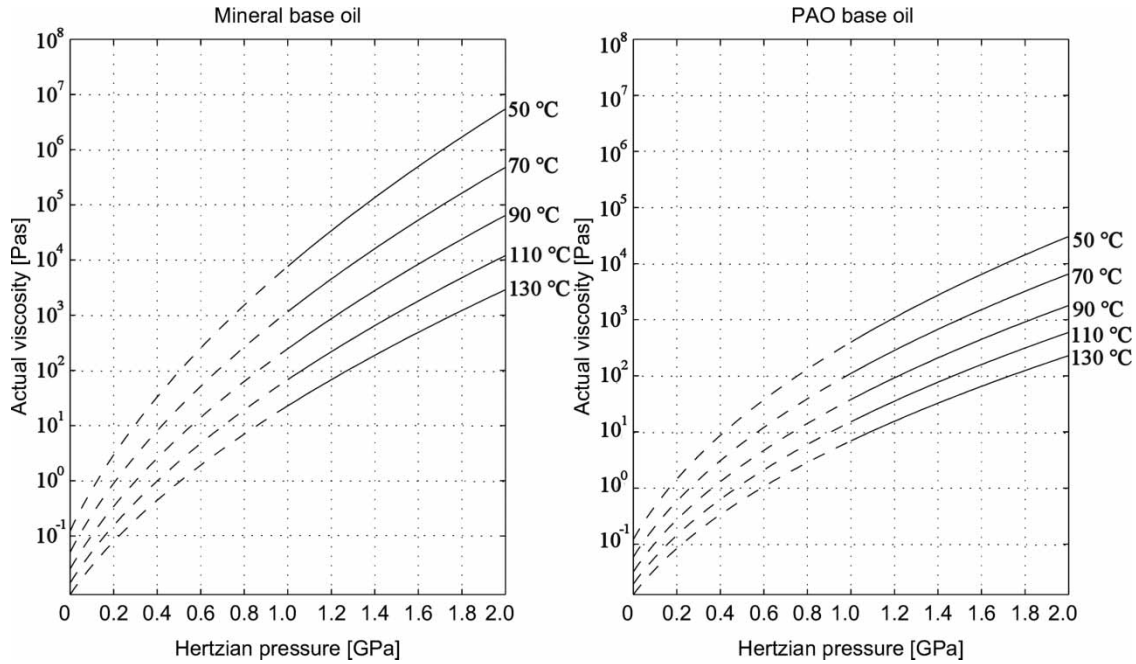

Fig. 8 The actual viscosity of mineral and PAO oils as a function of pressure at different fluid temperatures

but the influence of pressure is less significant for PAO oil than for mineral oil.

6 CONCLUSIONS

The objective of the work was to evaluate and develop further a method to determine the limiting shear stress and actual viscosity properties of lubricant using a numerical traction model and traction curves, measured at a wide range of temperatures and pressures with a twin-disc test device. The tests were performed in pure fluid film at high Hertzian pressures, which was possible due to the finely polished surfaces. The traction model is based on elliptical EHL contact with the non-Newtonian lubricant behaviour and surface-flash

temperature effects. The lubricant properties in the traction model were described in Roelands equation and limiting shear stress equations.

The properties of two different lubricants were measured by a wide range of operating conditions using a previously developed method. Each lubricant type was tested at 15 sets of conditions and each of which there was having nine separate test points resulting in 135 test points. Traction coefficients and bulk temperatures were obtained as a function of the sliding velocity, the Hertzian pressure, and the oil inlet temperature. The viscosity and limiting shear stress values used in the traction model were adjusted by iteration, so that the calculated results correlated with experimental values for all the test points. Generally, the calculated values correlate well with the experimental results. The corresponding mean difference for all PAO oil and mineral oil test points was 9 and 4 per cent, respectively.

The results show that a decrease in temperature increases the limiting shear stress. The influence of pressure on limiting shear stress and actual viscosity is less significant for PAO oil than for mineral oil, but the temperature has similar effects on both lubricants. As expected, PAO oil gives lower traction values than mineral oil.

The lubricant parameters obtained can be used as input values in gear-contact friction and power-loss calculations in future work.

ACKNOWLEDGEMENT

The authors gratefully acknowledge Neste Oil Oyj for providing the test lubricants.

REFERENCES

1 **Jacobson, B.** Measurement methods in tribology and their development. In Proceedings of the 12th Nordic Symposium on Tribology, Helsingør, Denmark, 2006.

2 **Fang, N., Chang, L., Johnston, G. J., Webster, M. N.,** and **Jackson, A.** An experimental/theoretical approach to modeling the viscous behavior of liquid lubricants under EHL conditions. In *Tribology research: from model experiment to industrial problem* (Eds G. Dalmaz, A. A. Lubrecht, D. Dowson, and M. Priest), Proceedings of the 27th Leeds–Lyon Symposium on *Tribology*, Lyon, France 2001, pp. 769–778 (Elsevier).

3 **Höglund, E.** and **Jabobson, B.** Experimental investigation of the shear strength of lubricants subjected to high pressure and temperature. *J. Tribol.*, 1986, **108**(4), 571–578.

4 **Höglund, E.** Influence of lubricant properties on elastohydrodynamic lubrication. *Wear*, 1999, **232**(2), 176–184.

5 **Jacobson B. O.** High-pressure chamber measurements. *Proc. IMechE, Part J: J. Engineering Tribology*, 2006, **220**(J3), 199–206.

6 **Wu, S.** and **Cheng, H. S.** Empirical determination of effective lubricant rheological parameters. *Tribol. Trans.*, 1994, **37**(1), 138–146.

7 **Ohno, N., Sunahara, K., Kumamoto, T.,** and **Hirano, F.** Prediction of liquid lubricant viscosity at high pressure from the density measurements. *Jpn. J. Tribol.*, 1999, **44**(4), 377–388.

8 **Bair, S.** Pressure–viscosity behaviour of lubricants to 1.4 GPa and its relation to ehd traction. *Tribol. Trans.*, 2000, **43**(1), 91–99.

9 **Moore, A. J.** The derivation of basic liquid flow properties from disc machine traction tests. In *Friction and traction*, Proceedings of the 7th Leeds–Lyon Symposium on *Tribology*, Leeds, UK, 1980, pp. 289–295.

10 **Jacobson, B.** A high pressure-short time shear strength analyzer for lubricants. *Trans. ASME J. Tribol.*, 1985, **107**, 220–223.

11 **Åhrström, B.-O.** *Friction in highly pressurized lubricants and its relation to therma-physical properties*. Doctoral Thesis, Luleå University of Technology, 2002.

12 **Workel, M. F., Dowson, D., Ehret, P.,** and **Taylor, C. M.** Design and development of a ball impact apparatus for the direct measurement of lubricant friction under high pressures and shear rates. *Proc. Instn Mech. Engrs, Part J: J. Engineering Tribology*, 2001, **215**, 211–222.

13 **Höglund, E.** The relationship between lubricant shear strength and chemical composition of the base oil. *Wear*, 1989, **130**, 213–224.

14 **Jacobson, B.** On the lubrication of heavily loaded spherical surfaces considering surface deformations and solidification of the lubricant. *Acta Polytech. Scand. Mech. Eng. Ser. 54*, 1970, p. 56.

15 **Höglund, E.** *Elastohydrodynamic lubrication, Interferometric measurements, lubricant rheology and subsurface stresses*. Doctoral Thesis, Luleå University of Technology, 1984.

16 **Ståhl, J.** and **Jacobson, B. O.** Compressibility of lubricants at high pressures. *Tribol. Trans.*, 2003, **46**, 592–599.

17 **Bair, S.** and **Winer, W. O.** The high shear stress rheology of liquid lubricants at pressures of 2 to 200 MPa. *Trans. ASME, J. Tribol.*, 1990, **112**, 246–253.

18 **King, H. E., Herbolzheimer, E.,** and **Crook, R. L.** The diamond-anvil cell as a high-pressure viscometer. *J. Appl. Phys.*, 1992, **71**, 2071–2080.

19 **Bair, S.** Measurements of real non_Newtonian response for liquid lubricants under moderate pressures. *Proc. Instn Mech. Engrs, Part J: J. Engineering Tribology*, 2001, **215**, 223–233.

20 **Johnson, K. L.** and **Cameron, R.** Shear behaviour of EHD oil film at high rolling contact pressure. *Proc. Instn Mech. Engrs, Part I: J. Systems and Control Engineering*, 1967, **182**, 307–319.

21 **Johnson, K. L.** and **Tevaarwerk, J. L.** Shear behaviour of elastohydrodynamic oil films. *Proc. R. Soc., Ser. A*, 1977, **356**, 215–236.

22 **Kleemola, J.** and **Lehtovaara A.** Introduction on high pressure twin disc test device. *Finn. J. Tribol.*, 2006, **25**, 8–17.

23 **Kleemola, J.** and **Lehtovaara A.** Experimental evaluation of friction between contacting discs for simulation of gear contact. *Tribotest*, 2007, **13**(1),13–20.

24 Lehtovaara, A. Calculation of sliding power loss in spur gear contacts. *Tribotest*, 2002, **9**(1), 23–34.

25 Hedlund, J. and **Lehtovaara, A.** Influence of lubricant on sliding friction in spur gear contacts. In Proceedings of the 10th Nordic Symposium on Tribology, Tromsø, Norway, 2002, pp. 55–64.

26 Hamrock, B. *Fundamentals of fluid film lubrication*, 1994, p. 690 (McGraw-Hill, Inc., New York).

27 Wu, S. and **Cheng, H. S.** A friction model of partial-EHL contacts and its application to power loss in spur gear. *Tribol. Trans.*, 1991, **34**, 398–407.

28 Gecim, B. and **Winer, W. O.** Lubricant limiting shear stress effect on EHD film thickness. *J. Lubr. Tech.*, 1980, **102**, 213–221.

29 Jaeger, J. C. Moving sources of heat and the temperature at sliding contacts. *Proc. R. Soc.*, 1942, **76**, 203–224.

30 Larsson, R., Larsson, P. O., Eriksson, E., Sjöberg, M., and **Höglund, E.** Lubricant properties for input to hydrodynamic and elastohydrodynamic lubrication analyses. *Proc. Instn Mech. Engrs, Part J: J. Engineering Tribology*, 2000, **214**, 17–27.

31 Clarke, A., Sharif, K. J., Evans, H. P., and **Snidle, R. W.** Elastohydrodynamic modelling of heat partition in rolling-sliding point contact. *Proc. IMechE, Part J: J. Engineering Tribology*, 2007, **221**(J3), 223–235.

32 Roelands, C. J. A. *Correlation aspects of the viscosity–temperature–pressure relationship of lubricating oils*, 1966 (Druk. V.R.B., Groningen, The Netherlands).

33 Höhn, B.-R., Michaelis, K., and **Doleschel, A.** Limitations of bench testing for gear lubricants. *ASTM Spec. Tech. Publ. 1404*, 2001, 15–32.

34 Höhn, B.-R., Michaelis, K., and **Doleschel, A.** Frictional behaviour of synthetic gear lubricants. In *Tribology research: from model experiment to industrial problem* (Eds G. Dalmaz, A. A. Lubrecht, D. Dowson, and M. Priest), Proceedings of the 27th Leeds–Lyon Symposium on *Tribology*, Lyon, France 2001, pp. 759–768 (Elsevier).

APPENDIX

Notation

a	semi-major axis of the Hertzian contact ellipse
$a_{1,2,3,4,5}$	constant
b	semi-minor axis of the Hertzian contact ellipse
c	specific heat
C_Z	non-dimensional constant in the Roelands viscosity equation
D_Z	non-dimensional constant in the Roelands viscosity equation
E	elasticity modulus
E'	reduced modulus of elasticity, $1/E' = 1/2[(1-\nu_1^2)/E_1 + (1-\nu_2^2)/E_2]$
F_N	normal force
F_μ	traction force
G	dimensionless material parameter, $G = \alpha E'$
G_0	non-dimensional constant in the Roelands viscosity equation
G_∞	limiting elastic shear modulus
h	film thickness
k	thermal conductivity
k_e	ellipticity parameter
p	fluid film pressure
p_o	maximum Hertzian pressure, $p_o = (3F_N/(2\pi ab))$
$\bar{p}$	mean fluid pressure
q	specific heat generation
R	reduced radius of curvature, $1/R = 1/((1/R_{x1}) + (1/R_{x2})) + 1/((1/R_{y1}) + (1/R_{y2}))$
Ra	surface Ra-value
R_x	radius of disc in x direction
R_y	radius of disc in y direction
S_0	non-dimensional constant in the Roelands viscosity equation
T	temperature
T_{bulk}	disc bulk temperature
T_{ref}	reference temperature
T_0	surface bulk temperature in rolling point
u	surface velocity
U	dimensionless load parameter, $U = \eta_0 V_R/E'R$
V_R	rolling velocity, $V_R = (u_1 + u_2)/2$
V_S	sliding velocity, $V_S = u_1 - u_2$
W	dimensionless load parameter $W = F_N/E'R^2$
x	coordinate
y	coordinate
z	coordinate
α	viscosity pressure coefficient
$\dot{\gamma}$	shear strain rate
η	actual viscosity
η_0	viscosity at atmospheric pressure
Λ	h/σ
μ	traction coefficient
μ_{cal}	calculated traction coefficient
μ_{exp}	experimental traction coefficient
ν	Poisson ratio
ρ	density
σ	combined surface rms roughness, $\sqrt{(1.3 \cdot \mathrm{Ra}_1)^2 + (1.3 \cdot \mathrm{Ra}_2)^2}$
τ	shear stress
τ_L	limiting shear stress
$\bar{\tau}_L$	mean limiting shear stress
ϕ_T	thermal reduction factor
ω	angular velocity

Subscripts

f	fluid
1	surface 1
2	surface 2

Paper IV

Kleemola, J. and Lehtovaara A.

Experimental simulation of gear contact along the line of action

Tribology International, 2009, 42(10), 1453-1459.

Tribology International 42 (2009) 1453–1459

Contents lists available at ScienceDirect

Tribology International

journal homepage: www.elsevier.com/locate/triboint

Experimental simulation of gear contact along the line of action

Jaakko Kleemola *, Arto Lehtovaara

Department of Mechanics and Design, Tampere University of Technology, P.O. Box 589, 33101 Tampere, Finland

ARTICLE INFO

Article history:
Received 29 September 2008
Received in revised form
23 January 2009
Accepted 2 June 2009
Available online 10 June 2009

Keywords:
Twin-disc
Gear
Line of action
Simulation

ABSTRACT

In highly loaded gears, lubricated rolling/sliding contact conditions change greatly along the line of action. This leads to variation in gear frictional properties and to failures such as pitting and scuffing that take place in different positions along the tooth flank. Information on instant contact behavior is therefore very useful, but this kind of measurement in real gears is extremely complicated. Single spur gear geometry has been simulated at 38 steady-state measuring points along the line of action using a twin-disc test device focusing on the friction coefficient and on temperature and lubrication conditions. Twin-disc simulations were adjusted to match real gear experiments by using similar maximum Hertzian pressure and surface velocities. The results show that the curve shapes for the mean friction coefficient as a function of pitch line velocity are similar to the corresponding experimental results with real gears. Further, the calculated thermal Λ-values of real gears and the measured mean contact resistance correspond well. This approach shows potential for simulating gear friction and failure mechanisms along the line of action.

1. Introduction

Highly loaded lubricated rolling/sliding contacts are common in various machines and machine elements. Typical examples are rolling bearings and gears. In the case of gears, contact conditions change greatly along the line of action. This leads to variations in the gear frictional properties and to failures such as pitting and scuffing that take place at different positions along the tooth flank. Information on instant contact behavior is therefore very useful in gaining a deeper understanding of these phenomena. This provides the basic information for estimation of gear train power losses and their lifetime.

Very often spur gear profiles are approximated by cylinders with the same radius of curvature as the gear teeth at the instant contact point, as shown in Fig. 1. This provides the basis of the twin-disc test devices, which typically represents only a single point along the line of action in real gears at constant load and speed conditions. In addition, Höhn et al. [1] list three main differences when gear and twin-disc contact is compared: (1) they have different kinds of surface topography and orientation, (2) film formation is continuous in discs but on gears a new oil film has to build up with every new engagement and (3) dynamic effects on discs are significantly smaller than in gears. Usually the arithmetic mean surface roughness (R_a-value) in discs is around 0.1 μm, which is four times less than the R_a-values in modern gears. Gear grinding is always done perpendicular to the rolling direction, while disc surfaces are nearly always finished along a line parallel to the rolling direction. The grinding direction affects the lubricant film thickness [2]. The manufacturing tolerances are smaller for twin-disc than for real gears.

Twin-disc test devices have been used widely to study gear related issues such as the influence of surface roughness on friction [2–4], lubricant rheological properties [5–11], development of coatings [12] or different kinds of surface failures [13–17]. Comparisons have been made between twin-disc and gear surface contact behavior in terms of film thickness, pressure and temperature distribution as well as in terms of surface failures [18–20]. In many gear power loss studies twin-disc results have been used as a reference measurement to verify calculated friction results [1,21,22]. However, the vast majority of the measurements have been made over a limited range of parameters, which do not cover all the conditions which exist for a gear pair contact along the line of action. This limits the comparisons which can be made between mean friction values obtained from twin-disc and those from gear tests. In real gear tests, the mean friction coefficient along the line of action is, in practice, the only friction value which can be measured.

The objective of this work is to evaluate gear contact along the line of action using a twin-disc test device focusing on the friction coefficient, the temperature and lubrication condition. An attempt is made to compare overall friction behavior in the twin-disc test device with that in real gear contacts as well as to show the measured data along the line of action. The details of the measured results are discussed.

* Corresponding author.
E-mail address: jaakko.kleemola@tut.fi (J. Kleemola).

0301-679X/$ - see front matter © 2009 Elsevier Ltd. All rights reserved.
doi:10.1016/j.triboint.2009.06.007

Nomenclature

b	half-width of Hertzian contact region
F_N	normal load
F_{Nmax}	maximum normal load
h	film thickness
M_{bear}	bearing friction moment
n	rotating speed
p	Hertzian pressure
p_{max}	maximum Hertzian pressure
r	radius of test disc
R_a	surface roughness R_a value
R_{ku}	kurtosis
R_q	root mean square roughness
R_{sk}	skewness
R_z	average of ten greatest peak-to-valley
u	surface velocity
u_{max}	maximum surface velocity
x	coordinate
y	coordinate
z	coordinate
η	viscosity
φ_T	thermal reduction factor
Λ	h/σ
μ	friction coefficient
ρ	radius
σ	combined surface rms roughness
σ_{max}	max. combined surface rms roughness
ω	angular velocity
ζ	density

Subscripts

1	disc 1
2	disc 2

2. Experimental

2.1. Test device

Simulated gear friction tests were performed with a previously developed twin-disc test device, which is described in more detail in Refs. [23,24]. In a twin-disc test device each disc is driven by a separate electric motor with adjustable rolling and sliding speeds. Loading and speeds can be varied on-line with automated computer control, which allows flexible testing.

The lubrication of the test disc is performed with circulating lubrication system where oil inlet temperature and flow rate are controlled and measured. Other measured signals from the twin-disc test device include the bulk disc temperature, mean contact resistance and friction moment in addition to load and shaft rotation speeds. The disc bulk temperature is measured 3 mm below the surface with a thermocouple and the signal is transmitted from the axle using a telemetry device. The mean contact resistance measurement was introduced into the test device to analyze the contact lubrication conditions. When there is no metal to metal contact the mean contact resistance is 1 kΩ but as metal to metal contact increases the mean contact resistance approaches 0 Ω. Signals are collected on a sampling card and are used both for on-line analysis and for later processing.

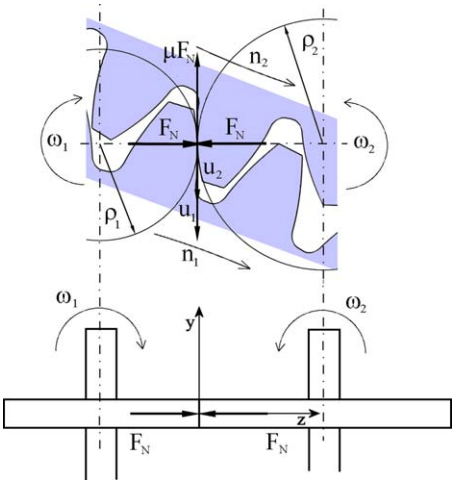

Fig. 1. Instant gear tooth contact and its approximation to equivalent cylinders.

The friction moment is measured from shaft 1 and includes components from supporting bearings and disc contact losses. Every test point was measured twice once in each sliding direction. This was carried out by reversing the speeds of the faster and slower rotating discs and it enables exclusion of the bearing losses from the measured friction moment as well as measurements of the bulk temperatures of both the slower and faster discs.

The disc contact conditions were designed to be as close as possible to real gear contacts in terms of line of action, material, grinding direction and surface roughness.

2.2. Test discs

The material for the test discs is case-hardening steel 20 NiCrMo2-2. The discs are case-hardened to a depth of 0.8–1 mm, with a specific surface hardness of 60–62 HRC. The test discs have a diameter of 70 mm and a thickness of 10 mm. They were ground in a direction perpendicular to the rolling direction to give a raised crown with a radius of 292 mm. This corresponds to the real gear flank surface topography, which is very seldom used in other studies. The grinding procedure is described in more detail in Ref. [23]. The surface roughness of the test discs was measured with a Wyko NT1100 optical profiler, which gives 3D-data from the disc surface. Table 1 shows the typical values of surface roughness parameters and their standard deviations. The parameters have been calculated from 1807 separate lines in the rolling direction of the surface, which was 1.24 mm long in the rolling direction and 6 mm wide. The surface roughness R_a-values of the test disc after the friction tests was close to 0.25 μm. This was more than half the surface roughness R_a-values

Table 1
Disc surface roughness parameters at the rolling direction.

Parameter		Mean (μm)	Std. dev. (μm)
Root mean square roughness	R_q	0.33	0.053
Average roughness	R_a	0.25	0.036
Average of the ten greatest peak-to-valley	R_z	1.58	0.27
Kurtosis	R_{ku}	4.85	3.85
Skewness	R_{sk}	−0.94	0.38

usually found in gears, which is better than the value usually used in twin-disc tests according to Höhn et al. [1].

2.3. Test procedure and test matrix

The test conditions for gear simulation were adjusted in line with real gear experiments with modified FZG test rig carried out by Järviö and Lehtovaara [25]. The main features of the test gears manufactured according to SFS 3390 are shown in Table 2.

The test gears were case hardened and the measured combined rms surface roughness after the tests varied between 0.54 and 0.64 μm. Gear measurements were made in a boundary and mixed lubrication regime according to the Λ-value, which was estimated by dividing the isothermal pitch point minimum film thickness [26] by combined rms surface roughness. The tests were made with one load level and five different rotation speeds. Both gear boxes were lubricated with a constant oil flow of 2.5 l/min in the mesh. Two lubricants, whose viscometric properties are shown in Table 3, were tested. Results are presented in more detail in Ref. [25].

The dimensionless distribution of normal force (F_N/F_{Nmax}), Hertzian maximum line pressure (p/p_{max}), surface velocities (u/u_{max}) and combined radius of curvature (ρ/ρ_{max}) along the line of action for the gear pair described in Table 2 are shown in Fig. 2a (upper). The teeth engagement starts at the left of the figure and the two sharp changes in load and pressure take place when two tooth engagement changes to single tooth engagement and the reverse. At the pitch point pure rolling is present, i.e. the sliding velocity $V_s = (u_1 - u_2)$ is zero. The rolling velocity is given by as $V_R = (u_1 + u_2)/2$.

The target was to create similar maximum Hertzian pressure and surface velocities, i.e. rolling and sliding velocities, in the twin-disc contact along the line of action. However, in the gear contact the combined radius changes along the line of action, but in the twin-disc contact this radius is constant. This is compensated for by changing the normal force according to Fig. 2a (lower) to obtain similar maximum Hertzian pressure at the midplane ($y = 0$) of the twin-disc elliptical contact. These similar rolling and sliding velocities can be obtained by separately adjusting the rotation speeds of the two discs with automated computer control.

Fig. 2b shows the detailed test points in the test cases 3 and 8, which will be described in Table 4. The simulation consists of 38 points along the line of action. Two lubricants were used. These were similar to those used in previous gear tests except that they were from different batches. The test discs were lubricated at a constant oil flow of 6 l/min.

The twin-disc tests were performed according Table 4, where maximum Hertzian pressure and surface velocity are given as minimum and maximum values along the line of action.

At the beginning of every test the device was warmed up for 1 h before starting measurements by circulating lubricant, at the test temperature, to achieve constant temperature conditions. The first test measurement was carried out under pure rolling conditions, i.e. at pitch point, for 30 min. After that, the steady state test points were measured according to Fig. 2b by moving left along the line of action. When that was complete the test device was returned to the pure rolling point and the rest of the test measurements made by moving right along the line of action. Each point was tested for 7 min except the rolling point and points where Hertzian pressure reduced rapidly. These points were tested for 37 min to achieve stable temperatures conditions. The mean value of each measured signal was calculated for the last 2 min for every test point.

Table 2
Main features of the simulated test gears.

Parameter		Pinion		Gear
Number of teeth	–	20		20
Pressure angle	deg		20	
Helix angle	deg		0	
Gear ratio	–		1	
Center distance	mm		91.5	
Normal module	mm		4.5	
Profile shift	–	0.176		0.176
Face width	mm	20		20
Contact ratio	–		1.45	

Table 3
Mian viscometric properties of test lubricants.

Type	Min	PAO
η at 40 °C, mm^2/s	210	205
η at 100 °C, mm^2/s	18	27
ζ at 15 °C, kg/m^3	891	834
VG class, –	220	220

3. Results and discussion

First of all, it was essential to find out how well the trends in lubrication conditions in the real gear match those in the twin-

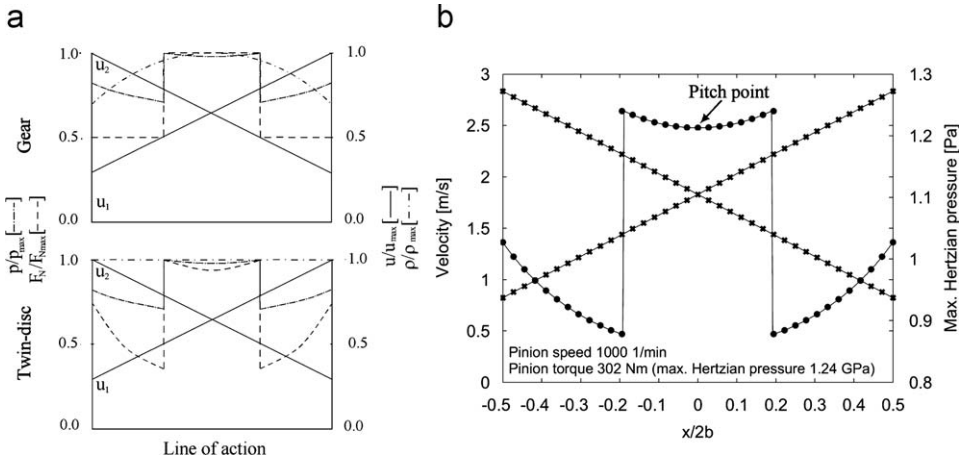

Fig. 2. Gear contact simulation using twin-disc device.

Table 4
Twin-disc test conditions.

Case	Hertzian max. pressure (GPa)	Surface velocities (m/s)	Pitch line velocity (m/s)	Oil inlet tem. T_{oil} (°C)	Oil type
1	1.24	1.65–5.67	0.96	60	Min
2	1.24	1.24–4.25	2.87	60	Min
3	1.24	0.82–2.83	4.80	60	Min
4	1.24	0.49–1.70	7.19	60	Min
5	1.24	0.17–0.57	9.58	60	Min
6	1.24	1.65–5.67	0.96	60	PAO
7	1.24	1.24–4.25	2.87	60	PAO
8	1.24	0.82–2.83	4.80	60	PAO
9	1.24	0.49–1.70	7.19	60	PAO
10	1.24	0.17–0.57	9.58	60	PAO

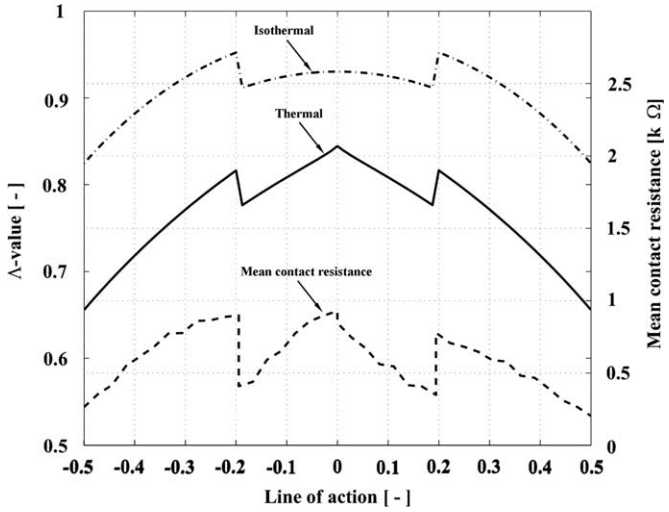

Fig. 3. The calculated isothermal (dash dot line) and thermal (solid line) Λ-values in gear line contact together with the measured mean contact resistance (dashed line) in case 2.

disc device along the line of action. This evaluation was done by calculating the isothermal and thermal Λ-values of real gears along the line of action and comparing these with the measured mean contact resistance, as shown in Fig. 3. The isothermal Λ-values were estimated by dividing the isothermal minimum film thickness [26] by the combined rms surface roughness. The thermal Λ-values multiplies the isothermal Λ-values by the thermal reduction factor [27], which takes into account the effect of velocity, i.e. temperature on film thickness.

Fig. 3 shows that the shape of the curves of the thermal Λ-values and the measured mean contact resistance correspond well, indicating that twin-disc measurements properly simulate the change of lubrication conditions in real gears. In disc contact the thermal Λ-values (0.5…2) are higher than in real gear contact due to lower surface roughness. At the lowest Λ-values, cases 5 and 10, measured mean contact resistance values no longer have a clear dependence on Λ-values and in the full ehl regime it will indicate only a possible disturbance of the film.

The second essential issue is to study the behavior of the mean friction coefficient along the line of action, which can also be measured in real gears. In the twin-disc case, the mean friction coefficient is a mean value of the friction based on 38 separate test points along the line of action. The mean friction coefficients for mineral and PAO lubricants from real gears [25] and from corresponding twin-disc simulations, as a function of gear pitch line velocity, are shown in Fig. 4.

Fig. 4 shows that the shape of the mean friction coefficient curves are similar for both lubricants, indicating that the twin-disc measurements properly simulate the friction behavior trends in real gears. However, there are clear differences in absolute friction values. In test gears the surface R_a-values were about 0.32 μm, and in twin-disc tests they were about 0.25 μm. Three separate test points 1, 2 and 3 are marked in Fig. 4. The calculated thermal Λ-value at pitch point for real gear test point 1 is 0.99 and for the simulated points 2 and 3 the corresponding values are 1.83 and 1.12, respectively. In the test points 1 and 3 the Λ-values are nearly the same and, in fact, the simulated and gear test friction coefficients are almost equal. This indicates that the main reason for the difference in absolute friction coefficient values is caused by surface roughness differences in discs and gears. A previous study [28] also supports this conclusion. Other possible reasons for this friction difference are the temperature difference between gear and disc contact and/or the fact that there is a continuous lubricant film on discs whereas on gears a new oil film has to build up with every new tooth engagement.

Twin-disc measurements are quicker and more cost effective to implement than real gear measurements. The twin-disc simulations give more local information about the friction coefficient, lubrication regime and temperature along at the line of action as shown in Fig. 4. This is essential for evaluation of gear failures. For example, it is generally known that pitting failure occurs at the point where contact pressure is still high (one tooth pair engagement), but sliding has already begun. The simulated results at this location, +0.1…+0.2 of the line of action, give logically high friction values combined with high temperatures and low film thickness, resulting in a increased risk of failure. Gear pitting tests cannot provide all that local information.

Scuffing is known to take place near the start and end points of tooth engagement, which shows again the effect of low film thickness and very high temperatures due to high sliding velocity. However, it must be noted that temperature build up, especially at tip and the root of the tooth flank, may include differences between simulated disc and real gear results. Yi and Quinonez [29] measured gear surface temperatures at five points along the line of action and they found that the highest temperature was close to the tooth dedentum. They concluded that even though the maximum sliding and maximum frictional power loss was at the tip of tooth, the highest temperature occurs at the tooth root. This was because of the windage effect produced by the rotational motion of the gear and the larger surface area at the tip circle for heat distribution. Otherwise a similar kind of surface temperature behavior was observed in gears and in twin-discs, i.e. the lowest temperature was at the pitch point and the temperature increased as the surface sliding velocity increased.

The results in Fig. 5 summarize all friction simulations made in different rolling and sliding velocities with twin-discs. In all cases mineral base oil gives higher friction coefficients than PAO base

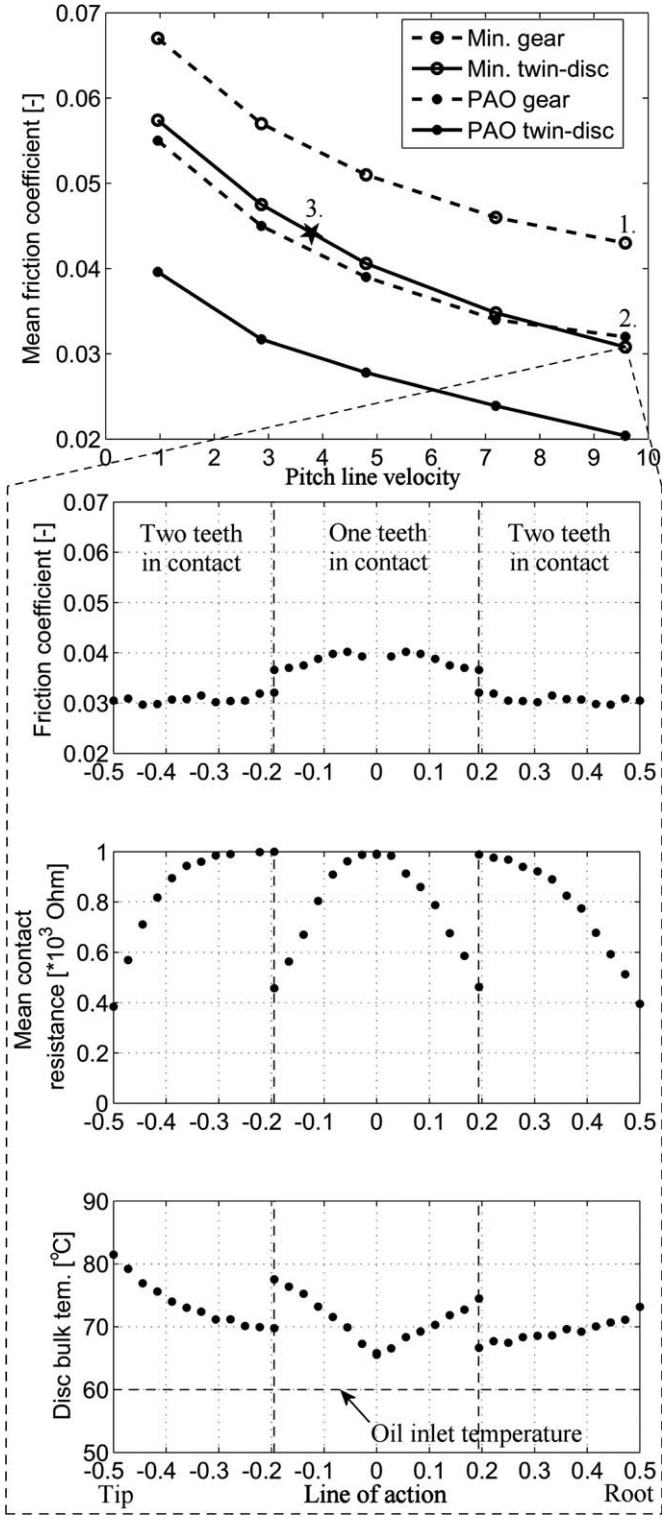

Fig. 4. The mean friction coefficient as a function of pitch line velocity from real gear tests and corresponding twin-disc tests together with the detailed view of simulated friction results in test case 1.

oil. An increase in the rolling velocity decreases the friction coefficient, because oil film thickness increases and the share of high boundary (asperity) friction decreases so that friction is mainly caused by lubricant shear stress. In the one tooth engagement zone the friction coefficient even starts to decrease with increasing distance from pitch point in high rolling/sliding velocities with mineral oil, indicating that it reaches the thermal friction region earlier than with PAO oil.

An interesting feature is the fact that in the area where two tooth engagement changes to single tooth engagement the friction coefficient begins to increase, when the rolling velocity decreases with both lubricants. A somewhat reverse situation occurs at high rolling velocities with mineral oil. In fact, the detailed frictional behavior in gear contact is a complicated result of the interaction of many different parameters leading to different outcomes, depending on operation conditions. A deeper analysis of the detailed friction behavior will be carried out with a gear contact friction model in future.

The sensitivity of measurements and the time scale for changes in lubrication conditions can be demonstrated by analyzing the slight variation with lubricant inlet temperature. The lubricant inlet temperature variation in a range of 58–61 °C and its effects on disc temperature, mean contact resistance and friction moment are shown in Fig. 6.

The results in Fig. 6 show clearly that the disc temperature, the mean contact resistance and the friction moment all logically follow changes in the lubricant inlet temperature, i.e. an increase of inlet temperature increases the bulk temperature and decreases the film thickness, thus increasing the friction moment. A lubricant inlet temperature increase of 2 °C reduces the calculated isothermal film thickness from 1.12 to 1.05 μm and this is clearly shown by the change in contact resistance. The friction moment also varies but its amplitude is not as significant as that of the mean contact resistance and the disc temperature. It can be also deduced that contact lubrication situation is sensitive for temperature changes. In gearboxes, this means that even slight changes in lubricant inlet temperature can alter the wear and friction behavior when gears are operated in mixed or boundary lubrication areas.

4. Conclusions

The objective of this work was to evaluate gear contact along the line of action using a twin-disc test device focusing on friction coefficient, temperature and lubrication conditions. Twin-disc simulations were adjusted to match real gear experiments by using similar maximum Hertzian pressure and surface velocities, i.e. rolling and sliding velocities, along the line of action. Single spur gear geometry was simulated with different pinion velocities and two different lubricants at 38 different steady-state measuring points along the line of action.

Mean contact resistance measurement was applied to characterize contact lubrication conditions. The calculated thermal Λ-values of real gears and the measured mean contact resistance correspond well. Further, the curve shape of the measured mean friction coefficient as a function of pitch line velocity is similar in real gear tests and in the corresponding twin-disc tests. The lower friction coefficient obtained with the twin-disc device is mainly explained by the better surface quality of the discs compared to real gears. These results indicate that twin-disc measurements properly simulate the change of lubrication conditions and the friction behavior trends in real gears.

The twin-disc simulations give more local information about the friction coefficient, lubrication conditions and temperature along at the line of action than the real gear measurements. This has potential when the mechanisms of gear failures are being evaluated. The simulated results showed local high friction values combined with high temperature and low film thickness, i.e. an increased risk of failure in locations that correspond to points where pitting and scuffing failures occur in real gears. However, it should be noted that temperature build up, especially at the tip

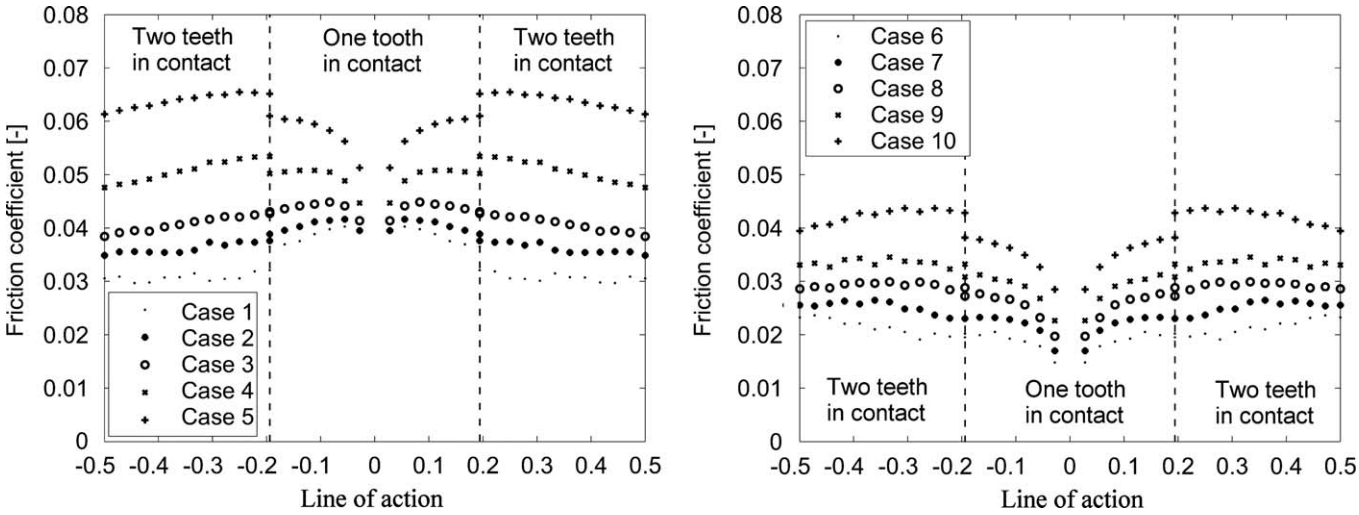

Fig. 5. The simulated friction coefficients along the line of action for mineral oil (left) and for PAO oil (right), Table 4.

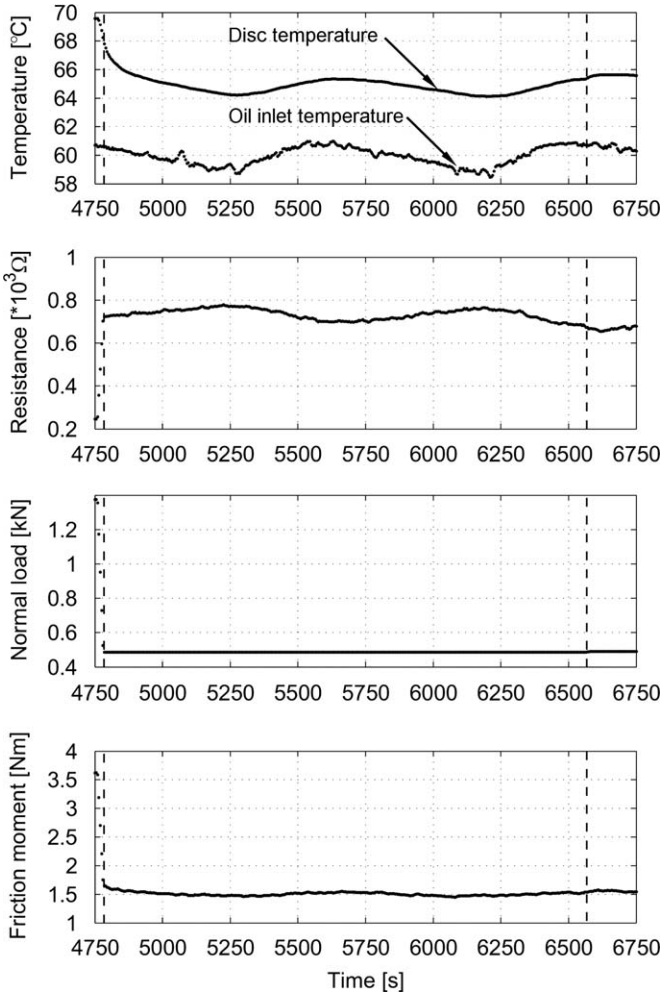

Fig. 6. The variation of the lubricant inlet temperature and its effect on disc temperature, mean contact resistance and friction moment. Inside the vertical dashed lines $u_1 = 2.16$ m/s, $u_2 = 3.33$ m/s and $F_N = 492$ N.

and at the root of the tooth flank, may include differences between simulated disc and real gear results. It was also demonstrated that contact lubrication conditions are sensitive to temperature changes.

The measured results show that mineral base oil reaches the thermal friction region with a lower sliding velocity than with PAO. The step-type increase in friction coefficient was observed at low rolling velocities when single tooth engagement changes to two tooth engagement, i.e. load decreases, but reversing step occurs at high rolling velocities.

The simulation of gear contact along the line of action using a twin-disc test device provides a better understanding of gear friction and failure mechanisms and models for evaluating them.

Acknowledgment

The authors gratefully acknowledge Neste Oil Oyj for providing the test lubricants.

References

[1] Höhn B-R, Michaelis K, Doleschel A. Frictional behaviour of synthetic gear lubricants. In: Proceedings of the 27th Leeds–Lyon symposium on tribology, 2000. Amsterdam: Elsevier; 2001. p. 759–68.
[2] Höhn B-R, Michaelis K, Kreil O. Influence of surface roughness on pressure distribution and film thickness in EHL-contacts. Tribol Int 2006;39(12): 1719–25.
[3] Xiao L, Björklund S, Rosen BG. The influence of surface roughness and the contact pressure distribution on friction in rolling/sliding contacts. Tribol Int 2007;40(4):694–8.
[4] Nanbu T, Chiba N, Kano M, Ushijima K. Effect of surface roughness on elastohydrodynamic traction: part 1. Lubr Sci 2005;17(3):281–93.
[5] Bair S, Winer WO. Friction/traction measurements with continuously variable slide-roll ratio and slide slip at various lambda ratios. In: Proceedings of the seventh Leeds–Lyon symposium on tribology, 1980. Guildford: Westbury House; 1981. p. 296–301.
[6] Johnson KL, Nayak L, Moore AJ. Determination of elastic shear modulus of lubricants from disc machine tests. In: Proceedings of the fifth Leeds–Lyon symposium on tribology, 1978. Mechanical Engineering Publication Limited: London; 1979. p. 204–8.
[7] Moore AJ. The derivation of basic liquid flow properties from disc machine traction tests. In: Proceedings of the seventh Leeds–Lyon symposium on tribology, 1980. Guildford: Westbury House; 1981. p. 289–95.
[8] Wu S, Cheng HS. Empirical determination of effective lubricant rheological parameters. Tribol Trans 1994;37(1):138–46.
[9] Johanson KL, Tevaarwerk JL. Shear behaviour of elastohydrodynamic oil films. Proc R Soc Lond Ser A 1977;356:215–36.
[10] Muraki M, Konishi S. Traction characteristics of an ehl oil film at high rolling speeds. In: Proceedings of the international tribology conference, Nagasaki, 2000. p. 597–602.
[11] Itoigawa F, Hakamata R, Nakamura T, Matsubara T. Study on ehl traction response at small slide–roll ratio. In: Proceedings of the international tribology conference, Nagasaki, 2000. p. 591–96.
[12] Amore RI, Martins RC, Seabra JO, Renevier NM, Teer DG. Molybdenum disulphide/titanium low friction coating for gears application. Tribol Int 2005;38(4):423–34.

[13] Widmark M, Melander A. Effect of material, heat treatment, grinding and shot peening on contact fatigue life of carburized steels. Int J Fatigue 1999;21(4):309–27.
[14] Oila A, Bull SJ. Assessment of the factors influencing micropitting in rolling/sliding contacts. Wear 2005;258(10):1510–24.
[15] Patching MJ. The effect of surface roughness on the micro-elastohydrodynamic lubrication and scuffing performance of aerospace gear tooth contacts. PhD dissertation, University of Wales; 1994. p. 259.
[16] Ville F, Nelias D, Tourlonias G, Flamand L, Sainsot P. On the two-disc machine: a polyvalent and powerful tool to study fundamental and industrial problems related to elastohydrodynamic lubrication. In: Proceedings of the 27th Leeds–Lyon symposium on tribology, 2000. Amsterdam: Elsevier; 2001. p. 393–402.
[17] Cheng W, Tu W. Semi-analytical modeling of spalling life of spur and helical gears. In: Proceedings of the 27th Leeds–Lyon symposium on tribology, 2000. Amsterdam: Elsevier; 2001. p. 599–605.
[18] Höhn B-R, Michaelis K, Kopatsch F. Determination of film thickness, pressure and temperature in elastohydrodynamic lubrication in the past 20 years in Germany. Proc Inst Mech Eng Part J 2001;215(3):235–42.
[19] Simon M. Messung von elasto-hydrodynamischen parametern und ihre auswirkung auf die grübchentragfähigkeit vergüteter scheiben und zahnräder. PhD dissertation, Technischen Universität München; 1984. p. 203.
[20] Höhn B-R, Michaelis K, Doleschel A. Limitations of bench testing for gear lubricants. ASTM Spec Tech Publ 2001;1404:15–32.
[21] Diab Y, Ville F, Velex P. Prediction of power losses due to tooth friction in gears. Tribol Trans 2006;49(2):260–70.
[22] Castro J, Seabra J. Coefficient of friction in mixed film lubrication: gear versus twin-discs. Proc Inst Mech Eng Part J 2007;221(3):399–411.
[23] Kleemola J, Lehtovaara A. Development of a high pressure twin disc test device for simulation of gear contact. Finn J Tribol 2006;25(2):8–17.
[24] Kleemola J, Lehtovaara A. Experimental evaluation of friction between contacting discs for simulation of gear contact. Tribotest 2007;13(1):13–20.
[25] Järviö O, Lehtovaara A. Experimental study of influence of lubricants on friction in spur gear contacts. Finn J Tribol 2002;21(1):20–7.
[26] Dowson D, Higginson GR. Elastohydrodynamic lubrication: the fundamentals of roller and gear lubrication. London: Pergamon Press; 1966.
[27] Wu S, Cheng HS. A friction model of partial-ehl contacts and its application to power loss in spur gear. Tribol Trans 1991;34:398–407.
[28] Johnson KL, Spence DI. Determination of gear tooth friction by disc machine. Tribol Int 1991;24(5):269–75.
[29] Yi J, Quinonez PD. Gear surface temperature monitoring. Proc Inst Mech Eng Part J 2005;219(2):99–105.

Paper V

Kleemola, J. and Lehtovaara A.

Evaluation of lubrication conditions in gear contacts using contact resistance and bulk temperature measurements

Proceedings of the Institution of Mechanical Engineers, Part J: Journal of Engineering Tribology, 2010, **224**(4), 367-375.

Evaluation of lubrication conditions in gear contacts using contact resistance and bulk temperature measurements

J Kleemola* and **A Lehtovaara**
Department of Mechanics and Design, Tampere University of Technology, Tampere, Finland

The manuscript was received on 9 May 2009 and was accepted after revision for publication on 20 November 2009.

DOI: 10.1243/13506501JET675

Abstract: Lubrication conditions have a major effect on lifetime and friction in gear contacts. Monitoring of relative changes in protecting film thickness provides an opportunity to understand the operating conditions before an initial fault appears. In this study, the lubrication conditions were detected on-line using contact resistance and bulk temperature measurements, which were applied to a modified FZG gear test device. Measurements were made with polished gear surfaces at operating conditions that are typical of industrial gears. The presented mean contact resistance includes the data points in different positions along the line of action and thus also considers transient effects. The bulk temperature and trend curves of the mean contact resistance at different pitch line velocities, loads, and oil inlet temperatures are reported and discussed as measures for analysing the lubrication condition.

Keywords: gear, lubrication condition, contact resistance, bulk temperature, polished surfaces

1 INTRODUCTION

The main task of a lubricant is to decrease friction and wear in contacting surfaces so that machine components have a satisfactory life. Decreased friction causes a reduced tangential force and surface temperature and further reduces the risk of overheating and surface damage. The lubrication regimes and friction are typically described by using the Stribeck curve. The boundary lubrication regime can be related to low velocity (or low ηV_R – value). In this regime, the friction coefficient is normally high, because the shear stress comes mainly from asperity contacts that carry the load. A mixed lubrication regime is achieved by increasing the velocity, which decreases the friction coefficient. With a further increase in velocity, an elastohydrodynamic lubrication (EHL) regime is reached, where the hydrodynamic pressure generated in the fluid film carries the load with no asperity contacts. In this regime, the friction coefficient stays almost constant [**1**]. Traditionally the lubrication regime may be characterized by the film parameter Λ, which is the ratio of film thickness and composite surface roughness. It is known that the use of this parameter has limitations in connection with thin film lubrication [**2**].

Industrial gear systems are often operated in a mixed lubrication regime or in micro-EHL conditions. In the gear contact load, surface velocities and radiuses are changing continuously along the line of action. At the instantaneous contact point, spur gear profiles are typically approximated by cylinders with the same radius of curvature as the gear teeth. This provides the basis of the twin-disc test devices, which typically represents a single point along the line of action in real gears at steady state, that is at constant radius, load, and speed conditions. Höhn *et al.* [**3**] list three main differences when gear and twin-disc contacts are compared:

(a) they have different kinds of surface topography and orientation;
(b) film formation is continuous in discs but on gears a new oil film has to build up with every new engagement;
(c) dynamic effects on discs are significantly smaller than in gears.

*Corresponding author: Department of Mechanics and Design, Tampere University of Technology, P.O. BOX 589, Tampere 33101, Finland.
email: jaakko.kleemola@tut.fi

Film thickness, which protects the gear from failure such as wear, scuffing, micropitting, and pitting, is strongly dependent on oil and surface temperatures in the gear contact inlet zone [**4**, **5**]. Studies have been made to calculate [**6**, **7**] and measure [**8**, **9**] gear (surface) temperatures; however, the surface temperature of an instantaneous contact point is very difficult to estimate either theoretically or experimentally.

Höhn *et al.* [**10**] reported thin fluid film measurement techniques used in twin-disc test devices and some of these techniques were also applied to real gears. These thin-film sensors allow measurement of surface temperature, film thickness, and pressure distribution at a lubricated Hertzian contact point. These sensors have a definite value in contact research, even though they require considerable effort for their manufacture and calibration together with the fact that they have a limited lifetime [**10**] and pressure level. The (electrical) contact resistance measurements have been used in many different kinds of test devices [**1**, **5**, **11**–**16**] to measure relative changes of film thickness in lubricated contacts. Kleemola and Lehtovaara [**5**] simulated gear contacts along the line of action using a twin-disc test device, where contact resistance measurements were recorded. It was concluded that the trends of calculated thermal Λ-values of real gears correspond well with the measured mean contact resistance. Lord and Larsson [**11**] studied ball and disc contact under pure rolling as well as under sliding conditions. Measurements were made using several different steel surfaces under nominal EHL conditions and contact was monitored using electrical resistance and capacitance measurement. It was concluded that the improved contact resistance measurements can be used to detect both the fluid full film and the solid tribofilm formed as a result of chemical reactions between the surface material and lubricant additives.

Contact resistance measurements seem to have properties that make it tempting to use them in gearboxes to evaluate, on-line, the relative changes in the oil film thickness. These measurements may give information about asperity loading conditions and the dominant lubrication mechanism. It also takes into account both the transient and temperature effects that occur in the gear contacts. This may further facilitate on-line detection of the relative changes in oil film thickness under tough operating conditions before and after initial faults appear. In future, this method may contribute or offer an alternative way of fault diagnostics in gearboxes. The temperature behaviour in gear contact is closely related to, for example, scuffing and needs to be monitored more closely than the oil inlet temperature.

The objective of this work was to detect and follow on-line lubrication conditions in gear contact using contact resistance and bulk temperature measurements, which were applied to a modified FZG gear test device. Measurements were made with polished gear surfaces. The most important observations are illustrated and discussed below.

2 LUBRICATED GEAR CONTACT

Heavily loaded gears typically operate in boundary, mixed or (micro-) EHL regimes depending on operating conditions such as speed, actual viscosity, and surface properties. Figure 1(a) shows the instantaneous spur gear teeth contact and related twin-disc cylinders with the same radius of curvature.

In Fig. 1(b), a gear contact along the line of action is shown, where the dimensionless distribution of normal force (F_N/F_{Nmax}), Hertzian maximum line pressure (p_0/p_{0max}), surface velocities (u/u_{max}), and combined radius of curvature (R'/R'_{max}) are also shown. The tooth engagement starts at the left of the figure and the two sudden changes in load and pressure take place when two-tooth engagement changes to single-tooth engagement and the reverse. At the pitch point pure rolling is present, that is the sliding velocity ($V_S = u_1 - u_2$) is zero. The rolling velocity is given by $V_R = (u_1 + u_2)/2$. Tooth contact radius, load, and velocities through the line of action can be calculated from involute gear geometry under the given conditions. Assuming steady-state conditions, the indication of the basic lubricant film thickness at a certain position in the line of action is given by the well-known Hamrock and Dowson film thickness formula with smooth surfaces [**17**]. A central isothermal film thickness can be calculated using equation (1)

$$h_c = 3.06U^{0.69}G^{0.56}W^{-0.10}R' \tag{1}$$

The central film thickness is dependent on the dynamic viscosity $\eta_0(T)$ under the inlet conditions and it can be calculated from the following equation [**18**]

$$\log(\log \eta_0 + 4.2) = -S_0 \log\left(1 + \frac{T}{135}\right) + \log G_0 \tag{2}$$

where S_0 and G_0 are lubricant parameters, which describe the viscosity dependence on temperature, and T is the lubricant film inlet temperature.

However, the gear contact enhances transient lubrication conditions due to the continuous change of operating parameters along the line of action, start of mesh cycle (impact with sliding) with a new oil film buildup and overall gear dynamic effects. These transient effects in lubrication together with rough surfaces and mixed lubrication lead to very complex formulation of gear contact behaviour, which is very challenging to estimate theoretically or experimentally. A recent overview of deterministic mixed lubrication modelling using roughness measurements

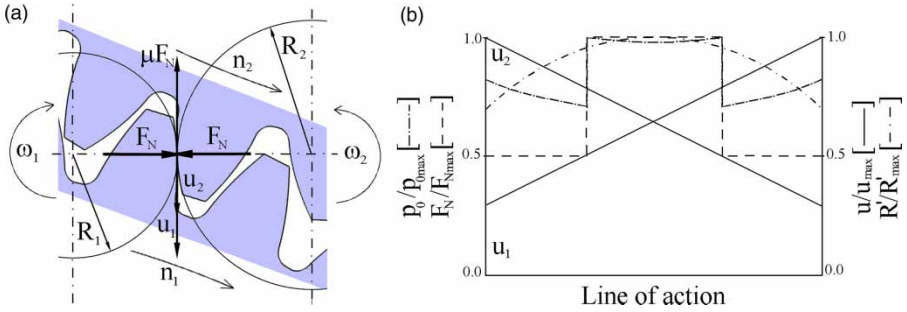

Fig. 1 Gear contact along the line of action

in gear applications is presented by Evans *et al.* [**19**]. Other essential papers dealing with the topic are studies by Larsson [**20**] and Wang *et al.* [**21**]. Cann *et al.* [**2**] studied the lambda ratio and reported that Λ values as high as 20 can give occasional metallic contact, while for well run-in surfaces, Λ as low as 0.3 can stop all metallic contact. Jacobson [**22**] stated that in EHL, contact sliding strongly increases the risk of metal-to-metal asperity contact in impact situations, especially with rough surfaces.

2.1 Friction coefficient

The friction coefficient changes along the line of action. At the instantaneous contact point the friction coefficient depends on the lubricant viscosity, the limiting shear stress, additive properties, and the severity of the asperity contacts. Based on the assumptions presented and discussed by Michaelis and Höhn [**23**], the mean coefficient of friction μ_m in a gear mesh can be presented as

$$\mu_m = \frac{P_s}{(PH_v)} \tag{3}$$

where the gear loss factor H_v is given by

$$H_v = \frac{\pi}{z_1}\frac{i+1}{i}(1-\varepsilon+\varepsilon_1^2+\varepsilon_2^2) \tag{4}$$

The transmitted power, P, is obtained by multiplying the applied torque by the shaft angular velocity, and the gear loss factor, H_v, is obtained by using the test gear geometry data shown in equation (4) and Table 1. The average sliding power loss, P_s, can be calculated as

$$P_S = P_L - P_{nl} - P_{bl} \tag{5}$$

The total power loss, P_L, and the no-load loss component, P_{nl}, are determined by experiment as is described later in section 3.3, test procedure and matrix. The load-dependent power loss, P_{bl}, for deep groove ball bearings was calculated according to reference [**24**]. The support bearing load-independent loss (viscous term) is part of the no-load losses.

Table 1 Gear tooth geometry

Parameter	Pinion	Gear
Number of teeth (dimensionless)	20	20
Pressure angle (°)	20	
Gear ratio (dimensionless)	1	
Centre distance (mm)	91.5	
Normal module (mm)	4.5	
Profile shift (dimensionless)	0.176	0.176
Face width (mm)	20	20
Contact ratio (dimensionless)	1.45	
Addendum contact ratio (dimensionless)	0.725	0.725

3 EXPERIMENT

3.1 Test device

Gear tests were carried out using a modified FZG test device, which is shown in Fig. 2. The loading of the test gears can be adjusted by applying appropriate torque to shaft 1 through the load clutch using a weight and rod. The applied moment is measured with a strain gauge transducer, which makes the application of the moment precise. The power necessary for rotation is fed in by the electric motor. The test rig has an adjustable speed control and the rotation speed of shaft 2 was measured with a pulse counter. The system friction moment was measured from shaft 2 using a torque meter.

The lubrication of gears and bearings is carried out with a separate pressure lubrication system, in which oil flowrate and inlet temperature can be controlled within a range of ± 0.05 l/min and ± 2 °C, respectively. The oil inlet and outlet temperatures are measured using thermocouples. The bulk temperature of the gear tooth was measured from one tooth with four different positions. The thermocouple head was 'cast' to the bottom of the tin piece, the shape and dimensions of which match with holes in the tooth. Thermocouple installations are shown in Figs 2 and 3.

This was carried out using k-thermocouples and a telemetry device. All signals were collected on a sampling card that was used for on-line analyses.

A contact resistance measuring device was incorporated in the test device to analyse relative changes in the oil film thickness. In the test device shaft 2 was

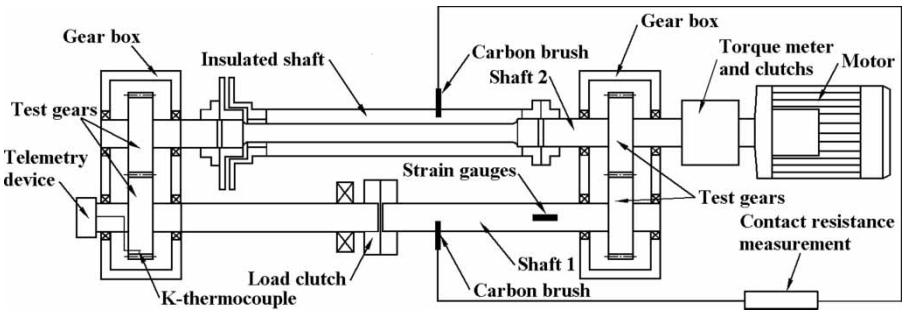

Fig. 2 Principle of the test rig

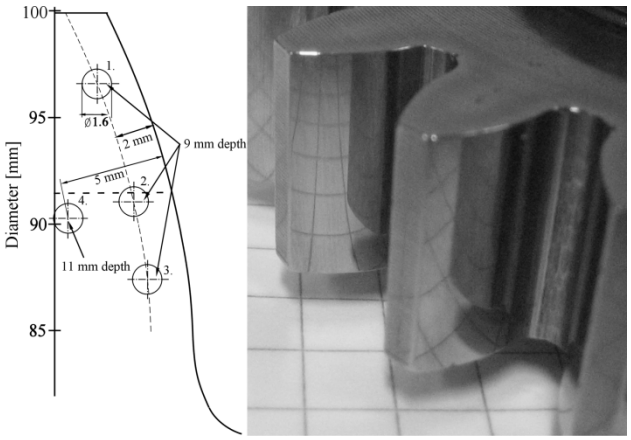

Fig. 3 Position of the k-thermocouple in the test gears and the surface of the polished gear

electrically insulated from the rest of the test device using an insulated layer between the bearings and bearing housings. Slip ring brushes were installed on both rotating shafts to transmit the signals. The insulated shaft carried a current of 5 mA with a voltage of 1 V, while the other shaft was connected to earth. Because shaft 2 was insulated, the only place where current can pass from shaft 2 to shaft 1 was through the gear contact situated in both gearboxes. The potential difference between the shafts and the current flowing between them were both measured using a sampling period of 1 ms. The contact resistance can be calculated by dividing the potential difference by the current. The maximum contact resistance was limited to 200 ohm with a separate resistor. The mean contact resistance was obtained by calculating average values for the contact resistance.

The total loss of torque from two gear pairs was obtained by using the torque meter, as shown in Fig. 2. The total power loss of one gear pair could be calculated from the measured total torque loss and shaft 2 rotation speed by assuming equal power loss in both gear boxes. The load-dependent losses of gears P_s and bearings P_{bl}, that is the total power loss P_L minus the no-load loss P_{nl}, were determined directly by measurement. Using equations (3) to (5), the mean friction coefficient of the gear contact can be calculated.

3.2 Test gears and lubricant

The material for the test gears is case-hardening steel 20 NiCrMo2–2. The gears are case hardened to a depth of 0.8–1 mm, with a specific surface hardness of 60–62 HRC. Test gears were case hardened, ground, and polished, which gives the gear surfaces a mirror-like finish, as shown in Fig. 3. Polishing has been done using a trough vibrator with chips and compounds, and the final surface roughness Ra-values were close to 0.05 μm. The main features of the gears are shown in Table 1.

The test lubricant was mineral base oil ISO VG 220 with kinematic viscosity at 40 and 100 °C of 220 and 19 mm^2/s, respectively. The density of the lubricant at 15 °C was 892 kg/m^3. The tests were carried out at steady oil inlet temperatures of 40, 60, and 80 °C and at a lubricant flowrate of 2.0 l/min.

3.3 Test procedure and matrix

Tests were carried out according to Table 2. The test device was warmed up for about 2 h before starting the measurements. At first a lubricant was circulated through the test device for about 30 min to bring the lubricant to the test temperature. During this time the torque was set for the system. The test device was run for about 1 h with a shaft 1 torque of 302 Nm and shaft 2 rotation speed of 1200 r/min, which gives a pitch line velocity of 5.76 m/s. This was done to warm up all components in the test device. Warming up the test device minimizes variations in the measurements. The test device was then stopped and the gear teeth were allowed to cool down to the lubricant inlet temperature.

Tests 1–6 were carried out as defined in Fig. 4 at intervals of 15 min. For Case 1, the torque was 302 Nm and the k-thermocouple was in tooth location 4 as shown in Table 2. Cases 2–4 have similar operating conditions to case 1, but before every test the gear teeth were cooled down to the lubricant inlet temperature and the thermocouple was moved to new locations 1, 2, and 3, respectively. Case 5 was run with a torque of 5 Nm to obtain data for no-load losses. Cases 1 and 6 are similar except that the torque was 135 Nm. In cases

Table 2 Test matrix

	Pitch line velocity (m/s)	Shaft 1 torque (Nm)	Lubricant inlet temperature (°c)	Location of k-thermocouple (dimensionless)	Time interval (min)
Case 1	0.96–9.58	302	60	4	15
Case 2	0.96–9.58	302	60	1	15
Case 3	0.96–9.58	302	60	2	15
Case 4	0.96–9.58	302	60	3	15
Case 5	0.96–9.58	5	60	3	15
Case 6	0.96–9.58	135	60	4	15
Case 7	0.96–9.58	135	40	4	1
Case 8	0.96–9.58	135	60	4	1
Case 9	0.96–9.58	135	80	4	1

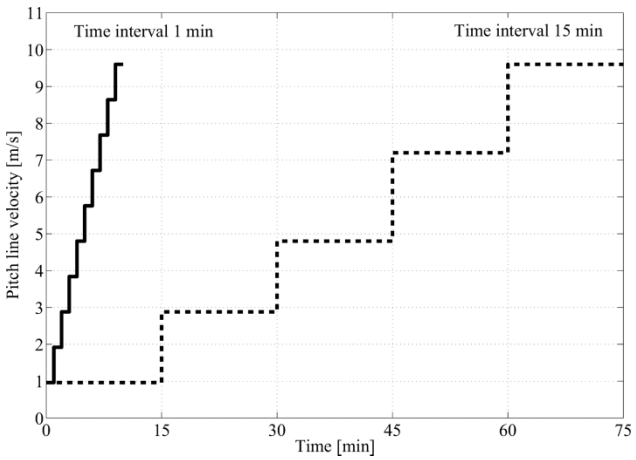

Fig. 4 Test procedure at each measuring point

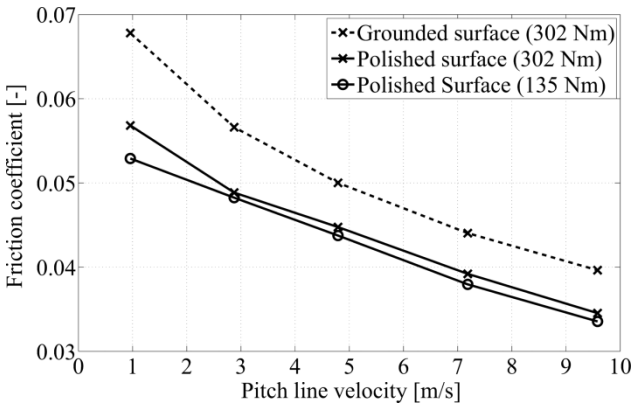

Fig. 5 Mean friction coefficients as a function of pitch line velocity for ground and polished gear surfaces at an oil inlet temperature of 60 °C and torques of 135 and 302 Nm

7–9, the time intervals were set to 1 min as shown in Fig. 4. These test cases were focused on the contact resistance behaviour.

In test cases 1–6, the point for determination of gear tooth bulk temperature at each pitch line velocity was selected so that the bulk temperature was stabilized and the oil inlet temperature was very close to 60 °C. At this point, the mean bulk temperature value was calculated from the measured signal at a time interval of 30 s before and 30 s after the selected point. The measured torque loss, that is the friction moment and the contact resistance were the mean values for the 1 min period at the end of each pitch line velocity. In cases 7–9, the gear tooth bulk temperature and contact resistance were the mean values for a 10 s period at the end of each pitch line velocity setting.

4 RESULTS AND DISCUSSION

The gear contact lubrication conditions were measured and followed on-line using the contact resistance and the bulk temperature measurement arrangement, which was implemented in the FZG test device. In this study the test gear surfaces were polished; otherwise the operation conditions were typical of those for an industrial gear. The contact resistance and bulk temperature were measured as a function of pitch line velocity, load, and oil inlet temperature.

The mean friction coefficient was determined for polished gears as described earlier in the text. The mean friction coefficients obtained were compared with the corresponding values for ground gears, which were measured with the same gear pairs as in a previous study [**25**]. The results are shown in Fig. 5.

Figure 5 shows that both mean friction coefficient curves have a similar downward trend as a function of pitch line velocity. The polished surface reduces the friction coefficient 10–20 per cent, which matches results from a previous study [**26**]. The value of the friction coefficient and the shape of the curve indicate that the measurements were mainly performed in a mixed lubrication regime. The steady-state-based lambda-value in the test varied in a range of 2–10 at pitch point using central film thickness and Ra surface roughness of 0.05 μm, but it is clearly lower when minimum film thickness is considered at the beginning of the mesh cycle. In addition, it is generally known that the gear contact enhances transient lubrication conditions at the beginning and along the line of action. Further, Cann *et al.* [**2**] studied the lambda ratio and reported that Λ values as high as 20 can give occasional metallic

contact, while for well run-in surfaces, Λ as low as 0.3 can stop all metallic contact. This means that changes in the mean contact resistance measurements should indicate changes in lubrication condition under these operating conditions.

The nature of the surface, and thus the bulk temperatures, is the dominant parameter when gear contact scuffing load-carrying capacity is evaluated [**27**]. The increase in temperature decreases the oil film thickness, which increases the risk of a scuffing failure. The measurement of the surface temperature in gear contacts is a very difficult task and requires a lot of effort to implement it as a routine measurement. Consequently bulk temperature measurement was more convenient for use in this study.

In Fig. 6, the bulk tooth temperatures are shown for each of the four locations indicated in Fig. 3. The oil inlet temperature was kept at 60 °C, but the measured bulk temperatures were higher in every test case. This is due to friction between contact surfaces causing heat, which is partially transferred to the gear. The bulk temperature increases with increasing pitch line velocity due to increasing power losses, that is heat generated in the gear contact. It seems that the bulk temperature is fairly independent of the location of measurement with the pitch line velocities used in this study. The maximum bulk temperature difference between the different locations was 6 °C and it increases as a function of the pitch line velocity.

As mentioned earlier, the test conditions include the mixed lubrication regime, where the mean contact resistance should indicate clear changes. In Fig. 7, the mean contact resistance and pitch line velocity are shown as a function of time. The single mean contact resistance value is a mean value for a period of

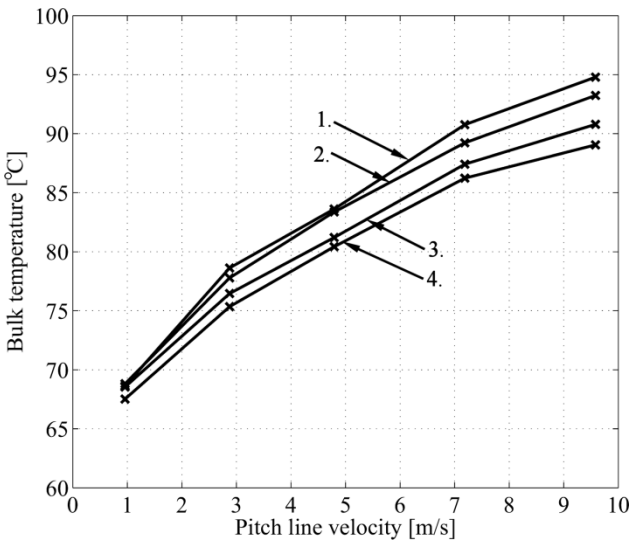

Fig. 6 Bulk temperatures as a function of pitch line velocity for polished surfaces at an oil inlet temperature of 60 °C and a torque of 302 Nm

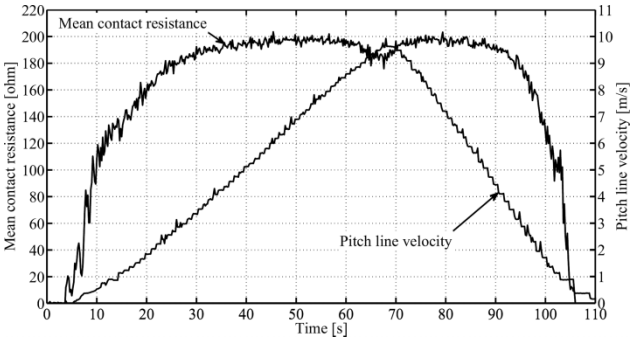

Fig. 7 Measured mean resistance and pitch line velocity as a function of time at an oil inlet temperature of 40 °C and a torque of 135 Nm

0.2 s with a sampling period of 1 ms. This means that the mean value includes the data points in different positions along the line of action and thus considers transient effects. It would have been interesting to see the detailed behaviour of resistance data during single tooth contact. However, this was not possible with the used test device, which has two gear pairs and each gear pair with one and two tooth pairs in contact.

Figure 7 shows that the measured mean contact resistance curve is already quite smooth with the mean value period used and that the signal is very sensitive to the change of pitch line velocity. Above a pitch line velocity of 3.8 m/s, the mean contact resistance does not change very much more because it was limited to 200 ohm. If the external resistor chosen were larger than 200 ohm, the mean contact resistance would increase further and would reach its maximum at a higher pitch line velocity. This was shown to happen in the initial tests using a potential difference of 2.5 V and a maximum resistance of 500 ohm.

To evaluate the behaviour of the lubrication process using contact resistance measurements, the tests were performed at different operating conditions according to Table 2. In Fig. 8, the behaviour of mean contact resistance is shown at three different oil inlet temperatures 40, 60, and 80 °C, together with the calculated film thickness trends at the pitch point. The bulk temperature-related film thickness is calculated from equation (1), where the dynamic viscosity, shown in equation (2), was determined using the measured bulk temperature from tooth position 4. The calculated thermal film thickness is the thermal correction factor φ_T [**28**] multiplied by the isothermal film thickness (equation (1)) based on the oil inlet temperature, which is traditionally used in gear film thickness estimation. In this study, the measured bulk temperature-related film thickness was also included, because it takes account of the temperature behaviour when the real gear operating conditions, such as pitch line velocity, are varied. Furthermore, this measurement may have potential, when the gearbox conditions are analysed on-line. The results show that the film

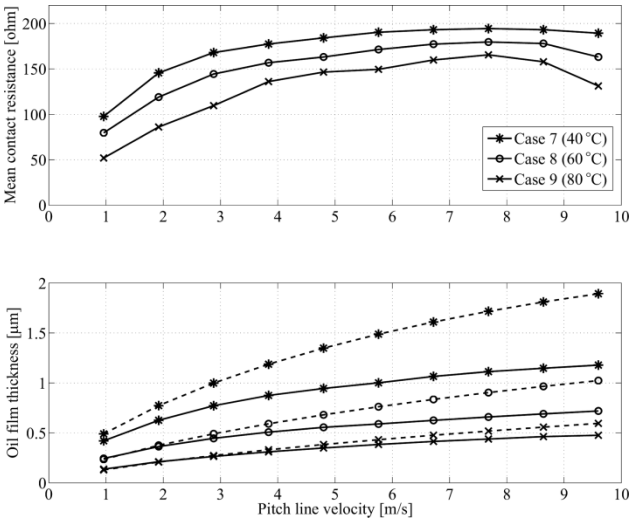

Fig. 8 Measured mean contact resistance, the calculated bulk temperature-related (solid line) and thermal (dashed line) central film thicknesses at a pitch point as a function of pitch line velocity at oil inlet temperatures of 40, 60, and 80 °C and a torque of 135 Nm

thickness trends are fairly similar in every test case, but the thermal film thickness values increase more rapidly than the corresponding bulk temperature-related film thicknesses. Here, the film thickness trend is shown as an indicative reference for steady-state conditions to screen the effect of the main operating parameters (load, velocity, and temperature) and transient behaviour in lubrication condition. In a previous study [**5**], gear contact was simulated along the line of action at discrete, steady state, with contacts using a twin-disc test device, where contact resistance measurements were recorded. The results showed that the trends of the calculated thermal Λ-values along the line of action correspond well with the measured mean contact resistance.

Figure 8 shows that the trend of the curves of the measured mean contact resistance and the calculated film thicknesses match well, indicating that the mean contact resistance measurement reflects the changes in oil film thickness under real gear operating conditions. When the mean contact resistance approaches its maximum or minimum value, its gradient becomes smaller than elsewhere. This may be the reason why the larger film thickness difference between cases 7 and 8 compared to that for cases 8 and 9 cannot be seen in corresponding mean contact resistance results. The mean contact resistance begins to drop at higher pitch line velocities, especially with an oil inlet temperature of 80 °C. One reason for this might be the dynamics of the gear contact and the fact that the oil film has to build up with every new engagement. The oil film may not stand the impact load combined with sliding when the gear tooth comes into contact at higher velocities. The other reason may be that the increase in oil film temperature with increasing velocity has the potential to reduce the oil film thickness despite the increase in entrainment velocity [**29**]. These reasons are related to non-steady-state lubrication conditions and cannot be derived with the film thickness calculations used. This kind of behaviour is very challenging when modelling gear contacts, because transient impact load and true inlet temperature need to be included in the study.

The tests were also performed with three different load levels. The results are shown in Fig. 9. Figure 9 shows that the increase in the load decreases the mean contact resistance. This trend corresponds with the film thickness calculations, which take account of the load and temperature effects. The drop in the mean contact resistance at higher pitch line velocities can also be seen in Fig. 9, especially with a torque of 302 Nm. At a torque of 5 Nm, a drop in the mean contact resistance at higher velocities is not apparent, indicating that the dynamics of the slip ring brushes do not cause the drop. Analysis of the results performed with the same test conditions in Figs 8 and 9 shows some difference in the contact resistance level. This may come from the contact resistance measuring arrangement, such as contact between the slip ring brushes and axes, which in the long term may change a little during the measurements.

The mean contact resistance measurement seems to indicate the correct trend in behaviour for a change in lubrication conditions with different operating parameters such as load, velocity, and temperature with the result that this kind of measurement may have some value as a 'tribosensor' in gearboxes. In future, the suitability of the mean contact resistance measurement should be evaluated with ground gear surfaces.

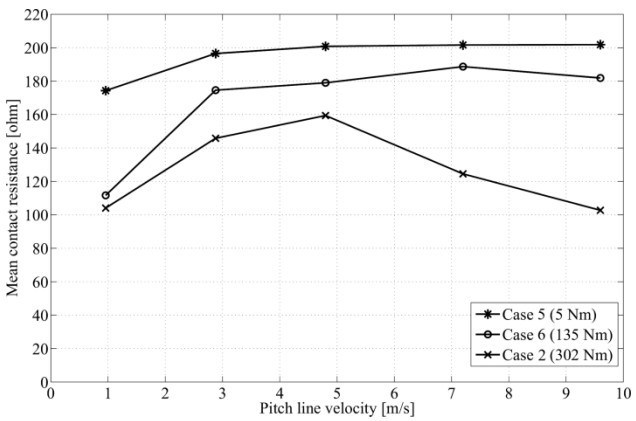

Fig. 9 Measured mean contact resistance as a function of pitch line velocity at torques of 5, 135, and 302 Nm and an oil inlet temperature of 60 °C

5 CONCLUSIONS

The objective of this work was to detect and follow on-line lubrication conditions in gear contacts using contact resistance and bulk temperature measurements in a modified FZG gear test device. Measurements were made in mixed lubrication conditions with polished gear surfaces at operating conditions that are typical of industrial gears. The presented mean contact resistance includes the data points in different positions along the line of action and thus also considers transient effects.

The trend in the curves of the measured mean contact resistance and the calculated steady-state-based film thicknesses correspond well with different operating parameters such as load, pitch line velocity, and oil inlet temperature. However, at the highest pitch line velocities some differences appeared, which may be due to the transient effects in gear contact. This indicates that the mean contact resistance measurements reflect the relative changes in lubrication conditions under used operating conditions. The measured contact resistance does not have a linear correlation with oil film thickness, at least when it approaches the maximum or minimum values.

Bulk temperature measurements give the actual temperature for gear contact and support the estimates of actual film thickness and lubrication conditions. The bulk temperature is closely linked to scuffing failure. The measured bulk temperatures were 8–35 °C higher than the oil inlet temperature depending on the operating conditions used. It appears that the bulk tooth temperature is largely independent of the location of the thermocouple resulting in a maximum difference of 6 °C at highest pitch line velocity.

In future, the mean contact resistance measurement should be evaluated with ground gear surfaces. Further study is also needed to adapt the measurement system to different lubrication and operating conditions. These actions should show whether this method can contribute or offer an alternative way for fault diagnostics in gearboxes.

REFERENCES

1 **Spikes, H. A.** Mixed lubrication – an overview. *Lubr. Sci.*, 1997, **9**(3), 221–253.

2 **Cann, P., Ioannides, E., Jacobson, B.,** and **Lubrecht, A. A.** The lambda ratio – a critical re-examination. *Wear*, 1994, **175**(1–2), 177–188.

3 **Höhn, B.-R., Michaelis, K.,** and **Doleschel, A.** Frictional behaviour of synthetic gear lubricants. In Proceedings of the 27th Leeds–Lyon Symposium on *Tribology*, 2001, pp. 759–768 (Elsevier, Amsterdam).

4 **Höhn, B.-R.** and **Michaelis, K.** Influence of oil temperature on gear failures. *Tribol. Int.*, 2004, **37**(2), 103–109.

5 **Kleemola, J.** and **Lehtovaara, A.** Experimental simulation of gear contact along the line of action. *Tribol. Int.*, 2009, **42**, 1453–1459.

6 **Patir, N.** and **Cheng, H. S.** Prediction of the bulk temperature in spur gears based on finite element temperature analysis. *ASLE Trans.*, 1979, **22**(1), 25–36.

7 **Long, H., Lord, A. A., Gethin, D. T.,** and **Roylance, B. J.** Operating temperatures of oil-lubricated medium-speed gears: numerical models and experimental results. *Proc. IMechE, Part G: J. Aerospace Engineering*, 2003, **217**(2), 87–106. DOI: 10.1243/095441003765208745.

8 **Deng, G., Kato, M., Maruyama, N., Morikawa, K.,** and **Hitomi, N.** Initial temperature evaluation for flash temperature index of gear tooth. *Trans. ASME, J. Tribol.*, 1995, **117**(3), 476–481.

9 **Yi, J.** and **Quinonez, P. D.** Gear surface temperature monitoring. *Proc. IMechE, Part J: J. Engineering Tribology*, 2005, **219**(2), 99–105. DOI: 10.1243/135065005X9745.

10 **Höhn, B.-R., Michaelis, K.,** and **Kopatsch, F.** Determination of film thickness, pressure and temperature in elastohydrodynamic lubrication in the past 20 years in Germany. *Proc. IMechE, Part J: J. Engineering Tribology*, 2001, **215**(3), 235–242. DOI: 10.1243/1350650011543501.

11 **Lord, J.** and **Larsson, R.** Film-forming capability in rough surface EHL investigated using contact resistance. *Tribol. Int.*, 2008, **41**(9–10), 831–838.

12 **Simon, M.** *Messung von elasto-hydrodynamischen parametern und ihre auswirkung auf die grübchentragfähigkeit vergüteter scheiben und zahnräder*. Doctoral Thesis, Technischen Universität München, 1984.

13 **Kuo, W.-F., Chiou, Y.-C.,** and **Lee, R.-T.** A study on lubrication mechanism and wear scar in sliding circular contacts. *Wear*, 1996, **201**(1–2), 217–226.

14 **Pepper, S. V.** Ultra starvation studied in the spiral orbit tribometer. *Tribol. Trans.*, 2008, **51**(6), 723–729.

15 **Kleemola, J.** and **Lehtovaara, A.** Experimental evaluation of friction between contacting discs for the simulation of gear contact. *Tribotest*, 2007, **13**(1), 13–20.

16 **Lugt, P. M., Severt, R. W. M., Fogelström, J.,** and **Tripp, J. H.** Influence of surface topography on friction, film breakdown and running-in in the mixed lubrication regime. *Proc. IMechE, Part J: J. Engineering Tribology*, 2001, **215**(6), 519–533. DOI: 10.1243/1350650011543772.

17 **Hamrock, B.** *Fundamentals of fluid film lubrication*, 1994, p. 690 (McGraw-Hill, Inc., New York).

18 **Larsson, R., Larsson, P. O., Eriksson, E., Sjöberg, M.,** and **Höglund, E.** Lubricant properties for input to hydrodynamic and elastohydrodynamic lubrication analyses. *Proc. IMechE, Part J: J. Engineering Tribology*, 2000, **214**, 17–27. DOI: 10.1243/1350650001542981.

19 **Evans, H. P., Snidle, R. W.,** and **Sharif, K. J.** Deterministic mixed lubrication modeling using roughness measurements in gear applications. *Tribol. Int.*, 2009, **42**(10), 1406–1417. DOI: 10.1016/j.triboint.2009.05.025.

20 **Larsson, R.** Transient non-Newtonian elastohydrodynamic lubrication analysis of an involute spur gear. *Wear*, 1997, **207**(1–2), 67–73.

21 **Wang, Y., Li, H., Tong, J.,** and **Yang, P.** Transient thermo-elastohydrodynamic lubrication analysis of an involute spur gear. *Tribol. Int.*, 2004, **37**(10), 773–782.

22 **Jacobson, B.** Nano-meter film rheology and asperity lubrication. *Trans. ASME, J. Tribol.*, 2002, **124**(3), 595–599.

23 Michaelis, K. and **Höhn, B.-R.** Influence of lubricants on power loss of cylindrical gears. *STLE Tribol. Trans.*, 1994, **37**(1), 161–167.

24 Andersson, N. E. and **Loewenthal, S. L.** Effect of geometry and operating conditions on spur gear system power loss. *Trans. ASME, J. Mech. Des.*, 1981, **103**(4), 151–159.

25 Järviö, O. and **Lehtovaara, A.** Experimental study of influence of lubricants on friction in spur gear contacts. *Finn. J. Tribol.*, 2002, **21**(2–3), 22–29.

26 Britton, R. D., Elcoate, C. D., Alanou, M. P., Evans, H. P., and **Snidle, R. W.** Effect of surface finish on gear tooth friction. *Trans. ASME, J. Tribol.*, 2000, **122**(1), 354–360.

27 Höhn, B.-R., Michaelis, K., and **Otto, H.-P.** Influence of immersion depth of dip lubricated gears on power loss, bulk temperature and scuffing load carrying capacity. *Int. J. Mech. Mater. Des.*, 2008, **4**(2), 145–156.

28 Wu, S. and **Cheng, H. S.** A friction model of partial-EHL contacts and its application to power loss in spur gear. *Tribol. Trans.*, 1991, **34**(3), 398–407.

29 Olver, A. V. Gear lubrication – a review. *Proc. IMechE, Part J: J. Engineering Tribology*, 2002, **216**(5), 255–267. DOI: 10.1243/135065002760364804.

APPENDIX

Notation

b	half-width of the Hertzian contact region $b = \sqrt{\frac{8F_N R'}{\pi L E'}}$
E	elasticity modulus
E'	effective elastic modulus, $1/E' = 1/2[(1-\nu_1^2)/E_1 + (1-\nu_2^2)/E_2]$
F_N	normal force
F_{Nmax}	maximum normal load
FZG	Forschungsstelle für Zahnräder und Getriebebau
G	dimensionless material parameter $G = \alpha E'$
G_0	non-dimensional constant in the Roelands viscosity equation
h_c	central film thickness
H_V	gear loss factor
i	gear ratio
L	face width of teeth
n	rotating speed
p_0	maximum Hertzian pressure at the contact $p_0 = \frac{2F_N}{\pi b L}$
p_{0max}	maximum Hertzian pressure at the line of action
P	transmitted power
P_{bl}	bearing power loss
P_L	total power loss
P_{nl}	no-load loss
P_S	sliding power loss
R	radius of curvature
R'	reduced radius of curvature, $1/R' = 1/(1/R_1 + 1/R_2)$
R'_{max}	maximum reduced radius of curvature
R_q	surface roughness RMS value
S_0	non-dimensional constant in the Roelands viscosity equation
T	temperature
u	surface velocity
u_{max}	maximum surface velocity
U	dimensionless load parameter $U = \eta_0 V_R/(E'R')$
V_R	rolling velocity $V_R = (u_1 + u_2)/2$
V_S	sliding velocity $V_S = u_1 - u_2$
W	dimensionless load parameter $W = F_N/(LE'R')$
z	number of teeth

α	viscosity pressure coefficient
ε	contact ratio
ε_1	addendum contact ratio of pinion
ε_2	addendum contact ratio of gear
η	actual viscosity
η_0	viscosity at atmospheric pressure
Λ	lambda value $\Lambda = h_c/\sigma$
μ	friction coefficient
μ_m	mean friction coefficient
ν	Poisson ratio
σ	combined surface RMS roughness $\sigma = \sqrt{R_{q1}^2 + R_{q2}^2}$
φ_T	thermal correction factor
ω	angular velocity

Subscripts

1	surface 1
2	surface 2

Tampereen teknillinen yliopisto
PL 527
33101 Tampere

Tampere University of Technology
P.O.B. 527
FI-33101 Tampere, Finland

ISBN 978-952-15-2367-0
ISSN 1459-2045